INSTITUTO TECNOLÓGICO DE COSTA RICA

VICERRECTORÍA DE INVESTIGACIÓN Y EXTENSIÓN

DIRECCIÓN DE PROYECTOS

ESCUELA DE INGENIERÍA FORESTAL

CENTRO DE INVESTIGACIÓN EN INNOVACIÓN FORESTAL

INFORME FINAL DE PROYECTO DE INVESTIGACIÓN

MODIFICACIÓN QUÍMICA DE LA ESTRUCTURA DE LA MADERA PARA EL MEJORAMIENTO DE LAS PROPIEDADES DE ESPECIES DE REFORESTACIÓN EN COSTA RICA

Código: 1401078

(DOCUMENTO I)

INVESTIGADORES:

Ing. Alexander Berrocal J. Dr.
Ing. Roger Moya R. Dr.
M.Sc. Johanna Gaitán Álvarez
Dr. Fabio Araya Carvajal

Mayo, 2020

ÍNDICE GENERAL

Pág.

1. Introducción

La madera es considerada un material sostenible y amigable con el ambiente, utilizada en una amplia variedad de usos estructurales y no estructurales (Barrantes y Salazar, 2012). Presenta buenas propiedades mecánicas que pueden ser mejoradas a través de técnicas o métodos ingenieriles como el uso de madera laminada y la incorporación de adhesivos, entre otros (Priadi y Hiziroglu, 2013).

Uno de los principales problemas con la madera, es que se trata de un material higroscópico (posee la capacidad de absorber o liberar humedad en relación a las condiciones ambientales de uso), lo que le genera una inestabilidad dimensional (Priadi y Hiziroglu, 2013). Además, bajo condiciones desfavorables, puede ser dañada y destruida rápidamente por factores bióticos como hongos, insectos y perforadadores marinos o por factores abióticos, como las condiciones ambientales (humedad relativa, lluvia, radiación UV, fuego etc.). Los agentes bióticos pueden atacar de múltiples maneras usando la madera para su alimentación y refugio (Islam et al. 2008). Utilizando como alimento a los polímeros de la pared celular como celulosa, hemicelulosas y lignina. Por otro lado, los factores abióticos, o del medio, producen en las estructuras de la madera foto-oxidación por radiación ultravioleta y erosión a nivel superficial (efecto del viento y la lluvia), generando depolimerización o fragmentación de la lignina, con lo cual se facilita la acción de los organismos bióticos (Garay et al. 2009).

En los países tropicales, las maderas de rápido crecimiento tienden a deteriorarse a mayor velocidad, en virtud de su naturaleza biológica, sus propiedades físicas y químicas; así como también producto de las condiciones ambientales que se tienen en estas regiones. Lo que implica que a la hora de realizar una construcción se prefieran otros tipos de materiales estructurales sustitutos en vez de la madera, argumentando su baja durabilidad producto de la degradación biótica y abiótica.

Con una mayor conciencia de la fragilidad del medio ambiente y la necesidad de la durabilidad de los productos de madera, se han desarrollado nuevas tecnologías para aumentar la vida útil de este material sin el uso de productos químicos tóxicos (Hill et al 2006; Rowell 2012; Gerardin 2016). Temas de sostenibilidad, captura de carbono y

desempeño convergen en esta búsqueda de nuevas tecnologías para mejorar la estabilidad, durabilidad y desempeño de la madera especialmente para uso en exteriores (Rowell 2016, Manthanis 2017).

A esto se le puede sumar las normas internacionales de limitar el uso de sustancias toxicas y que causen daños tanto en la salud de las personas, así como la contaminación del medio ambiente (Gerardin, 2016). Por lo que la búsqueda de nuevas tecnologías más amigables con el medio ambiente ha surgido y el incremento del interés por tratamientos sin la utilización de sustancias toxicas como los termo tratamientos, modificación químicas y modificación por impregmentación (Hill 2006, Rowell 2012); especialmente en especies de rápido crecimiento (Dong et al., 2015).

La modificación química en la madera ocurre cuando se da una reacción de algún reactivo con los polímeros de los componentes principales de la madera como lignina, hemicelulosa o celulosa; dando como resultado la formación de una banda estable covalente entre el reactivo y la pared celular de los polímeros (Hill 2006), provocando un cambio en las macromoléculas de la pared celular (Mantanis 2017). Estos cambios en la madera dan como resultado, mayor equilibrio en contenidos de humedad por lo que la madera es menos propensa al cambio dimensional por la pérdida de humedad, así como más resistente a los hongos o microrganismo que producen deterioro, por el bloqueo en la pared celular (Hill 2006; Rowell et al., 2009, Rowell 2012).

Basados en lo anterior, el objetivo de este estudio fue: Mejorar la estabilidad dimensional, durabilidad natural y retardación al fuego de la madera de diez especies utilizadas en la industria y construcción de Costa Rica mediante tratamientos modernos de modificación química de la madera, específicamente minerilización, acetilación y furfurilación.

Madera de albura de nueve especies, que presentan buena permeabilidad (Moya et al., 2015; Tenorio et al., 2016), provenientes de plantaciones forestales de rápido crecimiento en Costa Rica, fue utilizada. Las especies seleccionadas fueron *Cedrela odorata (C.o), Cordia alliodora (C.a), Enterolobium cyclocarpum (E.c), Gmelina arborea (G.a), Hieronyma alchorneoides (H.a), Samanea saman (S.s), Tectona grandis (T.g), Vochysia ferruginea (V.f)* y *Vochysia guatemalensis (V.g)*. La edad de las plantaciones donde se recolectó el

material varió entre los 4 y los 8 años de edad. En el muestreo fueron cortados tres árboles por especie en trozas de 1 metro de largo y luego fue aserrada en tablas de 7,5 cm de ancho x 2,5 cm de espesor. Estás tablas se dejaron secar al aire hasta que llegaran a un contenido de humedad entre 12-15% y luego se extrajeron piezas de dimensiones de 46 cm de largo x 7.5 cm de ancho y 2 cm de espesor, garantizando que la madera se compusiera de madera de albura. A partir de estas piezas se obtuvieron las probetas requeridas para los diferentes análisis realizados, la metodología específica para cada uno de los tratamientos se detalla en los capítulos de este informe.

Para el proceso de carbonatación, los resultados del (Análisis Termogravimétrico) TGA mostraron que las maderas con la mayor formación de $CaCO_3$ mostraron una señal más pronunciada a 200 °C en relación con la madera no tratada, por lo tanto, son más termoestables. La prueba de resistencia al fuego mostró que el tiempo de la llama en los compuestos de $CaCO_3$-madera fue más largo que el de la madera no tratada en el 50% de las especies analizadas, demostrando un efecto positivo por mineralización. La densidad de la madera, la resistencia a la descomposición, MOR y MOE en flexión y MOR en compresión se vieron ligeramente afectados por la mineralización. La absorción de agua aumentó, pero no tuvo ningún efecto negativo sobre la estabilidad dimensional. Fue posible concluir que en general, la mineralización puede ser un tratamiento químico para aumentar la estabilidad dimensional y la resistencia al fuego de las especies de madera dura sin modificar las propiedades físicas y mecánicas de la madera.

La absorción de la solución de $CaCl_2$ y $NaCO_3$ en las nueve especies de maderas latifoliadas varió de 42.2 a 168.0 l m^{-3} y de 69.5 a 214.6 l m^{-3} respectivamente, mientras que la retención de $CaCO_3$ in situ varió de 2.8 a 9.2 kg m^{-3}. Aunque las diferentes especies de madera mostraron una alta absorción de las soluciones, se encontró que en algunas de ellas el porcentaje de CO_3^{2-} no reaccionó, mientras que en otras el ion Ca^{2+} fue el que no reaccionó en la sal. El análisis SEM mostró la distribución de los cristales de $CaCO_3$ en los diferentes elementos anatómicos de la madera y mostró la formación de cristales de tipo calcita y vaterita, que también se evidenciaron en la difracción de rayos X y en el espectro FTIR.

Con respecto a la acetilación, la ganancia porcentual en peso (WPG) de la madera varió de 2.2% a 16.8%, con la madera de *Vochysia ferruginea* mostrando el valor más alto, y las especies de *Gmelina arborea* y *Tectona grandis* mostrando los WPG más bajos. La madera de especies como *Enterolobium cyclocarpum*, *Hieronyma alchorneoides* y *Samanea saman* mostraron diferencias estadísticas entre los tiempos de tratamiento, mientras que el resto de las especies estudiadas no mostraron diferencias significativas. En general, el tiempo de acetilación más efectivo fue de 2,5 h, para todas las especies. La relación de intensidad (RI) de los espectros FTIR fue mayor en los picos de 1732, 1372 y 1228 cm^{-1} para todas las especies, asociados con la lignina. Se encontró una buena correlación entre el RI de esos picos y WPG; así como también entre todos los IR y entre sí. Mientras tanto, el IR asociado a hemicelulosas y lignina (picos de 1592 y 1334 cm^{-1}, respectivamente) no mostró correlación con WPG, ni entre sí ni tampoco con los otros IR. Además, se sugiere que el IR a 1732 cm-1 (asociado a los grupos acetilo C = O) puede considerarse como un indicador confiable del grado de acetilación para las especies tropicales de madera dura.

El porcentaje de ganancia de peso (WPG) varió de 2.2% a 16.8%. Se observó una correlación estadística positiva entre WPG, factores pre-exponenciales en el análisis TGA y el ángulo de contacto inicial, mientras que se encontró una correlación estadística negativa entre la variación de humedad debido a cambios en las condiciones de equilibrio de humedad, absorción de agua y pérdida de peso debido al ataque de hongos. En aquellas especies con un WPG superior al 10% (*Vochysia ferruginea*, *V. guatemalensis*, *Cordia alliodora* y *Enterolobium cyclocarpum*), la estabilidad térmica, el ángulo de contacto y la resistencia al ataque biológico aumentaron, mientras que la hinchazón, la absorción y la variación del contenido de humedad disminuyeron. Para estas especies, los mejores comportamientos se obtuvieron con un tiempo de acetilación de 2,5 horas. Las propiedades de la madera en especies con un WPG inferior al 5% apenas se vieron afectadas por los diferentes tiempos de acetilación y mostraron poca diferencia en relación con la madera no tratada.

Finalmente, para la furfurilación la absorción de la disolución FA varió entre 90.8 y 308.7 (l m^{-3}) y en la disolución FA-NPs Ag varió entre 77.0 y 306.4 l m^{-3}. Para las propiedades de color se obtuvo que, en todas las especies en los parámetros L* y a* antes y después en ambos tratamientos, se presentaron diferencias estadísticas significativas; mientras que en

el parámetro b* los resultados variaron dependiendo de la especie y el tratamiento. Con respecto al ΔE del cambio de color se obtuvo que en todas las especies este valor fue mayor en el tratamiento FA-NPs Ag. La densidad de todas las especies, en los diferentes tratamientos, varió entre 335.65 y 848.91 (kg m^{-3}). La propiedad hinchamiento a lo ancho varió entre 0.26 a 1.00 mm y en espesor varió entre 0.21 a 1.11 mm. En cuanto a la absorción de agua por inmersión se obtuvo menor absorción de agua en las muestras previamente furfuriladas. La pérdida de peso por biodeterioro causado por el hongo de pudrición café *Lenzites acuta* varió entre 3.98% a 15.06%, mientras que por efecto del hongo de pudrición blanca *Tramates versicolor* varió entre 3.14% y 15.06%. Para el esfuerzo de dureza se observó que los valores en todas las especies y tratamientos varió entre 1089.60 N y 5505.61 N. En la mayoría de especies el valor de dureza incrementó en los tratamientos de furfurilación (FA y FA-NPs Ag). Al evaluar el desempeño de los tratamientos, mediante los espectros del análisis rayos-X FTIR, se observó la existencia de 4 señales importantes en los tratamientos FA y FA-NPs Ag que no se presentan en las muestras no tratadas, estas señales se logran observar en 899, 1562, 1652 y 1711 cm^{-1}. El comportamiento de descomposición térmica en el TGA de las nueve maderas furfuriladas presentó el mismo patrón que la madera sin tratar, sin embargo, se logró observar las diferencias en la descomposición de las especies a través de la curva de DTG. A través del análisis de microscopía de escaneo de láser confocal se logró observar una mayor cantidad de fluorescencia en la especie de mayor absorción, principalmente alrededor de los vasos en el tratameinto de FA, mientras que el tratamiento con FA-NPs sólo se observó en las fibras y en la no tratada no se presentó fluorescencia. De la misma forma, pero en menor cantidad, se observa fluorescencia en la especie de media absorción, principalmente en el tratameinto FA-NPs. Finalmente, en la especie de ligera absorción la fluorescencia es mínima y poco visible en los tratamientos de furfurilación.

En relación a los principales logros obtenidos en este proyecto se pueden mencionar:

1. Al menos cinco artículos científicos, uno de los cuales ya fue publicado (Revista BioResources), otro fue sometido (Revista Carbonates and Evaporites), uno está en edición para ser sometido (Revista Journal of Wood Science), uno está en revisión de uno de los autores internacionales para ser sometido y el último debe ser traducido para someterlo.

A partir de los resultados generados surgen algunas interrogantes que deberían ser abordadas a través de estudios posteriores en la misma línea:

a) Complementar los estudios de factibilidad técnica de aplicar la modificación química de maderas tropicales de rápido crecimiento, con estudios de factibilidad económica y de percepción que complementen la información generada para poder escalar estos procesos y poder implementarlos, a futuro, a escala comercial.

b) Valorar cuál de las tres opciones de modificación química tiene mayor potencial para ser escalada a nivel de planta piloto para probar su aplicación en madera de dimensiones comerciales.

c) Ampliar los estudios de evaluación del desempeño de los procesos de modificación química de la madera a través de técnicas tales como: análisis termo gravimétrico (TGA), microscopía electrónica de barrido, difracción de rayos X, espectroscopía infrarroja de la transformada de Fourier (FTIR) y microscopía de escaneo láser confocal entre otros; de tal manera que se generen más registros de la aplicación de estas técnicas en maderas tropicales de rápido crecimiento, incrementando el acervo de información disponible en esta materia.

Finalmente, con respecto a los beneficios inmediatos y futuros de los resultados obtenidos se debe destacar:

a) Un incremento en el acervo de información relevante de plantaciones de rápido crecimiento en diferentes zonas del país, con posibilidad de ser utilizada a nivel regional en materia de modificación química de maderas tropicales.

b) Haber generado experiencia práctica en la determinación del efecto de la modificación química, específicamente los procesos de carbonatación, acetilación y furfurilación, en el mejoramiento de propiedades físicas, mecánicas y de durabilidad en de maderas tropiacles de rápido crecimiento. Esta información se considera

relevante para determinar posibles usos futuros de estas maderas y obtener productos de un mayor valor agregado.

c) Contar con una base científica adecuada para futuros proyectos relacionados con los temas abordados en el proyecto, de tal forma que pueda incrementarse la información de propiedades de las maderas tropicales provenientes de plantaciones de rápido crecimiento, incrementando de esta forma la información existente a nivel nacional e internacional para esta temática.

d) Un aporte significativo la productividad académica de la Escuela de Ingeniería Forestal y del Instituto Tecnológico de Costa Rica, a través de al menos cinco publicaciones en índices superiores (Scopus y Web of Science).

2. Artículo 1. Effect of $CaCO_3$ in the wood properties of tropical hardwood species from fast-grown plantation in Costa Rica

Effect of $CaCO_3$ in the wood properties of tropical hardwood species from fast-grown plantation in Costa Rica

Róger MOYA*
Instituto Tecnológico de Costa Rica, Escuela de Ingeniería Forestal, Apartado 159-7050, Cartago, Costa Rica. Email: rmoya@itcr.ac.cr

Johana GAITÁN-ALVAREZ
Instituto Tecnológico de Costa Rica, Escuela de Ingeniería Forestal, Apartado 159-7050, Cartago, Costa Rica. Email: aberrocal@itcr.ac.cr

Alexander BERROCAL
Instituto Tecnológico de Costa Rica, Escuela de Ingeniería Forestal, Apartado 159-7050, Cartago, Costa Rica. Email: aberrocal@itcr.ac.cr

Fabio ARAYA
Instituto Tecnológico de Costa Rica, Escuela de Química, Apartado 159-7050, Cartago, Costa Rica. Email: aberrocal@itcr.ac.cr

*Authors correspondence, Email: rmoya@itcr.ac.cr

Effect of $CaCO_3$ in the wood properties of tropical hardwood species from fast-grown plantation in Costa Rica

ABSTRACT

Studies related to chemical modifications of wood, such as wood mineralization in tropical hardwoods, are scarce. The objective of this work is to evaluate the effect of the precipitation of $CaCO_3$ by means of subsequential in-situ mineral formation based on a solution-exchange process of two solution-exchange cycles by impregnation with $CaCl_2$ in ethanol and $NaHCO_3$ in water, on the structure of the wood and on the thermal, physical, mechanical and decay resistance properties of nine species commonly used in commercial reforestation in Costa Rica. The TGA results showed that the woods with the highest formation of CaCO3 showed a more pronounced signal at 200 °C in relation to untreated/wood, therefore are more thermostable. The fire-retardant test showed that flame time in $CaCO_3$/wood composites was longer than for untreated/wood in half of the species tested, presenting a positive effect of mineralization. Wood density, decay resistance, MOR and MOE in flexion and MOR in compression were slightly affected by mineralization. Water absorption increased, but it had no negative effect on the dimensional stability. In general, mineralization can be a chemical treatment to increase the dimensional stability and fire resistance of hardwood species without modifying the wood's physical and mechanical properties.

Keywords: wood treatment, wood chemical treatment, wood plantation, fast-growth plantation, wood properties.

INTRODUCTION

Minerals are common in living organisms where they maintain rigidity and hardness of the structures. The process of mineral formation by living organisms is known as biomineralization (Krajewska 2018). Minerals are also found in different shapes and sizes in natural deposits in the Earth's crust (Krajewska 2018). Biomineralization can be biologically controlled in the cell process (Benzerara et al. 2011; Kumari *et al.* 2016; Li *et al*. 2014) (Gadd 2010; Mukkamala *et al.* 2006) (Gadd et al. 2012, 2014; Li *et al.* 2014, 2015); there are around 60 different biological minerals (Anbu et al. 2016). The Earth's crust minerals constitute over

4% (Krajewska 2018) and are commonly found in rocks such as chalk, marble, travertine and tuff, among others (Krajewska 2018).

Among the wide range of minerals (from biomineralization and deposits of the Earth's crust) calcium carbonate ($CaCO_3$) is the main product, considered the most useful today (Dhami *et al.* 2013; Kumari *et al.* 2016; Rodriguez-Navarro *et al.* 2012). $CaCO_3$ appears as different polymorphs: calcite, aragonite and vaterite; two hydrated polymorphs (monohydrocalcit and ikaite) and several amorphous phases (ACC) (Dhami *et al.* 2014; Sánchez-Román *et al.* 2007). Calcite is the primary $CaCO_3$ product and it is the most thermodynamically stable polymorph of $CaCO_3$ (Ganendra *et al*. 2014; Okwadha and Li 2010). Vaterite, in turn, is considered a minor, metastable and transitional phase to calcite formation (Tourney and Ngwenya 2009). This mineral has been used for decades in construction and, more recently, it has been implemented in the agricultural, medical and engineering industries (Hoque 2013). Specifically, it is applied in the paper, paint, food, ceramics, construction, ink, adhesives, drugs, cable and plastic industries (Ozen *et al.* 2013). In the plastics industry for example, it is used as a loading agent to substitute high value polymers (Ozen *et al.* 2013). For water purification it can be used to eliminate ions of heavy metals such as Cu^{+2}, Pb^{+2}, Cd^{+2}, Zn^{+2} and Cr^{+5}(Hong *et al*. 2011). In the paper industry, for producing high gloss and greater opacity and whiteness (Barhoum *et al.* 2014; Wu *et al.* 2016).

On the other hand, wood has a porous network that poses a series of disadvantages, namely, high humidity and hygroscopicity, dimensional instability and high flammability (Uribe and Ayala 2015). However, this porous network is an optimal platform for the deposit of inorganic matter such as $CaCO_3$ (Merk *et al.* 2016), therefore minerals can be introduced in its hierarchical structure to help improve the material characteristics (Hübert *et al.* 2010; Shabir Mahr *et al.* 2012; Tampieri *et al.* 2009). Nevertheless, the process of precipitation of crystals of $CaCO_3$ is highly complex, since it depends on factors that affect the nucleation process and the subsequent crystal growth, which are often difficult to control (Declet *et al*. 2016).

Nevertheless, the first experiences on mineralization or $CaCO_3$ formation inside the wood were reported recently (Merk *et al.* 2015; Tsioptsias and Panayiotou 2011; Uribe and Ayala 2015). Tsioptsias and Pahayictou (Tsioptsias and Panayiotou 2011) introduced $CaCO_3$

using aqueous solutions and supercritical carbon dioxide in *Picea abies*, corroborating that under controlled conditions the treatment has fire retardant effects. Seeking fire retardancy, Merk *et al.* (Merk *et al*. 2015, 2016) used a modern and simple method based on a subsequential in-situ mineral formation based on a solution-exchange process in beech and spruce woods. Those studies showed that the formation of crystals of polycrystalline calcite and vaterite inside the wood occurs in lumina vessels and to a lesser extent in adjacent cell walls. Recently, using the methodology proposed by Merk *et al.* (Merk *et al.* 2016), Gaitán-Alvarez *et al.* (2020) studied $CaCO_3$ precipitation in tropical hardwoods and determined that it occurs in the form of calcite and vaterite, mainly in the vessels and rays of the species. They also determined that in-situ crystal formation is very difficult to control.

Despite the mentioned studies, the knowledge about the effect of $CaCO_3$ precipitation on the wood properties is limited; besides, the studies are limited to a few softwoods such as beech, spruce and picea and the processes of wood impregnation have been performed at a low scale (Burgert *et al.* 2016; Klaithong *et al.* 2013; Tsioptsias and Panayiotou 2011). Because of the great number of tropical timber species and the large variety of anatomical structures (Liu *et al.* 2018; Tenorio *et al.* 2016), studying the effect of $CaCO_3$ precipitation on wood properties becomes highly relevant in order to solve the problems of high moisture content, dimensional stability and natural decay, among others (Mantanis 2017).

Given this context, the present work aims at evaluating the effects of $CaCO_3$ precipitation on wood structure, on the thermal properties (thermal stability and fire retardancy); physical properties (density, moisture content, water absorption by immersion, swelling and moisture equilibrium); mechanical properties (static flexure and grain parallel compression) and durability properties (natural decay) of nine species commonly used in commercial reforestation in Costa Rica (*Cedrela odorata, Cordia alliodora, Enterolobium cyclocarpum, Gmelina arborea, Hieronyma alchornoides, Samanea saman, Tectona grandis, Vochysia ferruginea* and *Vochysia guatemalensis*). By studying these effects, it will be possible to treat tropical species with $CaCO_3$ to increment their fire retardancy and at the same time observe the changes in the wood properties.

MATERIALS AND METHODS

Sapwood from nine species from fast growth forest plantations in Costa Rica presenting good permeability was used ((Moya et al. 2015). The species were *Cedrela odorata* (*Co*), *Cordia alliodora* (*Ca*), *Enterolobium cyclocarpum* (*Ec*), *Gmelina arborea* (*Ga*), *Hieronyma alchorneoides* (*Ha*), *Samanea saman* (*Ss*), *Tectona grandis* (*Tg*), *Vochysia ferruginea* (*Vf*) and *Vochysia guatemalensis* (*Vg*). The age of the plantations that contributed the material ranged between 4 and 8 years. Three trees per species were cut down for sampling. Then, the samples were cut into 1 m long logs and sawn into 7.5 cm wide x 2.5 cm thick boards. These boards were air dried until reaching between 12-15% in moisture content. Then, pieces 46 cm long x 7.5 cm wide and 2 cm thick were extracted, making sure that the pieces were composed of sapwood.

The reagents used were ETI SODA (Turkey) solid-state sodium bicarbonate ($NaHCO_3$) and solid-state calcium chloride ($CaCl_2$) from CASO FCC FLAKES Solvay (USA). Absolute ethyl alcohol 99 % m/m of the brand Reactivos Químicos Gamma (Costa Rica), distributed by Laboratorios Químicos ARVI S.A, was used.

Mineralization process

The in-situ mineralization process was performed in 20 samples (46 cm long x 7.5 cm wide and 2 cm thick), using the vacuum and pressure equipment shown in the diagram in Fig. 1b. The samples were placed into a tank (25 cm diameter x 48 cm long and 27 litres capacity) for impregnation with salts. Calcium carbonate ($CaCO_3$) formation (Eq. 1) was performed by means of two impregnation cycles (Fig. 1a): impregnation with $CaCl_2$ (Eq. 2) and impregnation with $NaHCO_3$ (Eq. 3). In the $CaCl_2$ cycle, the wood was impregnated with $CaCl_2$ in an ethanol solution at 1 mol-l^{-1} concentration (Eq. 2), by first applying vacuum at -70 kPa (gauge) for 20 minutes and then immersing the samples totally into the solution and applying 690 kPa pressure for 30 minutes (Fig. 1a). In the $NaHCO_3$ cycle, the samples were impregnated with an aqueous solution at 1 mol-l^{-1} concentration (Eq. 2), by applying vacuum for 20 minutes, followed by 690 kPa pressure for 50 minutes. After finishing the first cycle, the samples were washed in distilled water and then were left to dry inside a chamber under controlled conditions (22°C and 66% relative humidity) until reaching 12% moisture content.

After the second cycle, the samples were washed in ethanol and then dried at 40°C for 4 hours. The details of this process can be consulted in Gaitán-Alvarez *et al*. (2020).

$$Ca^{2+} + CO_3^{2-} \rightarrow CaCO_3 \quad (1)$$

$$CaCl_2 * 2H_2O \rightarrow Ca^{2+} + 2Cl^- \quad (ethanol\ solution)\ (2)$$

$$NaHCO_3 \rightarrow\ Na^+ + H^+ + CO_3^{2-} \quad (aqueous\ solution)\ (3)$$

Evaluation of the mineralization process

In the $CaCl_2$ cycle, the samples were weighed before and after impregnation with $CaCl_2$. Thus, absorption of the $CaCl_2$ solution (Eq. 4) and salt retention (Eq. 5) were obtained. In the $NaHCO_3$ cycle, again the sample was weighed before and after impregnation with $NaHCO_3$ and again absorption of the $NaHCO_3$ solution (Eq. 4) and salt retention (Eq. 5) were obtained. The details regarding salt retention and $CaCO_3$ formation can be found in Gaitán-Alvarez et al. (2020).

$$Salt\ absorption\ \left(\frac{liters}{m^3}\right) = \frac{(Weight_{before\ impreg}(g) - Weight_{after\ impreg\ (g)}}{Volume\ of\ sample\ (cm^3)} \times \frac{(100\ cm)^3}{1\ m^3} \times \frac{1\ liters}{1000\ g} \quad (4)$$

$$Salt\ retention\ \left(\frac{kg}{m^3}\right) = Salt\ absorption\ \left(\frac{liters}{m^3}\right) \times \frac{salt\ concentration\ \left(\frac{salt\ weight\ in\ kg}{solution\ weight\ in\ kg}\right)}{solution\ density\ (\frac{weight\ in\ kg}{liters})} \quad (5)$$

Thermogravimetric analysis

The thermogravimetric analysis (TGA) was realized for $CaCO_3$/wood composites and untreated/wood 5 mg previously dried sawdust was used. The heating rate used was 20°C min^{-1} from 50°C to 800°C, in an ultra-high purity nitrogen atmosphere at a flow of 100 ml min^{-1}. A thermogravimetric analyzer from TA Instruments, model SDT Q600, was used. The TGA gave values of weight loss relative to temperature that were used to perform the derivative thermogravimetric analysis (DTG), which in turn was used to obtain the position and temperature at which the sample was degraded. The TGA data and its derivatives (DTG) were analyzed by means of TA Instruments Universal Analysis 2000 software.

Physical properties

The following physical properties were determined: density, moisture content (MC), water absorption of immersed wood in water, tangential and radial swelling of wood and moisture absorption due to changes in the condition of equilibrium moisture content (EMC) (from 12% to 18%). Sample density was determined for 20 $CaCO_3$/wood composites samples and 20 untreated/wood samples; the samples' volume and weight were measured and then the density (weight/volume) was determined. The MC was calculated for 20 $CaCO_3$/wood composites samples and 20 untreated/wood samples, following the procedures in ASTMD4442-42(ASTM 2016a). To determine the tangential and radial swelling and the percentage of water absorption, 20 samples 5 x 5 x 2 cm from each treatment were conditioned and weighed at 12% EMC and then conditioned for a period of 3-4 weeks at 18% EMC. After conditioning the samples were weighed and measured again. This procedure was based on the ASTM D4933-99 norm (ASTM 1999) but modified to the conditions in Costa Rica, where environmental moisture conditions are around 18%. Tangential and radial swelling were calculated by means of Eq. 6. Moisture absorption was determined through Equation 8 by obtaining first 12% and 18% moisture content with respect to dry weight (Eq. 7). The difference between both moisture measurements (12% and 18%) represented sample moisture absorption (Eq. 8).

$$Swelling\ \ (mm) = (g)\frac{measurement 12\%\ (mm) - measurement 18\%\ (mm)}{measurement\ 12\%\ (mm)} \times 100 (6)$$

$$Moisture\ content_{MC} = \frac{Weigh\ _{MC}\ (g) - Wei\ \ \ _{oven\ dried}\ (g)}{Weig\ \ \ _{oven\ dried}\ (g)} \times 100 \quad (7)$$

$$Moisture\ absorption = Moisture\ content_{18\%} - Moisture\ content_{12\%} \quad (8)$$

For weight gain from water immersion, 20 samples for each species/treatment previously weighed were immersed in water for 24 hours. After this period, the samples were weighed and weight gain was determined following Eq. 7, according to ASTM D4446 –13 (ASTM 1985).

Mechanical properties

The mechanical properties analyzed were resistance to static flexure and grain parallel compression. In both tests procedure B described in ASTM D-143 was used (ASTM 2016b). Twenty samples were taken from each species/treatment for each one of the tests. The tests were performed in a testing machine Tinius Olsen model H10KT in the case of static flexure and Tinius Olsen L60 for compression.

Fire retardancy

For this test, 10 $CaCO_3$/wood composite samples and 10 untreated/wood samples were used for each species. The sample size was 15 cm x 10 cm x 9 mm, in accordance with the methodology proposed by Taghiyari (Taghiyari 2012). The samples were placed in the device shown in Fig. 1c, specially designed for this test. Once the sample was placed at an angle of 45° and 27 mm from the flame, the test timing began, as follows: (i) *dark time*, the moment when the back of the sample exposed to the flame began to form a dark spot; (ii) *hole time*, which is the time when a hole begins to appear on the back of the sample exposed to fire; (iii) *flame time*, which is the moment when the flame begins to appear on the surface exposed to fire; (iv) *ember time*, which is when the embers begin to appear around the burning hole; (v) *end time* is the time when the test stops, when most of the surface of the sample has already been consumed by fire. Weight loss was also recorded during the curfew test, recording the weight before and after the test.

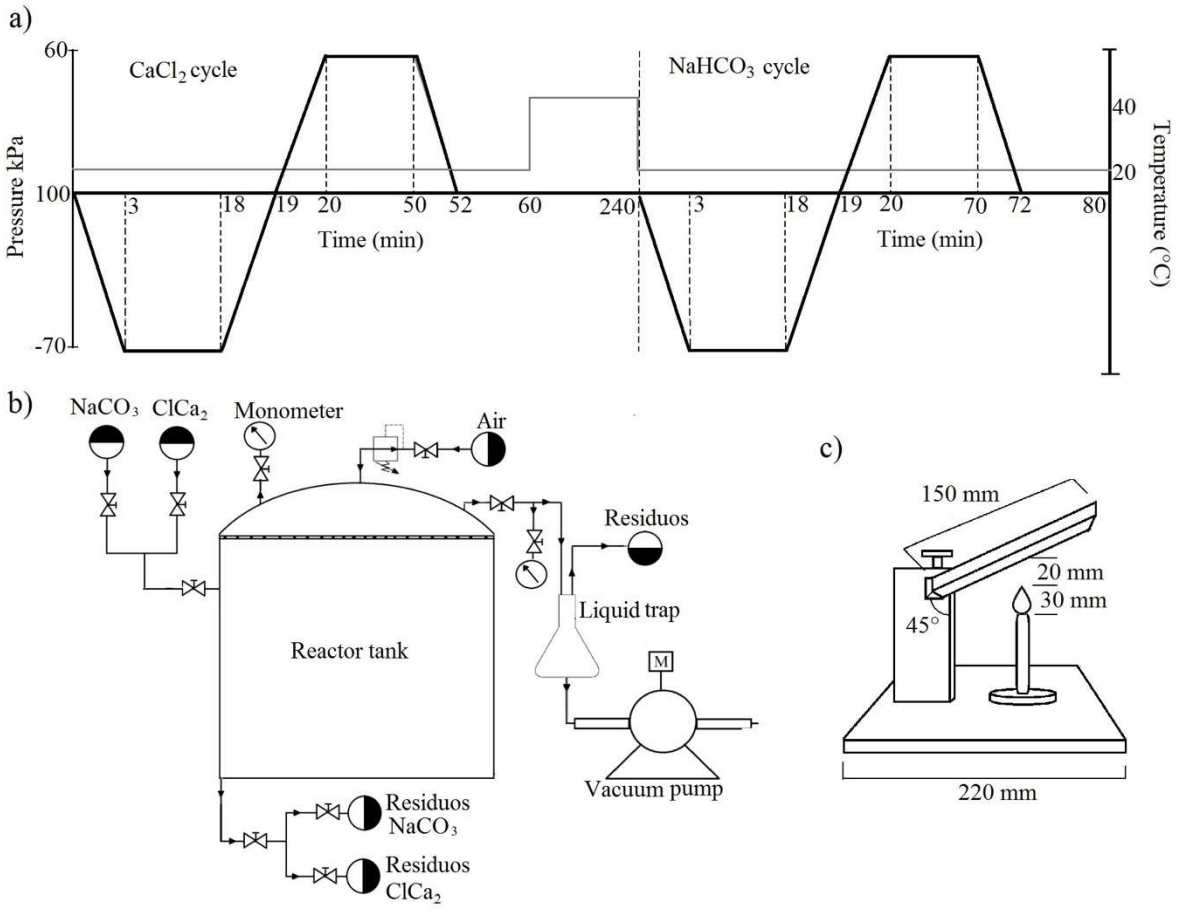

Fig 1. Pressure flow chart, temperature and time for in-situ mineralization (a); flow chart of equipment used for in-situ mineralization and (c) fire retardancy testing device especially designed for solid wood and wood composites. Source Taghiyari (Taghiyari 2012)

Durability

The methodology in ASTM D-2017-81 (ASTM 1995) was used to carry out the test of resistance to natural decay. In each treatment/species, 40 samples 2 cm wide x 2 cm long x 2 cm thick were prepared. Two types of fungi were used for this test, *Trametes versicolor* and *Lenzites acuta*, corresponding to white and brown rot, respectively. Twenty samples per species/treatment were subjected to degradation by each one of the fungi, for a period of 12 weeks.

Statistical analysis

The statistical analysis consisted primarily of checking the normality and homogeneity of the data and the elimination of "outliers". Then, the descriptive analysis consisted in determining the mean, standard deviation and coefficient of variation for each variable studied for each species and treatment. For each variable evaluated, an ANOVA analysis of variance was performed with a level of statistical significance of $p < 0.05$ to determine variability in response to the mineralization treatment. Tukey's test was used to determine the statistical significance of the differences between the means of the variables. This analysis was performed with the SAS 9.4 program (SAS Institute Inc., Cary, N.C.).

RESULTS

Absorption of the dissolutions of $CaCl_2$ and $NaCO_3$ in the different species varied from 42.2 to 168.0 l/m^3 and 69.5 to 214.6 l/m^3 (Table 1) respectively. The ANOVA for these two parameters showed that absorption of the $CaCl_2$ solution in-situ was higher in *Ec*, *Ha*, *Ss*, *Vf* and *Vg*, while lower absorptions were observed in *Co*, *Ga* and *Tg* (Table 1). Meanwhile, absorption of the $NaCO_3$ solution appears in greater quantities in *Ha*, *Ss* and *Vf*; and in lesser quantities in *Co*, *Ga* and *Tg* (Table 1). $CaCO_3$ retention in-situ varied from 2.8 to 9.2 kg/m^3 and was greater in *Ec*, *Ha*, *Ss*, *Vf* and *Vg*, and smaller in *Co, Ga* and *Tg,* with statistical differences between them (Table 1). Details of the formation and location of $CaCO_3$ crystals can be found in Gaitán-Alvarez *et al.* (2020). As for unreacted salts in the wood, surplus ions of Ca^{2+} and CO_3^{2+} could be observed within the same species, reaching up to 40% of the treated species (Table 1). Surplus of Ca^{2+} ions was observed in *Ca, Ec, Ss* and *Vg*, while in *Ca, Ga, Ha, Tg* and *Vf* the surplus ions were CO_3^{2+}. As for the amount of unreacted salt relative to volume, *Ec* presented the highest values with 3.8 and 6.0 g/m^3 of CO_3^{2-} and Ca^{2+} respectively, followed by *Vf* and *Vg*. The wood with less amounts of unreacted salts were *Co* and *Ca* wood (Table 1).

Table 1. Absorption of $CaCl_2$ and $NaCO_3$, and retention of $CaCO_3$ estimated in the in-situ mineralization process of nine woods from fast growth tropical species in Costa Rica

Wood	$CaCl_2$ absorption (l/m^3)	$NaCO_3$ absorption (l/m^3)	$CaCO_3$ amount in-situ (kg/m^3)	Unreacted Ca^{2+} (g/m^3)	Unreacted CO_3^{2-} (g/m^3)
Cedrela odorata (Co)	51.0 (13.4)^{A}	87.8 (14.1)^{A}	2.8 (0.7)^{A}	0.21 (131.76)	0.93 (43.11)
Cordia alliodora (Ca)	123.9 (42.1)^{B}	152.7 (43.4)^{B}	6.6 (2.3)^{B}	1.21 (106.66)	0.73 (85.19)
Enterolobium cyclocarpum (Ec)	167.9 (106.7)^{C}	175.4 (73.9)^{BC}	9.2 (5.8)^{C}	3.83 (146.14)	6.05 (128.94)
Gmelina arborea (Ga)	50.3 (3 .7)^{A}	69.5 (53.3)^{A}	2.4 (1.8)^{A}	1.72 (95.97)	1.60 (66.10)
Hieronyma alchornoides (Ha)	150.2 (56.9)^{BC}	195.1 (56.8)^{CDE}	8.2 (3.1)^{BC}	1.65 (75.15)	1.12 (85.08)
Samanea saman (Ss)	157.3 (25.4)^{BC}	208.1 (51.4)^{D}	8.6 (1.4)^{BC}	1.44 (74.21)	1.84 (40.16)
Tectona grandis (Tg)	42.2 (32.3)^{A}	72.3 (14.3)^{A}	2.6 (1.8)^{A}	2.47 (97.00)	1.05 (45.54)
Vochysia ferruginea (Vf)	158.1 (85.7)^{BC}	214.6 (67.8)^{D}	8.6 (4.7)^{BC}	3.15 (80.17)	3.66 (77.09)
Vochysia guatemalensis (Vg)	136.7 (30.7)^{BC}	177.2 (67.0)^{EB}	7.5 (1.7)^{BC}	1.61 (63.14)	2.21 (123.87)

Legend: the numbers in parentheses represent variation coefficients and different letters in each parameter represent significant statistical differences ($p<0.05$).

Thermogravimetric analysis

The TGA of the two different salts used for in-situ $CaCO_3$ formation showed that in the case of $CaCl_2$ used in the first cycle, decomposition occurred in two phases: the first phase with the highest peak at 149°C and the second phase with the highest peak at 200°C (Fig. 2a). Regarding $NaHCO_3$ decomposition occurred in one phase, the highest peak showing at 160°C (Fig. 2b). In $CaCO_3$ decomposition occurred in only one phase, with the maximum peak at 98°C (Fig. 2c).

In relation to $CaCO_3$/wood composites, thermal decomposition of the nine woods showed the same pattern of untreated wood in the TGA; however, the DTG curve showed differences in the $CaCO_3$/wood composites of the various species (Fig. 2a-l). The DTG curve presented three important decomposition stages: the first one appeared as a signal in the form of a slight curve after 200°C; the second stage showed at the highest peak of decompositions between 320°C and 360°C; and the third as a slight signal at the end after

380°C (Fig. 2d-l). All of the woods studied showed that the maximum decomposition peak of the $CaCO_3$/wood composites occurred before untreated/wood (Fig. 2d-l). The DTG curve also showed that in the woods with higher $CaCO_3$ formation (*Ec, Ss, Vf* and *Vg*) the signal at 200°C was more pronounced than the signal of untreated/wood at 200°C (Fig. 2f, i, k and l). Meanwhile, in the species with average retention (15.2 to 17.4 kg/m^3), such as *Ca* and *Ha* wood, the pronunciation of the curve at 200°C was slight, almost similar to untreated/wood (Fig. 2c and 2h). $CaCO_3$/wood composites of *Co*, *Ga* and *Tg* wood which presented the smallest values of $CaCO_3$ retention, follow the same behaviour of untreated/wood (Fig. 2e, 2g and 2j).

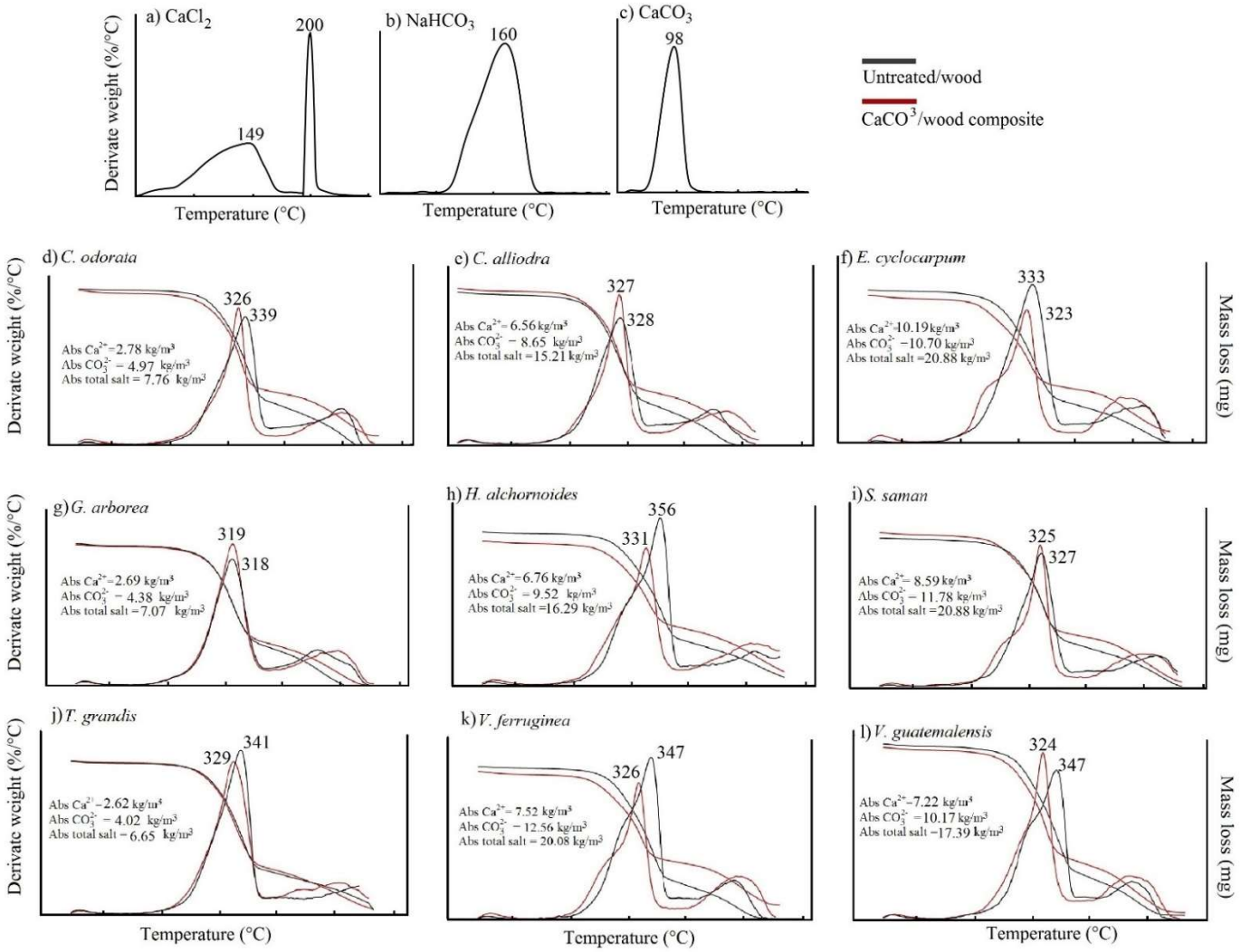

Fig 2. TGA and DTG analysis of $CaCO_3$/wood composites and untreated/wood of nine fast growth tropical species in Costa Rica

Fire resistance

In relation to flame time, $CaCO_3$/wood composites of *Ca, Ec, Ha* and *Vg* needed more time than untreated/wood of the same species (Table 2). The remaining species (*Ca, Ga, Sa*, *Tg* and *Vf*) showed no statistical differences between $CaCO_3$/wood composites and untreated/wood (Table 2). Ember time varied again between species, being statistically higher in $CaCO_3$/wood composites of *Co, Ec, Ha* and *Ss* in relation to untreated/wood. In $CaCO_3$/wood composites of *Ha* and *Tg* ember time was shorter than in untreated/wood. No statistical differences appeared in the remaining species (*Ca*, *Ga*, *Vf* and *Vg*) (Table 2). Dark time and hole time were not statistically affected between $CaCO_3$/wood composites and untreated/wood of *Ca, Ec, Ga, Ha, Vf* and *Vf.* Dark time increased statistically in $CaCO_3$/wood composites of *Ca* and *Ss*, but diminished statistically in $CaCO_3$/wood composites of *Tg* (Table 2). Lastly, the total testing time varied with the type of wood (Fig. 8b). In *Ca*, *Ga*, *Vf* and *Vg* woods it showed no statistical differences between $CaCO_3$/wood composites and untreated/wood (Fig. 3b). The end time in $CaCO_3$/wood composites of *Co, Ec* and *Ss* was statistically higher than in untreated/wood. On the other hand, in $CaCO_3$/wood composites of *Ha* and *Tg*, the end time was statistically lower than in untreated/wood (Fig. 3b). The evaluation of the weight loss at the end of the flame test demonstrated that all the mineralized woods showed less weight loss relative to untreated/wood; however, in $CaCO_3$/wood composites of *Ss* wood the weight loss was statistically higher than in $CaCO_3$/wood composites (Fig. 3b).

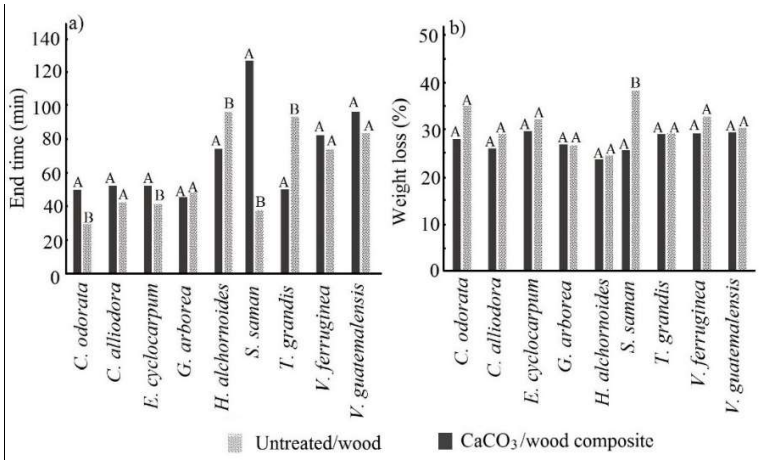

Fig 3. End time (a) and weight loss (b) in the fire retardant test of $CaCO_3$/wood composites and untreated/wood of nine fast growth tropical species in Costa Rica

Legend: different letters in each parameter represent significant statistical differences ($p<0.05$).

Table 2. Different times in the fire retardant test of $CaCO_3$/wood composites and untreated/wood of nine fast growth tropical species in Costa Rica

Species	Treatment	Flame time (min)	Ember time (min)	Dark time (min)	Hole time (min)
Cedrela odorata (Co)	$CaCO_3$/wood composite	0.8 (48.1)^A	2.3 (37.6)^A	23.0 (27.6)^A	29.9 (59.7)^A
	Untreated/wood	0.4 (11.6)^A	1.1 (11.5)^B	12.7 (21.0)^B	24.1 (9.6)^B
Cordia alliodora (Ca)	$CaCO_3$/wood composite	0.9 (26.4)^A	2.0 (31.9)^A	23.8 (10.9)^A	36.0 (8.8)^A
	Untreated/wood	0.5 (57.1)^B	1.5 (23.9)^A	23.5 (21.1)^A	33.2 (29.2)^A
Enterolobium cyclocarpum (Ec)	$CaCO_3$/wood composite	1.4 (31.4)^A	5.5 (56.3)^A	26.7 (19.1)^A	37.4 (10.8)^A
	Untreated/wood	0.6 (47.6)^B	2.8 (34.1)^B	23.1 (8.3)^A	32.3 (7.8)^B
Gmelina arborea (Ga)	$CaCO_3$/wood composite	0.6 (62.2)^A	1.9 (22.4)^A	24.7 (24.1)^A	37.6 (16.9)^A
	Untreated/wood	0.8 (44.2)^A	2.6 (25.7)^A	21.7 (30.4)^A	36.4 (28.4)^A
Hieronyma alchornoides (Ha)	$CaCO_3$/wood composite	1.9 (23.3)^A	3.2 (4.7)^A	20.2 (11.7)^A	53.9 (6.7)^A
	Untreated/wood	1.2 (11.0)^B	5.4 (17.7)^B	18.8 (11.1)^A	83.4 (19.5)^B
Samanea saman (Ss)	$CaCO_3$/wood composite	2.8 (14.0)^A	7.8 (27.0)^A	45.3 (11.5)^A	60.2 (5.5)^A
	Untreated/wood	2.2 (20.6)^A	4.7 (32.3)^B	12.2 (6.6)^B	28.4 (22.3)^B
Tectona grandis (Tg)	$CaCO_3$/wood composite	1.1 (18.4)^A	2.8 (18.4)^A	25.2 (13.9)^A	40.1 (13.5)^A
	Untreated/wood	1.3 (7.4)^A	6.2 (6.0)^B	57.2 (19.6)^B	79.7 (28.5)^B
Vochysia ferruginea (Vf)	$CaCO_3$/wood composite	0.7 (47.0)^A	2.6 (35.5)^A	34.8 (12.7)^A	49.3 (23.8)^A
	Untreated/wood	0.7 (43.1)^A	1.8 (31.7)^A	34.3 (5.2)^A	63.5 (29.6)^A
Vochysia guatemalensis (Vg)	$CaCO_3$/wood composite	0.9 (24.4)^A	1.9 (18.6)^A	35.2 (13.2)^A	86.1 (37.5)^A
	Untreated/wood	0.4 (36.7)^B	1.7 (27.0)^A	30.9 (2.7)^A	58.1 (33.3)^A

Legend: the numbers in parentheses represent variation coefficients and different letters in each parameter represent significant statistical differences ($p<0.05$)

Physical properties

Table 3 shows the values of the physical properties of $CaCO_3$/wood composites and untreated/wood. As regards to density, $CaCO_3$/wood composite of *Ca* was the only one to present a statistical difference higher than in untreated/wood. MC in $CaCO_3$/wood composites of *Ec, Ss*, *Vf* and *Vg* was statistically higher than untreated/wood, while the remaining woods showed no statistical differences. Moisture absorption was from 12% to 18% in all woods. The percentage of absorption was statistically higher in $CaCO_3$/wood composites than in untreated/wood (Table 3). As for water absorption by immersion, in all

the species studied except *Vg*, $CaCO_3$/wood composite presented a statistically higher percentage of absorbed water than in untreated wood (Fig. 4). Width swelling was statistically lower only in untreated/wood of *Ha* than in untreated/wood. Meanwhile, $CaCO_3$/wood composites of *Ec* and *Ga* presented higher thickness swelling than untreated/wood (Table 3).

Table 3. Some physical properties evaluated of $CaCO_3$/wood composites and untreated/wood of nine fast growth tropical species in Costa Rica

Species	Treatment	Density (g/cm^3)	Moisture content (%)	Moisture absorption (%)	Wide swelling (mm)	Thickness swelling (mm)
Cedrela odorata (Co)	$CaCO_3$/wood composite	257.3 (8.0)^A	12.8 (40.5)^A	4.2 (10.7)^A	0.5 (17.3)^A	0.6 (63.4)^A
	Untreated/wood	266.4 (8.1)^A	10.9 (58.3)^A	1.5 (9.9)^B	0.4 (114.3)^A	0.3 (1.8)^A
Cordia allidora (Ca)	$CaCO_3$/wood composite	387.26 (6.7)^A	11.8 (13.4)^A	4.6 (24.0)^A	0.8 (33.1)^A	0.7 (118.4)^A
	Untreated/wood	341.2 (11.4)^B	10.9 (7.5)^A	2.7 (8.3)^B	0.8 (73.1)^A	1.2 (83.3)^A
Enterolobium cyclocarpum (Ec)	$CaCO_3$/wood composite	397.9 (15.9)^A	12.6 (13.8)^A	8.2 (30.4)^A	1.6 (74.8)^A	0.4 (126.6)^A
	Untreated/wood	395.5 (10.3)^A	11.2 (11.4)^B	4.2 (19.4)^B	1.6 (57.9)^A	0.9 (93.4)^B
Gmelina arborea (Ga)	$CaCO_3$/wood composite	400.9 (10.1)^A	12.0 (14.9)^A	2.6 (44.6)^A	0.5 (66.0)^A	0.3 (100.6)^A
	Untreated/wood	418.9 (9.3)^A	13.5 (7.6)^A	1.6 (41.8)^B	0.3 (142.3)^A	0.6 (57.9)^B
Hieronyma alchornoides (Ha)	$CaCO_3$/wood composite	541.8 (9.5)^A	11.4 (34.9)^A	3.5 (12.9)^A	0.4 (104.8)^A	0.8 (72.8)^A
	Untreated/wood	518.9 (5.1)^A	12.7 (4.3)^A	2.2 (15.0)^B	0.7 (51.6)^B	1.3 (83.4)^A
Samanea saman (ss)	$CaCO_3$/wood composite	535.2 (4.7)^A	11.5 (8.1)^A	6.7 (30.4)^A	1.6 (71.8)^A	0.6 (75.8)^A
	Untreated/wood	521.6 (5.1)^A	10.8 (4.1)^B	3.9 (19.4)^B	2.1 (43.1)^A	0.8 (81.4)^A
Tectona grandis (Tg)	$CaCO_3$/wood composite	544.8 (10.5)^A	11.9 (16.6)^A	5.2 (23.4)^A	2.5 (117.8)^A	0.9 (90.3)^A
	Untreated/wood	541.9 (9.7)^A	11.8 (11.6)^A	4.4 (6.2)^B	2.2 (45.4)^A	1.5 (73.9)^A
Vochysia ferruginea (Vf)	$CaCO_3$/wood composite	321.9 (7.0)^A	11.9 (7.0)^A	6.6 (32.5)^A	1.1 (66.6)^A	0.5 (112.7)^A
	Untreated/wood	317.8 (9.7)^A	9.2 (35.9)^B	3.0 (9.6)^B	0.8 (77.4)^A	0.8 (49.7)^A
Vochysia guatemalensis (Vg)	$CaCO_3$/wood composite	297.7 (7.4)^A	11.2 (10.7)^A	8.5 (11.9)^A	3.9 (112.9)^A	0.9 (93.9)^A
	Untreated/wood	304.9 (6.0)^A	9.7 (8.0)^B	4.8 (7.7)^B	3.4 (40.2)^A	1.2 (77.5)^A

Legend: the numbers in parentheses represent variation coefficients and different letters in each parameter represent significant statistical differences ($p<0.05$).

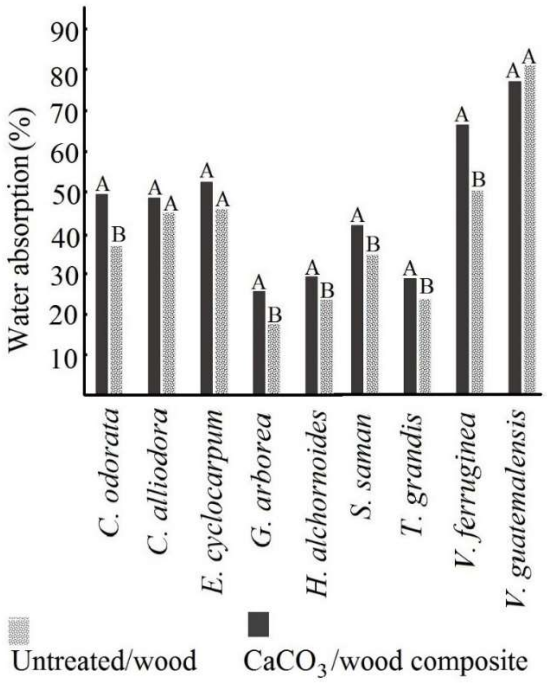

Fig 4. Water absorption by immersion of $CaCO_3$/wood composites and untreated/wood of nine fast growth tropical species in Costa Rica

Legend: different letters in each parameter represent significant statistical differences ($p<0.05$)

Mechanical properties

The mechanical properties of $CaCO_3$/wood composites and untreated/wood presented few significant differences, except for mineralized wood of *Ca* regarding flexural MOR and MOE and compression MOR, which were statistically higher than in untreated/wood (Table 4); and $CaCO_3$/wood composites of *Ss*, in which flexural MOR and MOE diminished statistically (Table 4).

Table 4. Mechanical properties of $CaCO_3$/wood composites and untreated/wood of nine fast growth tropical species in Costa Rica

Species	Treatment	Flexion test		Compression test	
		MOR (MPa)	MOE (Gpa)	MOR (Mpa)	MOE (Gpa)
Cedrela odorata (Co)	$CaCO_3$/wood composite	35.9 (9.9)^A	5.4 (15.6)^A	29.9 (25.3)^A	0.9 (20.0)^A
	Untreated/wood	34.9 (11.1)^A	5.6 (13.9)^A	31.9 (16.5)^A	0.9 (27.1)^A
Cordia alliodora (Ca)	$CaCO_3$/wood composite	58.2 (10.8)^A	8.4 (9.5)^A	40.0 (11.1)^A	0.9 (24.2)^A
	Untreated/wood	47.3 (20.9)^B	6.6 (24.9)^B	29.7 (28.4)^B	0.7 (51.4)^A
Enterolobium cyclocarpum (Ec)	$CaCO_3$/wood composite	37.1 (38.7)^A	4.1 (30.3)^A	14.3 (44.3)^A	21.9 (91.7)^A
	Untreated/wood	38.3 (23.9)^A	4.6 (26.6)^A	16.2 (26.4)^A	13.6 (72.4)^A
Gmelina arborea (Ga)	$CaCO_3$/wood composite	58.8 (16.1)^A	8.3 (22.9)^A	43.6 (13.3)^A	1.9 (20.7)^A
	Untreated/wood	58.3 (18.4)^A	9.0 (18.6)^A	36.5 (29.2)^B	1.6 (30.4)^A
Hieronyma alchornoides (Ha)	$CaCO_3$/wood composite	72.4 (17.0)^A	9.6 (23.9)^A	38.1 (16.7)^A	1.8 (57.4)^A
	Untreated/wood	75.6 (14.0)^A	10.3 (18.6)^A	35.4 (16.6)^A	1.4 (29.4)^A
Samanea saman (Ss)	$CaCO_3$/wood composite	60.9 (15.4)^A	6.4 (12.0)^A	23.8 (31.3)^A	21.9 (91.7)^A
	Untreated/wood	68.4 (10.9)^B	7.3 (11.5)^B	27.6 (21.3)^A	13.6 (72.4)^A
Tectona grandis (Tg)	$CaCO_3$/wood composite	82.2 (8.8)^A	10.2 (15.0)^A	29.2 (31.5)^A	36.8 (69.0)^A
	Untreated/wood	79.5 (14.3)^A	9.5 (21.0)^A	29.4 (20.5)^A	30.0 (82.6)^A
Vochysia ferruginea (Vf)	$CaCO_3$/wood composite	34.8 (13.2)^A	5.7 (16.0)^A	31.6 (12.5)^A	0.9 (36.5)^A
	Untreated/wood	35.9 (13.3)^A	5.8 (12.5)^A	29.6 (34.4)^A	0.9 (38.0)^A
Vochysia guatemalensis (Vg)	$CaCO_3$/wood composite	31.2 (14.2)^A	4.7 (16.7)^A	14.9 (12.3)^A	6.8 (63.6)^A
	Untreated/wood	34.0 (14.9)^B	4.9 (16.2)^A	16.9 (18.9)^B	7.2 (41.1)^A

Legend: the numbers in parentheses represent variation coefficients and different letters in each parameter represent significant statistical differences ($p<0.05$)

Decay durability

As for resistance to brown fungus (*L. acuta*) decay, the weight loss percentage was statistically higher in $CaCO_3$/wood composites of *Ca* and *Ec* than in untreated/wood, while $CaCO_3$/wood composites of *Ha* presented less weight loss than untreated/wood (Fig. 5a). As for weight loss due to decomposition caused by *T. versicolor*, no differences appeared between $CaCO_3$/wood composites and untreated/wood of *Co*, *Ga*, *Ha*, *Tg*, *Vf* and *Vg*, while $CaCO_3$/wood composites of *Ca*, *Ec* and *Ss*, presented weight loss statistically higher than in untreated/wood (Fig. 5b).

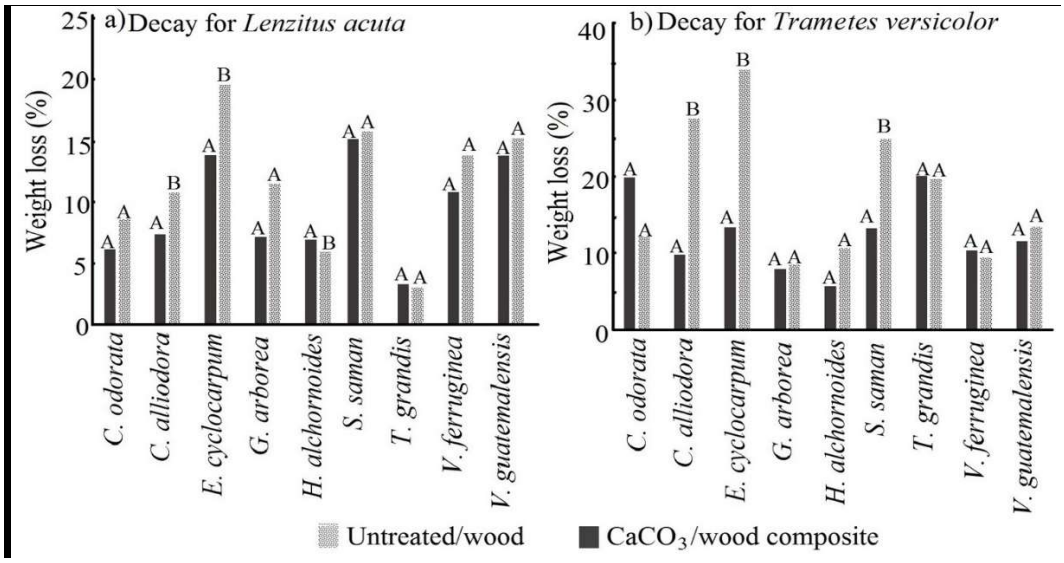

Fig 5. Weight loss due to natural decay to *Lenzitus acuta* (a) and *Trametes versicolor* (b) of $CaCO_3$/wood composites and untreated/wood of nine fast growth tropical species in Costa Rica

Legend: different letters in each parameter represent significant statistical differences ($p<0.05$)

DISCUSSION

The TGA showed that, except for *Co* and *Ss*, at the beginning $CaCO_3$/wood composites of the species lost weight faster than untreated/wood; however, after 350°C the opposite behaviour occurred: untreated/wood lost weight faster (Fig. 6 d-l). This effect is more pronounced in $CaCO_3$/wood composites above 16.29 kg/m^3 (*Ec, Ha, Ss, Vf* and *Vg*) (Fig. 2f, 2h, 2i, 2k and 2l). These results agree with those obtained by Tsioptsias and Pnayiotou (Tsioptsias and Panayiotou 2011), who found the same behaviour in $CaCO_3$/wood composites of *Picea abies*. Fast initial degradation of $CaCO_3$/wood composites was due to early endothermal degradation of $CaCO_3$, water and CO_2 (Dash et al. 2000), where most degradation occurred before reaching 100°C (Fig. 2c). However, at higher temperatures (>350°C), $CaCO_3$/wood composites turned more stable to combustion due to aragonite transforming into calcite at 387°C(Gallagher 2003), which decomposed into CaO and CO_2 at temperatures above 850°C (Singh and Singh 2007).

Although adequate absorptions were achieved to have the amount of ions (Ca^{2+} or CO_3^{2+}) sufficient for $CaCO_3$formation, the stoichiometry is not suitable for the formation of this salt

(Table 1). Salt formation, is a complex mechanism that includes the polymorphism exhibited by crystals of calcium carbonate, calcium oxalate and different polymorphs of the same compound that can transform each other. Crystal formation also influences the environmental temperature, concentration, pH, viscosity, additives and so on (Zeng *et al.* 2018), which are conditions difficult to control in processes and equipment used in commercial preservation intended for application in wood mineralization.

The fire resistance analysis confirmed the previous results. $CaCO_3$/wood composites of species showing greater in-situ $CaCO_3$ formation, like *Ec, Ss, Vf* and *Vg* (Table 1), resisted fire better (Fig. 3; Table 2). These results agree with those obtained by Merk *et al.,* (Merk *et al.* 2015, 2016) and Tsioptsias and Panayiotou (Tsioptsias and Panayiotou 2011) in $CaCO_3$/wood composites of beech and spruce. Merk *et al*.(Merk et al. 2015) explained that impregnating the wood with $CaCO_3$ affects the thermal decomposition of the cellulose by reducing formation of volatiles. Similarly, Yao et al. (Yao *et al.* 2008) indicated that minerals embedded in the tissues dilute the amount of fuel material and constitute a barrier to heat transmission and weight transport during pyrolysis. However, other authors (Hull *et al.* 2011; Walters and Lyon 2003) indicated that $CaCO_3$ limits the supply of oxygen and volatile material. Therefore, incrementing the quantity of embedded $CaCO_3$ crystals in *Ec, Ss, Vf* and *Vg* reduces the flammability of the mineralized material and increases its thermal stability and fire resistance (Fig. 2; Table 2).

Regarding the physical properties, the results showed that the mineralization process did not affect the density and the MC of wood (Table 2). Lack of differences between $CaCO_3$/wood composites and untreated/wood was explained by the fact that the quantity of in-situ formed $CaCO_3$ (Table 1), between 2.8 and 9.2 kg/m^3, was slightly significant for the values of wood density before the process of mineralization, which varied between 266 and 550 kg/m^3. Likewise, similarities between treated and untreated wood suggested that the structural components (or other types) of the wood (cellulose, hemicellulose and lignin) were not significantly affected by the chemical substances (water and ethanol) used in the in-situ mineralization process.

If statistically affected, the MC diminished. This is so because the $CaCO_3$ crystals are adhered to the cell wall, creating bonds with hydroxyl groups of the wall (Butylina *et al*. 2012;

Merk *et al.* 2016) and preventing association of these groups with water molecules present in the environment or making water molecules associate with more hydroxyl groups in the outer side of the wood, so that cell wall swelling would diminish (Stark and Gardner 2008). The obstacle posed by the affinity of the $CaCO_3$/wood composites produces reduction of the wood's equilibrium moisture content when exposed to temperature and relative humidity close to 12%, which the samples were conditioned to, after in-situ $CaCO_3$ formation.

A remarkable aspect of the results of physical properties of $CaCO_3$/wood composites of tropical woods in fast growing plantations was the increase in moisture absorption, from 12% to 18%, and water absorption after immersing 24 hours in water (Table 2 and Fig. 4), which contradicts the studies carried out by Merk *et al.* (Merk *et al.* 2015, 2016). This contradiction may be explained by lack of efficiency of the method of in-situ $CaCO_3$ formation in wood samples in which permeability plays an important role; or, CaCO3 crystal formation in specific sites (vessel lumina, rays and axial parenchyma) of the hierarchical structure of the wood (Gaitán-Álvarez *et al.,* 2020). As we found in this study, in the process of mineralization there was a percentage of NaCl or small quantities of unreacted Ca^{2+}, $CO3^{2-}$ (Gaitán-Álvarez *et al.,* 2020) that probably remained deposited in the wood (Merk et al. 2016). These salts are highly water soluble (Harvie *et al.* 1984), enabling $CaCO_3$/wood composites to absorb more water, as occurred with composites of several species (Table 1). In fact, $CaCO_3$/wood composites of the species with higher percentage of unreacted salts (*Ec, Ss, Vf* and *Vg*) presented the highest percentage of moisture absorption in the samples impregnated (Fig. 6). These results suggest that salts, instead of the wood structure, retained the absorbed water and that the process of formation in-situ should be improved for bigger wood samples.

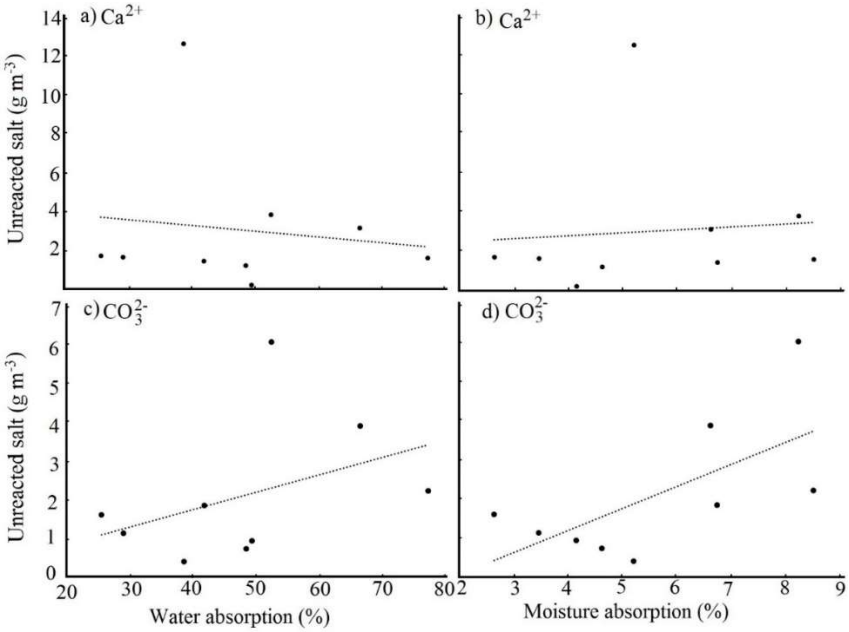

Fig 6. Correlation between unreacted salts and water absorption (a, c), and moisture absorption (b, d).

The scarce difference in swelling (wide and thickness) between treated and untreated wood suggests that high water absorption in $CaCO_3$/wood composites was associated to $CaCl_2$ and $NaCO_3$ salts that did not react to form $CaCO_3$. Although high moisture absorption (Table 2) was observed, few species presented statistical difference in swelling, or remained the same in both the impregnated and untreated samples (Table 2). This situation could be explained by the fact that calcium carbonate crystals adhered to the cell wall create bonds with hydroxyl groups of the wall (Butylina *et al.* 2012), hindering association with moisture.

It has been affirmed that adding mineral to the structure of cellulose, such as $CaCO_3$, improves the mechanical properties of flexion, compression and tension of materials (Hadal *et al.* 2004; Huuhilo *et al.* 2010) or wood-plastic composites (Cheng *et al.* 2015; Leong *et al.* 2004; Sun *et al.* 2006). However, this study disagrees with that affirmation since the results showed there were few changes in the mechanical properties (Table 3). This lack of agreement of the results of this study with those of other studies shows that the effects of $CaCO_3$ formation on mechanical properties of solid wood are scarcely known and that formation of this mineral in wood composites will have little effect on the wood properties (Table 3).

Although addition of $CaCO_3$ to increase wood durability is used(Steenkjær Hastrup *et al*. 2006), the effect of this salt ($CaCO_{3)}$ on decay resistance in tropical species was not regular for all wood species tested nor for the type of fungus used. For *L. acuata*, $CaCO_3$/wood composites showed greater weight loss in *Ca* and *Ec* woods than in untreated/wood, while with *T. versicolor* the weight loss was also greater in $CaCO_3$/wood composites of *Ca*, *Ec* and *Ss* (Fig. 5). As these results are not acceptably efficient, the performance of the application of mineralization as an alternative to wood decay should be evaluated.

CONCLUSIONS

1. According to the results, the deposit of $CaCO_3$ crystals in the cell structure of hardwoods influences differently the wood properties in the different species tested, probably because of irregularity of the deposit. In-situ $CaCO_3$ mineralization increases water absorption, but increments the dimensional stability, having little effects on the mechanical properties and decay resistance of some wood species; however, the major advantage of this treatment is that $CaCO_3$/wood composites increased fire resistance, as it creates a barrier that hinders the exchange of oxygen and volatile material with the outer environment.
2. Mineralization can be carried out in tropical hardwood species, but each species will show a different behaviour, so the effects on each species must be studied. Despite this, mineralization is a promising treatment to solve the problem of dimensional stability and fire resistance of forest plantation woods.

ACKNOWLEDGMENTS

The authors wish to thank the Vicerrectoría de Investigación y Extensión at the Instituto Tecnológico de Costa Rica (ITCR) for the project financing.

REFERENCES CITED

Anbu, P., Kang, C.-H., Shin, Y.-J., and So, J.S. (2016). “Formations of calcium carbonate minerals by bacteria and its multiple applications,” *SpringerPlus* 5(1), 250. DOI: 10.1186/s40064-016-1869-2

ASTM. (1985). “Standard test method for anti-swelling effectiveness of water-repellent formulations and differential swelling of untreated wood when exposed to liquid water environments,” *Annual book of ASTM standards. Section 4, Construction. Volume*

04.09, Wood, 702–706. DOI: 10.1520/D4446-08R12.when

ASTM. (1995). “Standard Method of Accelerated Laboratory Test of Natural Decay Resistance of,” 81(Reapproved 1994), 1–5.

ASTM. (1999). “Standard Guide for Moisture Conditioning of Wood and Wood-Based Materials 1,” *Current*, i(Reapproved), 1–8. DOI: 10.1520/D4933-99R10.2

ASTM. (2016a). “Standard Test Methods for Direct Moisture Content Measurement of Wood and Wood-Based Materials,” *Annual Book of ASTM Standards. Volume 4.10 (Woods)*, (A. S. F. T. Materials, ed.), American Society For Testing and Materials. DOI: 10.1520/D4442-16

ASTM. (2016b). “Standard Methods of Testing Small Clear Specimens of Timber,” *Annual Book of ASTM Standards. Volume 4.10 (Woods)*, (A. S. F. T. Materials, ed.), American Society For Testing and Materials.

Barhoum, A., Rahier, H., Abou-Zaied, R. E., Rehan, M., Dufour, T., Hill, G., and Dufresne, A. (2014). “Effect of Cationic and Anionic Surfactants on the Application of Calcium Carbonate Nanoparticles in Paper Coating,” *ACS Applied Materials & Interfaces* 6(4), 2734–2744. DOI: 10.1021/am405278j

Benzerara, K., Miot, J., Morin, G., Ona-Nguema, G., Skouri-Panet, F., and Férard, C. (2011). “Significance, mechanisms and environmental implications of microbial biomineralization,” *Comptes Rendus Geoscience* 343(2–3), 160–167. DOI: 10.1016/j.crte.2010.09.002

Burgert, I., Keplinger, T., Cabane, E., Merk, V., and Rüggeberg, M. (2016). “Biomaterial Wood: Wood-Based and Bioinspired Materials,” in: *Secondary Xylem Biology*, 259–281. DOI: 10.1016/B978-0-12-802185-9.00013-9

Butylina, S., Hyvärinen, M., and Kärki, T. (2012). “Accelerated weathering of wood–polypropylene composites containing minerals,” *Composites Part A: Applied Science and Manufacturing* 43(11), 2087–2094. DOI: 10.1016/j.compositesa.2012.07.003

Cheng, H., Gao, J., Wang, G., Shi, S. Q., Zhang, S., and Cai, L. (2015). “Enhancement of mechanical properties of composites made of calcium carbonate modified bamboo fibers and polypropylene,” *Holzforschung* 69(2), 215–221. DOI: 10.1515/hf-2014-0020

Dash, S., Kamruddin, M., Ajikumar, P., Tyagi, A., and Raj, B. (2000). “Nanocrystalline and metastable phase formation in vacuum thermal decomposition of calcium carbonate,” *Thermochimica Acta* 363(1–2), 129–135. DOI: 10.1016/S0040-6031(00)00604-3

Declet, A., Reyes, E., and Suárez, O. M. (2016). “Calcium carbonate precipitation: A review of the carbonate crystallization process and applications in bioinspired composites,” *Reviews on Advanced Materials Science* 44(1), 87-107.

Dhami, N. K., Reddy, M. S., and Mukherjee, A. (2013). “Biomineralization of calcium carbonates and their engineered applications: a review,” *Frontiers in Microbiology* 4, 314. DOI: 10.3389/fmicb.2013.00314

Dhami, N. K., Reddy, M. S., and Mukherjee, A. (2014). “Synergistic Role of Bacterial Urease and Carbonic Anhydrase in Carbonate Mineralization,” *Applied Biochemistry and Biotechnology* 172(5), 2552–2561. DOI: 10.1007/s12010-013-0694-0

Gadd, G. M. (2010). “Metals, minerals and microbes: geomicrobiology and bioremediation,” *Microbiology* 156(3), 609–643. DOI: 10.1099/mic.0.037143-0

Gadd, G. M., Bahri-Esfahani, J., Li, Q., Rhee, Y. J., Wei, Z., Fomina, M., and Liang, X. (2014). “Oxalate production by fungi: significance in geomycology, biodeterioration and bioremediation,” *Fungal Biology Reviews* 28(2–3), 36–55. DOI: 10.1016/j.fbr.2014.05.001

Gadd, G. M., Rhee, Y. J., Stephenson, K., and Wei, Z. (2012). “Geomycology: metals, actinides and biominerals,” *Environmental Microbiology Reports* 4(3), 270–296. DOI: 10.1111/j.1758-2229.2011.00283.x

Gaitán- Alvarez, J., Moya, R., Berrocal, A., Araya, F. (2020). "In-situ mineralization of calcium carbonate of tropical hardwood species from fast-grown plantations in Costa Rica". Carbonates and calcites. (submmited) 2020.

Gallagher, P. K. (2003). “Handbook of thermal analysis and calorimetry: vol 2- applications to inorganic and miscellaneous materials miscellaneous materials,” *Elsevier*, 2(1), 905. DOI: 10.1007/s13398-014-0173-7.2

Ganendra, G., De Muynck, W., Ho, A., Arvaniti, E. C., Hosseinkhani, B., Ramos, J. A., Rahier, H., and Boon, N. (2014). “Formate Oxidation-Driven Calcium Carbonate Precipitation by Methylocystis parvus OBBP,” *Applied and Environmental Microbiology* 80(15), 4659–4667. DOI: 10.1128/AEM.01349-14

Hadal, R., Dasari, A., Rohrmann, J., and Misra, R. D. (2004). “Effect of wollastonite and talc on the micromechanisms of tensile deformation in polypropylene composites,” *Materials Science and Engineering* 372(1–2), 296–315. DOI: 10.1016/j.msea.2004.01.003

Harvie, C. E., Møller, N., and Weare, J. H. (1984). “The prediction of mineral solubilities in natural waters: The Na-K-Mg-Ca-H-Cl-SO4-OH-HCO3-CO3-CO2-H2O system to high ionic strengths at 25°C,” *Geochimica et Cosmochimica Acta* 48(4), 723–751. DOI: 10.1016/0016-7037(84)90098-X

Hong, K.S., Lee, H. M., Bae, J. S., Ha, M. G., Jin, J. S., Hong, T. E., Kim, J. P., and Jeong, E. D. (2011). “Removal of Heavy Metal Ions by using Calcium Carbonate Extracted from Starfish Treated by Protease and Amylase,” *Journal of Analytical Science and Technology* 2(2), 75–82. DOI: 10.5355/JAST.2011.75

Hoque, M. E. (2013). “Processing and Characterization of Cockle Shell Calcium Carbonate ($CaCO_3$) Bioceramic for Potential Application in Bone Tissue Engineering,” *Journal of Material Science & Engineering* 02(04), 4. DOI: 10.4172/2169-0022.1000132

Hübert, T., Unger, B., and Bücker, M. (2010). “Sol–gel derived TiO2 wood composites,”

Journal of Sol-Gel Science and Technology 53(2), 384–389. DOI: 10.1007/s10971-009-2107-y

Hull, T. R., Witkowski, A., and Hollingbery, L. (2011). "Fire retardant action of mineral fillers," *Polymer Degradation and Stability* 96(8), 1462–1469. DOI: 10.1016/j.polymdegradstab.2011.05.006

Huuhilo, T., Martikka, O., Butylina, S., and Kärki, T. (2010). "Mineral fillers for wood–plastic composites," *Wood Material Science & Engineering* 5(1), 34–40. DOI: 10.1080/17480270903582189

Klaithong, S., Opdenbosch, D. Van, Zollfrank, C., and Plank, J. (2013). "Preparation of CaCO3 and CaO Replicas Retaining the Hierarchical Structure of SpruceWood," *Zeitschrift für Naturforschung* 68(5–6), 533–538. DOI: 10.5560/znb.2013-3062

Krajewska, B. (2018). "Urease-aided calcium carbonate mineralization for engineering applications: A review," *Journal of Advanced Research* 13, 59–67. DOI: 10.1016/j.jare.2017.10.009

Kumari, D., Qian, X.-Y., Pan, X., Achal, V., Li, Q., and Gadd, G. M. (2016). "Microbially-induced Carbonate Precipitation for Immobilization of Toxic Metals," in: *Advances in Applied Microbiology*, 79–108. DOI: 10.1016/bs.aambs.2015.12.002

Leong, Y. W., Abu Bakar, M. B., Ishak, Z. A. M., Ariffin, A., and Pukanszky, B. (2004). "Comparison of the mechanical properties and interfacial interactions between talc, kaolin, and calcium carbonate filled polypropylene composites," *Journal of Applied Polymer Science* 91(5), 3315–3326. DOI: 10.1002/app.13542

Li, Q., Csetenyi, L., and Gadd, G. M. (2014). "Biomineralization of Metal Carbonates by Neurospora crassa," *Environmental Science & Technology* 48(24), 14409–14416. DOI: 10.1021/es5042546

Li, Q., Csetenyi, L., Paton, G. I., and Gadd, G. M. (2015). "CaCO 3 and SrCO 3 bioprecipitation by fungi isolated from calcareous soil," *Environmental Microbiology* 17(8), 3082–3097. DOI: 10.1111/1462-2920.12954

Liu, C. L. C., Kuchma, O., and Krutovsky, K. V. (2018). "Mixed-species versus monocultures in plantation forestry: Development, benefits, ecosystem services and perspectives for the future," *Global Ecology and Conservation* 15, 419. DOI: 10.1016/j.gecco.2018.e00419

Mantanis, G. I. (2017). "Wood chemical modification," *BioResources* 12(2), 4478–4489.

Merk, V., Chanana, M., Gaan, S., and Burgert, I. (2016). "Mineralization of wood by calcium carbonate insertion for improved flame retardancy," *Holzforschung* 70(9), 867–876. DOI: 10.1515/hf-2015-0228

Merk, V., Chanana, M., Keplinger, T., Gaan, S., and Burgert, I. (2015). "Hybrid wood materials with improved fire retardance by bio-inspired mineralisation on the nano- and submicron level," *Green Chemistry* 17(3), 1423–1428. DOI: 10.1039/C4GC01862A

Moya, R., Salas, C., Berrocal, A., and Valverde, J. C. (2015). “Evaluation of chemical compositions, air-dry, preservation and workability of eight fastgrowing plantation species in Costa Rica,” *Madera Bosques*, 21, 31-47.

Mukkamala, S. B., Anson, C. E., and Powell, A. K. (2006). “Modelling calcium carbonate biomineralisation processes,” *Journal of Inorganic Biochemistry*100(5–6), 1128–1138. DOI: 10.1016/j.jinorgbio.2006.02.012

Okwadha, G. D. O., and Li, J. (2010). “Optimum conditions for microbial carbonate precipitation,” *Chemosphere* 81(9), 1143–1148. DOI: 10.1016/j.chemosphere.2010.09.066

Ozen, I., Simsek, S., and Eren, F. (2013). “Production and characterization of polyethylene/calcium carbonate composite materials by using calcium carbonate dry and wet coated with different fatty acids,” *Polymers and Polymer Composites* 21(3), 183–188. DOI: 10.1177/096739111302100310

Rodriguez-Navarro, C., Jroundi, F., Schiro, M., Ruiz-Agudo, E., and González-Muñoz, M. T. (2012). “Influence of substrate mineralogy on bacterial mineralization of calcium carbonate: implications for stone conservation.,” *Applied and environmental microbiology* 78(11), 4017–29. DOI: 10.1128/AEM.07044-11

Sánchez-Román, M., Rivadeneyra, M. A., Vasconcelos, C., and McKenzie, J. A. (2007). “Biomineralization of carbonate and phosphate by moderately halophilic bacteria,” *FEMS Microbiology Ecology* 61(2), 273–284. DOI: 10.1111/j.1574-6941.2007.00336.x

Shabir Mahr, M., Hübert, T., Sabel, M., Schartel, B., Bahr, H., and Militz, H. (2012). “Fire retardancy of sol–gel derived titania wood-inorganic composites,” *Journal of Materials Science* 47(19), 6849–6861. DOI: 10.1007/s10853-012-6628-3

Singh, N. B., and Singh, N. P. (2007). “Formation of CaO from thermal decomposition of calcium carbonate in the presence of carboxylic acids,” *Journal of Thermal Analysis and Calorimetry* 89(1), 159–162. DOI: 10.1007/s10973-006-7565-7

Stark, N. M., and Gardner, D. J. (2008). “Outdoor durability of wood–polymer composites,” in: *Wood–Polymer Composites*, 142–165. DOI: 10.1533/9781845694579.142

Steenkjær Hastrup, A. C., Jensen, B., Clausen, C., and Green III, F. (2006). “The effect of $CaCl_2$ on growth rate, wood decay and oxalic acid accumulation in Serpula lacrymans and related brown-rot fungi,” *Holzforschung* 60(3), 339–345. DOI: 10.1515/HF.2006.054

Sun, S., Li, C., Zhang, L., Du, H., and Burnell-Gray, J. (2006). “Interfacial structures and mechanical properties of PVC composites reinforced by $CaCO_3$ with different particle sizes and surface treatments,” *Polymer International* 55(2), 158–164. DOI: 10.1002/pi.1932

Taghiyari, H. R. (2012). “Fire-retarding properties of nano-silver in solid woods,” *Wood Science and Technology* 46(5), 939–952. DOI: 10.1007/s00226-011-0455-6

Tampieri, A., Sprio, S., Ruffini, A., Celotti, G., Lesci, I. G., and Roveri, N. (2009). "From wood to bone: multi-step process to convert wood hierarchical structures into biomimetic hydroxyapatite scaffolds for bone tissue engineering," *Journal of Materials Chemistry* 19(28), 49-73. DOI: 10.1039/b900333a

Tenorio, C., Moya, R., Salas, C., and Berrocal, A. (2016). "Evaluation of wood properties from six native species of forest plantations in Costa Rica," *Bosque* 37(1). DOI: 10.4067/S0717-92002016000100008

Tourney, J., and Ngwenya, B. T. (2009). "Bacterial extracellular polymeric substances (EPS) mediate CaCO3 morphology and polymorphism," *Chemical Geology* 262(3–4), 138–146. DOI: 10.1016/j.chemgeo.2009.01.006

Tsioptsias, C., and Panayiotou, C. (2011). "Thermal stability and hydrophobicity enhancement of wood through impregnation with aqueous solutions and supercritical carbon dioxide," *Journal of Materials Science* 46(16), 5406–5411. DOI: 10.1007/s10853-011-5480-1

Uribe, B. E. B., and Ayala, O. A. (2015). "Characterization of three wood species (Oak, Teak and Chanul) before and after heat treatment," *Journal of the Indian Academy of Wood Science* 12(1), 54–62. DOI: 10.1007/s13196-015-0144-4

Walters, R. N., and Lyon, R. E. (2003). "Molar group contributions to polymer flammability," *Journal of Applied Polymer Science* 87(3), 548–563. DOI: 10.1002/app.11466

Wu, Y., Zhao, C., Jiang, Y., and Han, W. (2016). "Study on modification of calcium carbonate for paper filler," in: *Proceedings of the 2016 4th International Conference on Machinery, Materials and Computing Technology*, Atlantis Press, Paris, France. DOI: 10.2991/icmmct-16.2016.80

Yao, F., Wu, Q., Lei, Y., Guo, W., and Xu, Y. (2008). "Thermal decomposition kinetics of natural fibers: Activation energy with dynamic thermogravimetric analysis," *Polymer Degradation and Stability* 93(1), 90–98. DOI: 10.1016/j.polymdegradstab.2007.10.012

Zeng, Y., Cao, J., Wang, Z., Guo, J., Zhou, Q., and Lu, J. (2018). "Insights into the Confined Crystallization in Microfluidics of Amorphous Calcium Carbonate," *Crystal Growth & Design* 18(11), 6538–6546. DOI: 10.1021/acs.cgd.8b00675

Article submitted:

3. Artículo 2. In-situ mineralization of calcium carbonate of tropical hardwood species from fast-grown plantations in Costa Rica

In-situ mineralization of calcium carbonate of tropical hardwood species from fast-grown plantations in Costa Rica

Johana GAITAN-ALVAREZ

Instituto Tecnológico de Costa Rica, Escuela de Ingeniería Forestal, Apartado 159-7050, Cartago, Costa Rica. Email: jgaitan@tcr.ac.cr https://orcid.org/0000-0003-4243-5910

Róger MOYA*

Instituto Tecnológico de Costa Rica, Escuela de Ingeniería Forestal, Apartado 159-7050, Cartago, Costa Rica. E-mail: rmoya@itcr.ac.cr https://orcid.org/0000-0002-6201-8383

Alexander BERROCAL

Instituto Tecnológico de Costa Rica, Escuela de Ingeniería Forestal, Apartado 159-7050, Cartago, Costa Rica. Email: aberrocal@itcr.ac.cr https://orcid.org/0000-0003-2041-4772

Fabio ARAYA

Instituto Tecnológico de Costa Rica, Escuela de Química, Instituto Tecnológico de Costa Rica, Cartago 159-7050, Costa Rica. Email: fdaraya@itcr.ac.cr

*Authors correspondence, Email: rmoya@itcr.ac.cr

In-situ mineralization of calcium carbonate of tropical hardwood species from fast-grown plantations in Costa Rica

Abstract

Chemical modifications of the cellular structure of wood aiming at solving problems of dimensional stability, durability and fire resistance, such as mineralization, have been applied in the past. However, knowledge of these treatments applied to tropical wood is almost inexistent. For this reason, the aim of the present work is to impregnate nine hardwood species used in commercial reforestation in Costa Rica, by means of subsequential in-situ mineral formation based on a solution-exchange process of two solution-exchange cycles by impregnating with $CaCl_2$ in ethanol and $NaHCO_3$ in water with $CaCO_3$. The results showed that the absorption of the $CaCl_2$ and $NaCO_3$ solution in the different wood species varied from 42.2 to 168.0 l m^{-3} and 69.5 to 214.6 l m^{-3} respectively, while the retention of in-situ $CaCO_3$ varied from 2.8 to 9.2 kg/m^3. Although the different wood species showed high absorption of the solutions, it was found that in some of them the percentage of CO_3^{2-} did not react, while in others the Ca^{2+} ion was unreacted salt. The SEM analysis showed the distribution of the $CaCO_3$ crystals in the different anatomical features and showed the formation of calcite and vaterite type crystals, which was also evidenced in the X-ray diffraction and FTIR spectrum.

Keywords: fast-growth plantation, preservation, wood chemical treatment, wood plantation wood treatment.

Introduction

Wood can be utilized untreated or after some type of modification (Rowell 2014, 2016), such as the application of coating or finishing (Singh et al. 2013; Cogulet et al. 2018) and certain preservation treatments (Mishra et al. 2018; Teng et al. 2018). Wood modifications may involve utilization of chemical substances, generally harmful to the environment (Schultz et al. 2007; Jones et al. 2019). In recent years, new technologies have been developed to increase the useful life of woods without using toxic substances (Gérardin 2016; Teng et al.

2018). In the search for new technologies to improve the durability of wood, non-biocide treatments (Teacă et al. 2019) and chemical modifications (Mantanis 2017; Jiang et al. 2018; Lee et al. 2018; Papadopoulos et al. 2019) have been developed. Wood mineralization is one of these chemical modifications, which consists of impregnating the wood with mineral salts such as titanium (Hübert et al. 2010; Shabir Mahr et al. 2012), sodium phosphate (Tampieri et al. 2009), calcium carbonate (Meldrum 2003; Merk et al. 2015) and struvite (Guo et al. 2019), dissolved in different liquid solvents to impregnate the wood (Ansell 2015; Guo et al. 2019).

Wood mineralization with calcium carbonate ($CaCO_3$) requires a high technical set-up for supercritical gases (Tsioptsias and Panayiotou 2011), or harmful precursors and reactions, which for example involve elemental calcium, methanol, and hydrogen (Klaithong et al. 2013; Merk et al. 2015, 2016). Nevertheless, Merk et al. (Merk et al. 2016) propose an innovative and simple wood mineralization strategy, which involves a subsequential in-situ mineral formation based on a solution-exchange process. These authors propose two solution-exchange cycles with $CaCl_2$ in ethanol and $NaHCO_3$ in water. According to their report, $CaCO_3$ formation was adequately distributed in the lumina of cells of earlywood, and in less proportion in latewood of Norway spruce. They also mention that salt penetration was the expected for softwood species. Other studies on mineralization have focused on softwood, such as Norway spruce and European beech wood (Merk et al. 2015, 2016; Guo et al. 2019), as well as small scale methods difficult to apply at a larger industrial scale (Burgert et al. 2016; Ma et al. 2016).

Additionally, reforestation programs with hardwood species aiming at wood production are being implemented in many tropical climate countries such as Costa Rica in Central America (Tenorio et al. 2016; Liu et al. 2018). Hardwoods differ from softwoods in their hierarchical and chemical structure (Van der Graaff and Baas 1974; Pandey 1999; Gibson 2012). Softwoods have a more uniform hierarchical structure consisting mainly of parallel hollow tubes called tracheids, with a thick cell wall of cellulose microfibrils composite embedded into a matrix of hemicelluloses and lignin. The traquead (85–95% of total cells) are highly elongated tracheids that provide both structural support and a conduction path for fluids (through small openings, called bordered pits, along their sides) (Fratzl and Weinkamer 2007; Klaithong et al. 2013).

Hardwoods in turn are composed of fiber cells (35-70% of total cells) which give mechanical support, while liquid flow is carried out by the vessels (6-55% of total wood cells) that are enlarged cells with thin walls and large pore spaces. Both wood types (softwoods and hardwoods) have rays made up of smaller, more rectangular parenchyma cells that store sugars; in softwoods, the rays make up 5-12% of the wood, while in hardwoods, they make up 10-32% (Gibson 2012).

Because of these structural differences between softwood and hardwood, liquid flow inside the wood is different. In softwood species, liquid flow occurs longitudinally and transversally, the longitudinal sense being the easier one (Bolton and Petty 1978; Usta 2005), since this way the liquid moves first through the tracheid lumina and then through the bordered pits to another trachea, located in the pitted cross wall (Usta 2005). Transversally, liquid flow occurs through the rays, and is considered insignificant (Bolton and Petty 1978). Liquid flow mechanisms in hardwoods are more complex, for more anatomical features are involved. In the longitudinal sense liquid flow is 10-13 times greater than in transversal sense and occurs mainly through the vessels (Ahmed and Chun 2011). Vessels are hollow tubes interconnected at the ends with other vessels by means of perforation plates. However, liquid flow can be interrupted by obstacles in the lumen of the vessel (Thomas 1976), considering also the longitudinal flow, frequency, quantity and type of porosity of the wood (Ahmed and Chun 2009).

Hardwood fibers contribute little to liquid flow, since these only have a small number of minute pits, which hinders an adequate liquid flow in the wood (Emaminasab et al. 2017). As for the longitudinal parenchyma, if associated to vessels (paratracheal parenchyma), it helps conduction by means of wall pits. Lateral flow occurs mainly through the rays, where the type (homogeneous or heterogeneous), the number of cells the rays are composed of, their frequency, parenchyma lumen diameter and length, and end wall pit number and diameter, play an important role (Ahmed and Chun 2009). Liquid flow through the rays comes from the vessels through radio-vascular pits and continues laterally through the lumen of ray cells, passing to other ray cells through the pits at the ends or the punctures in the lateral pits with other rays (Ahmed and Chun 2011).

Therefore, the treatments involving liquid flow, such as in-situ mineralization in hardwood species in tropical climates, should be studied appropriately. In this context, the objective of the present work is to impregnate 9 hardwood species (*Cedrela odorata, Cordia alliodora, Enterolobium cyclocarpum, Gmelina arborea, Hieronima alchornoides, Samanea saman, Tectona grandis, Vochysia ferruginea and Vochysia guatemalensis*) by means of subsequential in-situ mineral formation based on a solution-exchange process of two solution-exchange cycles by impregnating with $CaCl_2$ in ethanol and $NaHCO_3$ in water with $CaCO_3$, in order to know the potential of formation of $CaCO_3$ in the different anatomical elements, based on the quantity of impregnated salts and the quantity of reacted and unreacted salt, by means of the TGA, FTIR, SEM and XDR techniques.

Materials and methods

Highly permeable sapwood from nine wood species from fast-growth forest plantations in Costa Rica was used (Moya et al. 2015). The species used were *Cedrela odorata* (*Co*), *Cordia alliodora* (*Ca*), *Enterolobium cyclocarpum* (*Ec*), *Gmelina arborea* (*Ga*), *Hieronyma alchorneoides* (*Ha*), *Samanea saman* (*Sa*), *Tectona grandis* (*Tg*), *Vochysia ferruginea* (*Vf*) and *Vochysia guatemalensis* (*Vg*). The age of the plantations that contributed the material ranged between 4 and 8 years. Three trees per species were cut down for sampling. Then, the samples were cut into 1 m long logs and sawn into 7.5 cm wide x 2.5 cm thick boards. These boards were air dried until reaching between 12-15% moisture content. Then, pieces 46 cm long x 7.5 cm wide and 2 cm thick were extracted, making sure that the pieces were composed of sapwood.

The reagents used were ETI SODA (Turkey) solid state sodium bicarbonate ($NaHCO_3$) (http://www.etisoda.com/en/products/sodium-bicarbonate/food-type-sodium-bicarbonate) and solid state calcium chloride ($CaCl_2$) from CASO FCC FLAKES Solvay (USA) (https://www.solvay.com/en/product/caso-fcc-flakes). Ethyl alcohol 99% m m^{-1} absolute of the brand Reactivos Químicos Gamma (Costa Rica) (http://www.arvicr.com/productos/hospitalarios/laboratorio/etanol-qp.html#tab2), distributed by Laboratorios Químicos ARVI S.A, was used.

Process of mineralization

The in-situ mineralization process was performed in 20 samples (46 cm long x 7.5 cm wide and 2 cm thick), using the vacuum and pressure equipment shown in the diagram in Figure 1b. The samples were placed into a tank (25 cm diameter x 48 cm long and 27 litres capacity) for impregnation with salts. Calcium carbonate ($CaCO_3$) formation was performed by means of two impregnation cycles (Equation 1): $CaCl_2$ cycle (Equation 2) and $NaHCO_3$ cycle (Equation 3).

$$Ca^{2+} + CO_3^{2-} \rightarrow CaCO_3 \qquad (1)$$

$$CaCl_2 * 2H_2O \rightarrow Ca^{2+} + 2Cl^- \quad (ethanol\ solution)\ (2)$$

$$NaHCO_3 \rightarrow\ Na^+ + H^+ + CO_3^{2-} \quad (aqueous\ solution)\ (3)$$

(i) $CaCl_2$ cycle: wood was impregnated with this salt in an ethanol solution at 1 mol^{-1} concentration (Equation 2). First, vacuum at -70 kPa (gauge) for 20 minutes was performed; then, the samples were totally immersed into the solution and 690kPa pressure was applied for 30 minutes. Following, the excess of solution was vacuum extracted. The samples were taken out of the tank, washed in ethanol and then kiln-dried at 40°C for 4 hours, so that the samples reached again less than 30% moisture content to ensure that the cell lumens were empty (Skaar 2012).

(ii) $NaHCO_3$ cycle: the samples were impregnated with an aqueous solution at 1 mol^{-1} concentration (Equation 2). During impregnation, vacuum was first applied at -70 kPa for 20 minutes, then the samples were immersed in the aqueous solution of $NaHCO_3$ and 690 kPa pressure was applied during 50 minutes (Figure 1a). After this period, the samples were taken out and washed in distilled water. Lastly, the samples were left to dry inside a chamber under controlled conditions (22°C and 66% relative humidity) until reaching 12% moisture content.

[Fig. 1]

Evaluation of the mineralization process

In the $CaCl_2$ cycle the samples were weighed before and after impregnation with $CaCl_2$. Thus, absorption of the solution (Equation 4) and retention of the salt (Equation 5) of $CaCl_2$ were obtained. In the $NaHCO_3$ cycle, again the sample was weighed before and after impregnation with $NaHCO_3$ and again absorption of the solution (Equation 4) and retention of the salt (Equation 5) of $NaHCO_3$ were obtained. Retention of de Ca^{2+} and CO_3^{2-} was obtained from the value of retention of each one of these salts. Because the process of absorption of salts occurs at different stages and it is not possible to control the amount of moles necessary to carry out the reaction of the formation of $CaCO_3$, the surpluses of Ca^{2+} or CO_3^{2-} were calculated considering that the balance is given by the reaction (Equation 1). The excess salt was reported as weight relative to the volume of wood (Equation 3).

$$Salt\ absortion\ \left(\frac{liters}{m^3}\right) = \frac{(Weigth_{before\ impregnation}(g) - Weigth_{after\ impregnation\ (g)}}{Volume\ of\ sample\ (cm^3)} x\ \frac{(100\ cm)^3}{1\ m^3} x\ \frac{1\ liters}{1000\ g} \quad (4)$$

$$Salt\ retention\ \left(\frac{kg}{m^3}\right) = Salt\ absortion\ \left(\frac{liters}{m^3}\right) x\ \frac{salt\ concentration\ \left(\frac{salt\ weigth\ in\ kg}{solution\ weigth\ in\ kg}\right)}{solution\ density\ (\frac{weigth\ in\ kg}{liters})} \quad (5)$$

Scanning electron microscope

From each treatment (impregnated and not impregnated) for each species, samples 5mm wide x 5mm thick x 10mm long were prepared, cutting two of their corners in the form of a truncated pyramid. Then, in the cross section of the sample, a cut was made using an American Optical Corp model 860 microtome to achieve a smooth surface. Scanning electron microscopy (SEM) was performed on a Table MicroscopeTM 3000 equipment without gold or carbon film covering the sample. The formation of $CaCO_3$ was observed in the different anatomical elements, in order to determine where the salt formation occurred.

FTIR X-ray spectroscopy

Samples of impregnated and non-impregnated wood were taken from each species and these were ground to a size of 420 µm and 250 µm (40 and 60 mesh, respectively). The samples were dried in the oven at 105°C until reaching constant weight. The Fournier Transform Infrared Spectroscopy (FTIR) scan was then performed using a Nicolet 380 FTIR (Thermo Scientific) spectrometer with a single reflective cell (equipped with a diamond crystal). The equipment was configured to perform readings accumulating 32 scans with a resolution of 1 cm^{-1}, with a background correction before each measurement. The obtained FTIR spectra were processed with Spotlight 1.5.1, HyperView 3.2 and Spectrum 6.2.0 software developed by Perkin Elmer. Inc.

X-ray diffraction

Two species with high and medium in-situ $CaCO_3$ impregnation were selected: *Sa* with high impregnation and *Ha* with medium impregnation. The X-ray diffractometry (XRD) was performed on a PANanalytical Empyrcan Series 2 diffractometer (Cu-Kα, 6° - 40° 20), in conjunction with the PANalytical High Score Plus software. Sawdust from the impregnated and non-impregnated samples was used, placing it on a rectangle of neoprene on a glass plate for measurement. For XRD spectra the Analysis of the samples was done within the range of the characteristic bands of $CaCO_3$ particles, with 2h ranging from 10° to 50°.

Statistical analysis: First, the normality and homogeneity of the absorption and retention data and the presence of extreme data or “outliers” were checked. Then the average, standard deviation and coefficient of variation for each variable for each species and treatment were calculated. Next, an ANOVA analysis of variance was performed with a level of statistical significance of $p<0.05$. Finally, Tukey’s test was used to determine the statistical significance of the difference between the means of the variables. This analysis was performed in the SAS 9.4 program (SAS Institute Inc., Cary, N.C.).

Results

Evaluation of the process of mineralization

Absorption of $CaCl_2$ and $NaCO_3$ solutions in the different species varied between 42.2 to 168.0 l m^{-3} and 69.5 to 214.6 l m^{-3} (Table 1), respectively. However, it is important to highlight that in all species, the absorption of $CaCl_2$ was lower than the absorption of $NaCO_3$, therefore the amount of $CaCO_3$ in-situ corresponds to the retention of the lesser amount of salt ($CaCl_2$) absorbed (Table 1). The ANOVA for these two parameters showed that the absorption of the solution of $CaCl_2$ and therefore of $CaCO_3$ formed in-situ was greater in *Ec*, *Ha*, *Ss*, *Vf* and *Vg*, while the lowest absorptions were found in *Co*, *Ga* and *Tg* (Table 1). Meanwhile, the absorption of the $NaCO_3$ solution mostly occurred in *Ha*, *Ss* and *Vf*, and in smaller quantity in *Co*, *Ga* and *Tg* (Table 1). The retention of Ca^{2+} and CO_3^{2-} in the different woods varied between 2.4 to 9.2 kg m^{-3} and between 3.9 to 12.2 kg m^{-3} respectively, resulting in the amount of $CaCO_3$ formed in-situ ranging from 2.8 to 9.2 kg m^{-3}. The retention of both salts (of Ca^{2+} and CO_3^{2-}) was higher in *Ec*, *Ha*, *Ss*, *Vf* and *Vg*, and smaller in *Co*, *Ga* and *Tg*, presenting statistical differences between them (Table 1).

[Table 1]

As for the unreacted salts in the wood (which can reach up to 40% of the treated wood species), excess ions such as Ca^{2+} and CO_3^{2-} can be observed in the same species (Figure 2a). In *Ca*, *Ec*, *Ss* and *Vg*, the excess ions were Ca^{2+}, while excess ions in *Ca*, *Ga*, *Ha*, *Tg* and *Vf* were CO_3^{2-} (Figure 2a). Regarding the amount of unreacted salt in relation to volume, *Ec* wood had the highest values with 3.8 and 6.0 g m^{-3} of CO_3^{2-} and Ca^{2+} respectively, followed by *Vf* and *Vg*, while the woods with less unreacted salts were *Co* and *Ca* (Figure 2b).

[Fig. 2]

Scanning electron microscope

SEM images showed that $CaCl_2$ crystals are of the type six-sided needles (Figure 3a); $NaHCO_3$ crystals are spheroidal (Figure 3b) and $CaCO_3$ crystals are rhomboidal and

spheroidal (Figure 3c). The mineralization process by means of in-situ formation of $CaCO_3$ occurred mainly inside the vessels lumina, then in the rays and finally in the fiber lumina (Figure 3d-l). In woods with a smaller amount of $CaCO_3$ formed (less than 8.0 kg of $CaCO_3$ m^{-3}), which correspond to *Tg*, *Ga* and *Co*, the SEM images showed lower formation of this salt in the anatomical elements of the wood. $CaCO_3$ crystals formed in vessels lumina and slightly in the rays, while no crystals were observed in the fibers (Figure 3 d, e and f). In woods with medium salt absorption, between 15.0 and 17.5 kg of $CaCO_3$ m^{-3}, such as *Ca*, *Ha* and *Vg*, a greater salt formation was observed in the vessels lumina and in the wood rays and some crystals in the fiber lumina (Figure 3g, h and i). Finally, in woods with the highest salt formation (between 20.0 and 21.0 of $CaCO_3$ m^{-3}), corresponding to *Vf*, *Ss* and *Ec*, a greater amount of crystals in vessels lumina and in the rays in relation to the other species was observed, while in the fiber lumina the greatest amount of crystals appeared, which was not observed in the previously described species (Figure 3j, k and l).

[Fig. 3]

The following aspects regarding formation of crystals of $CaCO_3$ are noteworthy in all species: (i) the crystals formed were of the types calcite (Figure 4a), vaterite (Figure 4b) and amorphous (Figure 4c), while crystals of the types aragonite, crystalline monohydrate and hexahydrate were not observed; (ii) the crystals are adhered to the inside walls of the lumina of different anatomical elements (Figure 4d); (iii) crystals form dispersed in the lumina of the anatomical elements (Figure 3d-e, 3h-i); (iv) crystals form in small heaps in the lumina of vessels and fibers (Figure 3f, 3j, 3l) and (v) crystal formation in the lumina of rays creates larger crystal heaps (Figure 3f and 3l) than those formed in the lumina of vessels and fibers.

[Fig. 4]

FTIR spectroscopy

FTIR spectrum showed a peak at 873 cm^{-1} and another at 1463 cm^{-1} in wood mineralized with $CaCO_3^{2+}$ (Figure 5a). Both signals are rather noticeable in woods of *Co, Ca* and *Ss* (Figure 5b, c, g), while in woods of *Ec, Ga, Ha, Tg, Vf* and *Vg* the peak's signal is quite weak or null (Figure 5 d, e, f, h, i and j).

[Figure 5]

X-ray diffraction

The XRD patterns of the $CaCO_3$/wood composites showed strong diffraction peaks at 29°, which correspond to (110) planes of calcite (JCPDS number 98-003-3842) in both woods chosen (Figure 6a-b).

[Fig. 6]

Discussion

The absorption and retention results of individual salts ($CaCl_2$ and $NaHCO_3$, from 42.2 to 168.0 l m^{-3} and 69.5 to 214.6 l m^{-3}, respectively (Table 1)), regarding $CaCO_3$ formation, showed similar values as those obtained when these 9 species were treated in preservation processes with commercial aqueous substances, to increase wood durability (Moya et al. 2015), which reported absorptions between 50 and 450 l m^{-3}. These results show that utilization of the vacuum-pressure method commonly used in commercial preservation (Teng et al. 2018), can be used in subsequential in-situ mineral formation in tropical woods based on a solution-exchange process by impregnation with $CaCl_2$ in ethanol (first cycle) and $NaHCO_3$ in water con $CaCO_3$ (second cycle). However, as occurs with modern treatments for wood preservation, the type of solvents or chemicals used may affect the materials from which the wood treatment equipment is made of.

Although adequate absorptions were achieved to obtain the quantity of ions (Ca^{2-} or CO_3^{2+}) needed for $CaCO_3$ formation, the stoichiometry was not appropriate for the formation of this salt. The benefit of the excess Ca^{2+} or CO_3^{2-} ions for $CaCO_3$ formation was small in all species (Figure 2a), affecting the economic efficiency of the process of in-situ mineralization. Another aspect left aside was the complex mechanism of crystallization reaction in solutions (Leng and Salmon 2009), as the ones used in the present condition of in-situ wood mineralization. Salt formation is a complex mechanism that includes the polymorphism exhibited by crystals of calcium carbonate, calcium oxalate and different polymorphs of the same compound that can transform each other. Crystal formation also influences the environmental temperature, concentration, pH, viscosity, additives and so on (Zeng et al.

2018), conditions that are difficult to control in the processes and in the equipment used in commercial preservation, whose application is intended in wood mineralization.

Likewise, absorption and retention, as well as the percentage of the ions that react and their surpluses vary in the different tropical hardwood species. Such variability is attributed to wood permeability or fluid flow in the wood (Thomas 1976; Ahmed and Chun 2009), which vary depending on the anatomical elements composing it. In hardwood species liquid flow occurs mainly in the longitudinal direction through vessels lumina (Ahmed and Chun 2011), continuing at the ends to another vessel through the perforation plates; nevertheless, liquid flow can be interrupted by the presence of tyloids or gums in vessels lumina (Thomas 1976; Ahmed and Chun 2009) Longitudinal flow also occurs through the longitudinal parenchyma, which is connected to the vessels by wall pits. Radial flow occurs through the radial parenchyma, which is fed by the radio-vascular punctuations. Then, the liquid flows transversally through the lumen of the ray cells, passing to other ray cells through the pits at the ends or the punctures in lateral pits with other rays (Ahmed and Chun 2011). Radial flow is favoured when the rays are composed of more than 3 series in width (Ahmed and Chun 2011). These variations that occur in the previous anatomical features produce variations in the absorption and retention of salt ions (Table 1, Figure 1) or the formation of $CaCO_3$.

According to the dimensions and characteristics of the anatomical elements that help the liquid flow inside the wood (Table 2), it is expected that large vessel lumina diameter, larger amounts of vessel cells, diameter of pits and presence or not of ornamentations, large and compound rays over 3 series and the 3 types of parenchyma, allow for greater fluid flow and therefore greater absorption and retention of salts. Specifically, the species *Ec*, *Ha*, *Ss*, *Vf* and *Vg* have larger anatomical features (Table 2), among which vessel diameter (over 120 µm), ray width (from 2 to 10 cell series or over 252 µm) and frequency (over 5 rays mm^{-2}), and several types of parenchyma that aid the flow of solutions to form a greater amount of in-situ $CaCO_3$, stand out. In contrast, the smallest in-situ formed $CaCO_3$ occurred in the species *Co*, *Ga* and *Tg* (Table 1), which presented adverse anatomical elements, such as smaller and less frequent rays, deposits of gums and tyloses in the vessels, and scarce parenchyma associated with the vessels (Table 2), which do not benefit the introduction of salts.

[Table 2]

The forms of the $CaCO_3$ particles (vaterite, calcite and amorphous) (Figure 4a-c), it agrees with the study conducted by Ma et al., (Ma et al. 2016), which established six well defined polymorphic $CaCO_3$ particles: vaterite, aragonite, calcite, amorphous, crystalline monohydrate and hexahydrate. In contrast, the forms aragonite, crystalline monohydrate and hexahydrate were not observed. According to several studies, the three forms found are the most commonly found during the synthesis of $CaCO_3$. Better control of the process and other types of substances are needed to obtain the other three forms that were not observed (Ma et al. 2016; Jimoh et al. 2018; Krajewska 2018). Therefore, the results suggest that in-situ formation of $CaCO_3$ in wood produces particles of the forms vaterite, calcite and amorphous.

$CaCO_3$ formation occurs mainly in the vessel lumina, followed by the radial and axial parenchyma and, to a less extent, in the fibers (Figure 3-4). This pattern of deposit in-situ in the different anatomical elements of $CaCO_3$ is attributed to the fluid transport mechanisms within the hierarchical structure (Fratzl and Weinkamer 2007; Klaithong et al. 2013). The main hardwood fluid flow anatomical feature are the vessels (Ahmed and Chun 2011); therefore, greater in-situ formation of $CaCO_3$ crystals are to be expected. However, flow can be obstructed by tylides (Fujii et al. 2001), which was reflected in some species such as *G. arborea* and *C. alliodora* (Table 2). After the vessels, the rays are the next anatomical feature as regards liquid flow inside the wood, particularly in radial conduction (Ahmed and Chun 2009). Therefore, formation of $CaCO_3$ crystals in those anatomical features are to be expected. In the case of fibers in hardwood species, these constitute tree anatomical features for structural support, not used to transport liquid (Thomas 1976), thus, little in-situ formation of $CaCO_3$ crystals is expected in the fibers. Noteworthy, during the mineralization not all the deposits found correspond to $CaCO_3$; secondary products, such as $NaCl_2$, or small amounts of unreacted salts can be found, which in our case varied from over 50% of CO_3^{2-}, with unreacted salt over 50% for *Ca* (Figure 2a). Not to be overlooked is the fact that a percentage of the impregnated salt will be precipitated prematurely on the surface of the wood, causing an accumulation of minerals in this area due to the ease of reaction of the salt used (Merk et al. 2016).

The FTIR and X-ray diffraction analyses showed presence of $CaCO_3$ in the different species and the intensity of the spectra signals, which was different according to the quantity of salts formed in-situ in the various species (Figure 5-6). As for the FTIR spectrum, it shows in-situ $CaCO_3$ formation in those species where salt absorption and retention was greater (*Ec*, *Ha*, *Ss*, *Vf* and *Vg*) (Table 1); there is less intensity at the 1420 cm^{-1} band, corresponding to the $CaCO_3$ calcite type, and at the 873- 878 cm^{-1} band, corresponding to both $CaCO_3$ calcite and vaterite types (Figure 4 a-j). According to Saraya et al. (Saraya and Rokbaa 2016) and Mantilaka et al. (Mantilaka et al. 2014) these vibrations are attributed to the molecular structure of the CO_3^{2-} ions. However, other vibrations also attributed to the carbonate ion (Wang et al. 2010; Zhang et al. 2012), were not as evident in the FTIR spectrum, as 1080 cm^{-1} and 700 cm^{-1} bands. In the case of the X-ray diffraction analysis (Figure 6), the strong diffraction peaks at 29° is attributed to the in-situ $CaCO_3$ formation, specifically, the presence of calcite and vaterite (Kralj et al. 1994; Merk et al. 2016).

Conclusions

The results of the present work showed deposits of $CaCO_3$ crystals in the structure of the wood cells, which is confirmed by the SEM images, FTIR spectrum and XDR, which also showed $CaCO_3$ formation of the type calcite and vaterite. However, there is an irregularity in the in-situ formation of $CaCO_3$. This is so because the hierarchical structure of the wood is complex and these structures are characteristic of each of the species, so there are various degrees of absorption of the different salts used in the in-situ formation of $CaCO_3$, demonstrating that the quantity of this salt varies according to the wood species. The variation per species of $CaCO_3$ formation occurs firstly in the vessel lumina, then in the ray lumina, but scarcely in the fiber lumina. This deposit pattern of $CaCO_3$ occurs because the first two anatomical features are specialized elements in the conduction of liquids, whereas the fibres do not have the conditions for transporting salt solutions.

Lastly, mineralization in tropical species by means of subsequential in-situ mineral formation based on a solution-exchange process of two solution-exchange cycles by impregnation with $CaCl_2$ in ethanol and $NaHCO_3$ in water with $CaCO_3$ can be performed utilizing the traditional commercial wood preservation equipment. Nevertheless, each species will

behave differently regarding absorption and formation of $CaCO_3$ because of their different internal mechanisms for liquid flow.

Acknowledgement

The authors wish to thank the Vicerrectoría de Investigación y Extensión at the Instituto Tecnológico de Costa Rica (ITCR).

References

Ahmed SA, Chun SK (2011) Permeability of *Tectona grandis* L. as affected by wood structure. Wood Sci Technol 45:487–500. doi: 10.1007/s00226-010-0335-5

Ahmed SA, Chun SK (2009) Observation of liquid permeability related to anatomical characteristics in *Samanea saman*. Turkish J Agric For 33:155–163. doi: 10.3906/tar-0807-13

Ansell MP (2015) Carbonised and mineralised wood composites. In: Wood Composites. Elsevier, 395–409

Bolton AJ, Petty JA (1978) A model describing axial flow of liquids through conifer wood. Wood Sci Technol 12:37–48. doi: 10.1007/BF00390009

Burgert I, Keplinger T, Cabane E, et al (2016) Biomaterial Wood: Wood-Based and Bioinspired Materials. In: Secondary Xylem Biology. Elsevier, 259–281

Cogulet A, Blanchet P, Landry V, Morris P (2018) Weathering of wood coated with semi-clear coating: Study of interactions between photo and biodegradation. Int Biodeterior Biodegradation 129:33–41. doi: 10.1016/j.ibiod.2018.01.002

Emaminasab M, Tarmian A, Oladi R, et al. (2017) Fluid permeability in poplar tension and normal wood in relation to ray and vessel properties. Wood Sci Technol 51:261–272. doi: 10.1007/s00226-016-0860-y

Fratzl P, Weinkamer R (2007) Nature's hierarchical materials. Prog Mater Sci 52:1263–1334. doi: 10.1016/j.pmatsci.2007.06.001

Fujii T, Lee S-J, Kuroda N, Suzuki Y (2001) Conductive function of intervessel pits through a growth ring boundary of machilus thunbergii. IAWA J 22:1–14. doi: 10.1163/22941932-90000264

Gérardin P (2016) New alternatives for wood preservation based on thermal and chemical modification of wood— a review. Ann For Sci 73:559–570. doi: 10.1007/s13595-015-0531-4

Gibson LJ (2012) The hierarchical structure and mechanics of plant materials. J R Soc Interface 9:2749–2766. doi: 10.1098/rsif.2012.0341

Guo H, Luković M, Mendoza M, et al (2019) Bioinspired struvite mineralization for fire-resistant wood. ACS Appl Mater Interfaces 11:5427–5434. doi: 10.1021/acsami.8b19967

Hübert T, Unger B, Bücker M (2010) Sol–gel derived TiO2 wood composites. J Sol-Gel Sci Technol 53:384–389. doi: 10.1007/s10971-009-2107-y

Jiang F, Li T, Li Y, et al (2018) Wood-Based Nanotechnologies toward Sustainability. Adv Mater 30:1703453. doi: 10.1002/adma.201703453

Jimoh OA, Ariffin KS, Hussin HBin, Temitope AE (2018) Synthesis of precipitated calcium carbonate: a review. Carbonates and Evaporites 33:331–346. doi: 10.1007/s13146-017-0341-x

Jones AS, Marini J, Solo-Gabriele HM, et al. (2019) Arsenic, copper, and chromium from treated wood products in the U.S. disposal sector. Waste Manag 87:731–740. doi: 10.1016/j.wasman.2019.03.004

Klaithong S, Opdenbosch DVan, Zollfrank C, Plank J (2013) Preparation of $CaCO_3$ and CaO replicas retaining the hierarchical structure of sprucewood. Zeitschrift für Naturforsch B 68:533–538. doi: 10.5560/znb.2013-3062

Krajewska B (2018) Urease-aided calcium carbonate mineralization for engineering applications: A review. J Adv Res 13:59–67

Kralj D, Brečević L, Nielsen AE (1994) Vaterite growth and dissolution in aqueous solution II. Kinetics of dissolution. J Cryst Growth 143:269–276. doi: 10.1016/0022-0248(94)90067-1

Lee SH, Ashaari Z, Lum WC, et al. (2018) Thermal treatment of wood using vegetable oils: A review. Constr Build Mater 181:408–419. doi: 10.1016/j.conbuildmat.2018.06.058

Leng J, Salmon J-B (2009) Microfluidic crystallization. Lab Chip 9:24–34. doi: 10.1039/B807653G

Liu CLC, Kuchma O, Krutovsky KV (2018) Mixed-species versus monocultures in plantation forestry: Development, benefits, ecosystem services and perspectives for the future. Glob Ecol Conserv 15.

Ma MG, Liu S, Fu LH (2016) Calcium Carbonate and Cellulose/Calcium Carbonate Composites: Synthesis, Characterization, and Biomedical Applications. Mater Sci Forum 875:24–44. doi: 10.4028/www.scientific.net/MSF.875.24

Mantanis GI (2017) Chemical modification of wood by acetylation or furfurylation: A review of the present scaled-up technologies George. BioResources 12:4478–4489.

Mantilaka MM, Rajapakse RMG, Karunaratne DG, Pitawala HM (2014) Preparation of amorphous calcium carbonate nanoparticles from impure dolomitic marble with the aid of poly(acrylic acid) as a stabilizer. Adv Powder Technol 25:591–598. doi: 10.1016/j.apt.2013.09.008

Meldrum FC (2003) Calcium carbonate in biomineralisation and biomimetic chemistry. Int Mater Rev 48:187–224. doi: 10.1179/095066003225005836

Merk V, Chanana M, Gaan S, Burgert I (2016) Mineralization of wood by calcium carbonate insertion for improved flame retardancy. Holzforschung 70:867–876. doi: 10.1515/hf-2015-0228

Merk V, Chanana M, Keplinger T, et al. (2015) Hybrid wood materials with improved fire retardance by bio-inspired mineralisation on the nano- and submicron level. Green Chem 17:1423–1428. doi: 10.1039/C4GC01862A

Mishra PK, Giagli K, Tsalagkas D, et al (2018) Changing face of wood science in modern era: Contribution of nanotechnology. Recent Pat Nanotechnol 12:13–21. doi: 10.2174/1872210511666170808111512

Moya R, Salas C, Berrocal A, Valverde JC (2015) Evaluation of chemical compositions, air-dry, preservation and workability of eight fastgrowing plantation species in costa rica. Madera Bosques 21: 31-47.

Pandey KK (1999) A study of chemical structure of soft and hardwood and wood polymers by FTIR spectroscopy. J Appl Polym Sci 71:1969–1975. doi: 10.1002/(SICI)1097-4628(19990321)71:12<1969::AID-APP6>3.3.CO;2-4

Papadopoulos AN, Bikiaris DN, Mitropoulos AC, Kyzas GZ (2019) Nanomaterials and chemical modifications for enhanced key wood properties: A review. Nanomaterials 9:607. doi: 10.3390/nano9040607

Rowell R (2016) Dimensional stability and fungal durability of acetylated wood. Drewno 59:139–150. doi: 10.12841/wood.1644-3985.C14.04

Rowell RM (2014) Acetylation of wood-A review. Int J Ligno Prod 1:1-27.

Saraya ME-SI, Rokbaa HH (2016) Preparation of vaterite calcium carbonate in the form of spherical nano-size particles with the aid of polycarboxylate superplasticizer as a capping age. Am J Nanomater 4:44–51. doi: 10.12691/ajn-4-2-3

Schultz TP, Nicholas DD, Preston AF (2007) A brief review of the past, present and future of wood preservation. Pest Manag Sci 63:784–788. doi: 10.1002/ps.1386

Shabir, Mahr M, Hübert T, Sabel M, et al. (2012) Fire retardancy of sol–gel derived titania wood-inorganic composites. J Mater Sci 47:6849–6861. doi: 10.1007/s10853-012-6628-3

Singh AP, Park B-D, Nuryawan A, Kazayawoko M (2013) Advances in probing wood-coating interface by microscopy: A review. J Surf Eng Mater Adv Technol 03:49–54. doi: 10.4236/jsemat.2013.31A007

Skaar C (2012) Wood-water relations. Springer Science & Business Media.

Tampieri A, Sprio S, Ruffini A, et al. (2009) From wood to bone: multi-step process to convert wood hierarchical structures into biomimetic hydroxyapatite scaffolds for bone tissue

engineering. J Mater Chem 19:49-73. doi: 10.1039/b900333a

Teacă C-A, Roşu D, Mustaţă F, et al. (2019) Natural bio-based products for wood coating and protection against degradation: A review. BioResources 14:4873–4901.

Teng T-J, Mat Arip MN, Sudesh K, et al. (2018) Conventional technology and nanotechnology in wood preservation: A review. BioResources 13:9220-9252. doi: 10.15376/biores.13.4.Teng

Tenorio C, Moya R, Salas C, Berrocal A (2016) Evaluation of wood properties from six native species of forest plantations in Costa Rica. Bosque 37:71-81. doi: 10.4067/S0717-92002016000100008

Thomas RJ (1976) Anatomical features affecting liquid penetrability in three hardwood species. Wood fiber Sci 4:256–263

Tsioptsias C, Panayiotou C (2011) Thermal stability and hydrophobicity enhancement of wood through impregnation with aqueous solutions and supercritical carbon dioxide. J Mater Sci 46:5406–5411. doi: 10.1007/s10853-011-5480-1

Usta I (2005) A review of the configuration of bordered pits to simulate the fluid flow. Maderas Cienc Tecnol 7:121-132. doi: 10.4067/S0718-221X2005000200006

Van der Graaff N, Baas P (1974) Wood anatomical variation in relation to. Blumea 22:101–121

Wang Y, Moo YX, Chen C, et al. (2010) Fast precipitation of uniform $CaCO_3$ nanospheres and their transformation to hollow hydroxyapatite nanospheres. J Colloid Interface Sci 352:393–400. doi: 10.1016/j.jcis.2010.08.060

Zeng Y, Cao J, Wang Z, et al. (2018) Insights into the confined crystallization in microfluidics of amorphous calcium carbonate. Cryst growth Des 18:6538–6546. doi: 10.1021/acs.cgd.8b00675

Zhang Z, Xie Y, Xu X, et al. (2012) Transformation of amorphous calcium carbonate into aragonite. J Cryst Growth 343:62–67. doi: 10.1016/j.jcrysgro.2012.01.025

Tables

Table 1 Absorption of $CaCl_2$ and $NaCO_3$, and retention of Ca^{+} and CO_3^{2-} in the in-situ mineralization process of nine woods from fast growth tropical species in Costa Rica.

Wood	Absorption $CaCl_2$ (l m^{-3})	Absorption $NaCO_3$ (l m^{-3})	Retention Ca^{2+} (kg m^{-3})	Retention CO_3^{2-} (kg m^{-3})	Quantity of in situ $CaCO_3$ (kg m^{-3})
Cedrela odorata (Co)	51.0 (13.4)^{A}	87.8 (14.1)^{A}	2.8 (0.7)^{A}	5.0 (0.8)^{A}	2.8 (0.7)^{A}
Cordia alliodora (Ca)	123.9 (42.1)^{B}	152.7 (43.4)^{B}	6.6 (2.3)^{B}	8.6 (2.5)^{B}	6.6 (2.3)^{B}
Enterolobium cyclocarpum (Ec)	167.9 (106.7)^{C}	175.4 (73.9)^{BC}	9.2 (5.8)^{C}	9.9 (4.2)^{BC}	9.2 (5.8)^{C}
Gmelina arborea (Ga)	50.3 (3 .7)^{A}	69.5 (53.3)^{A}	2.4 (1.8)^{A}	3.9 (3.0)^{A}	2.4 (1.8)^{A}
Hieronyma alchornoides (Ha)	150.2 (56.9)^{BC}	195.1 (56.8)^{CDE}	8.2 (3.1)^{BC}	11.0 (3.2)^{CD}	8.2 (3.1)^{BC}
Samanea saman (Ss)	157.3 (25.4)^{BC}	208.1 (51.4)^{D}	8.6 (1.4)^{BC}	11.8 (2.9)^{D}	8.6 (1.4)^{BC}
Tectona grandis (Tg)	42.2 (32.3)^{A}	72.3 (14.3)^{A}	2.6 (1.8)^{A}	4.0 (0.8)^{A}	2.6 (1.8)^{A}
Vochysia ferruginea (Vf)	158.1 (85.7)^{BC}	214.6 (67.8)^{D}	8.6 (4.7)^{BC}	12.1 (3.8)^{D}	8.6 (4.7)^{BC}
Vochysia guatemalensis (Vg)	136.7 (30.7)^{BC}	177.2 (67.0)^{EB}	7.5 (1.7)^{BC}	10.0 (3.8)^{B}	7.5 (1.7)^{BC}

Legend: numbers between parentheses correspond to the coefficient of variation and different letters in each parameter represent statistically significant differences ($p<0.05$).

Table 2 Vessel characteristics of nine fast growth tropical species in Costa Rica.

Species		*Cedrela odorata*	*Cordia alliodora*	*Enterolobium cyclocarpum*	*Gmelina arborea*	*Hieronyma alchorneoides*	*Samanea saman*	*Tectona grandis*	*Vochysia ferruginea*	*Vochysia guatemalensis*
	FP (Vessel mm^{-2})	9	7	6	5	17	4-5	4	2-3	3
	DV (µm)	125	166	167	189	116	152	150	145	169
	Deposits	G	T	G	T	G	G	G	-	-
	DPI	3	3	3	5	10	4	6	4	3
Radial parenchyma	Ray height	104	870	252	270	560	250	440	580	229
	Cells in ray width	4-10	2-6	1-3	1-3, 4-10	2-4	2-3	1-3, 4-10	1-3	1-3, 4-10
	Ray frequency	2	3	6-7	6	7	6-7	5	5	3
Axial Parenchyma	PA	-	-	-	-	+	+	-	-	-
	PP	+	+	+	+	+	+	+	+	+
	PB	-	+	-	-	-	-	+	-	+

Legend: FP= pore frequency, LV= vessel length, DV= vessel diameter, T= tyloses, G= gums, DIP= intervascular punctuation diameter, PA= apotracheal parenchyma, PP= paratracheal parenchyma, PB= banded parenchyma.

Figures

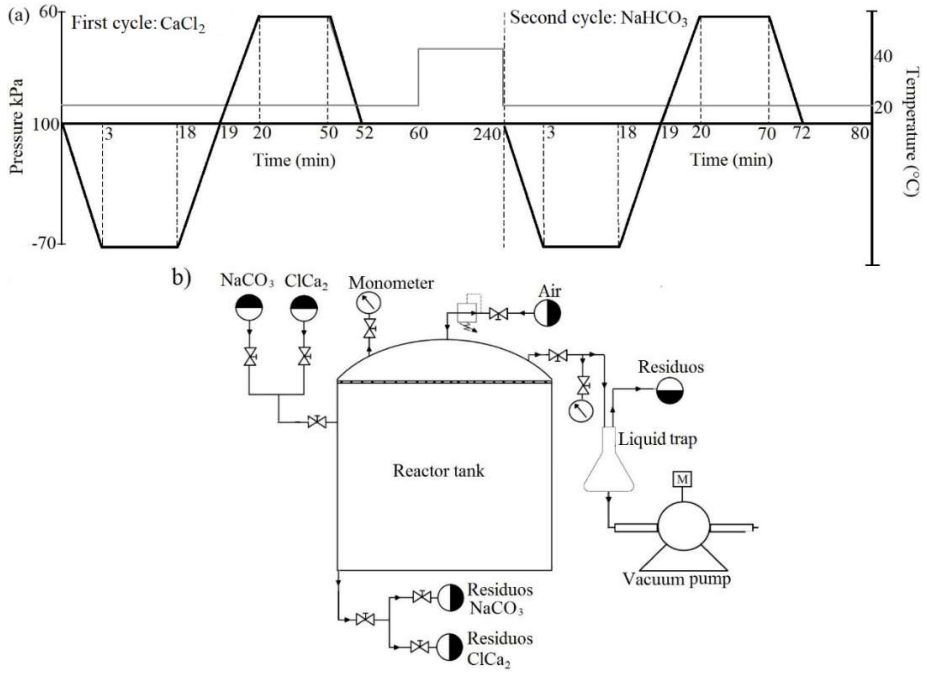

Fig. 1 Pressure flow chart, temperature and time for in-situ mineralization (a) and flow chart of equipment used for in-situ mineralization (b)

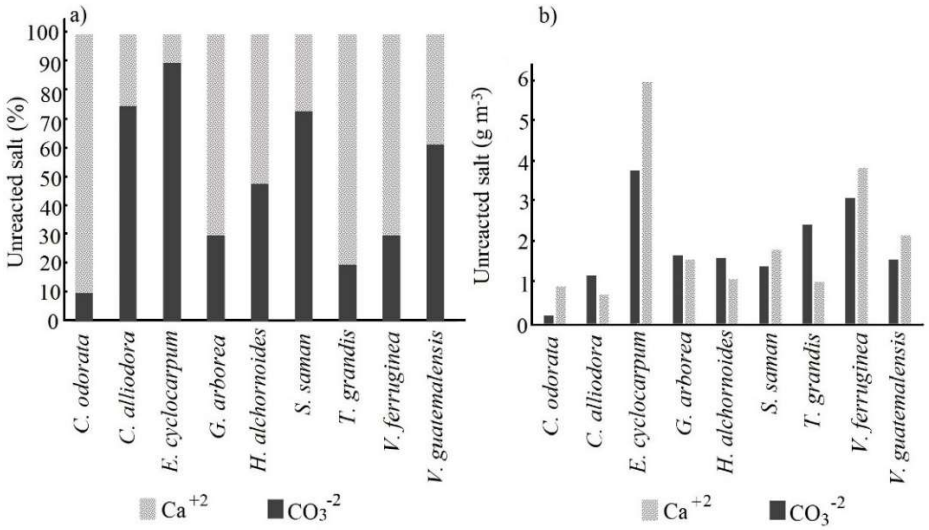

Fig. 2 Percentage (a) and value (b) of the unreacted salt of Ca^{2+} and CO_3^{2-}, in the in-situ mineralization process of nine fast growth tropical species in Costa Rica.

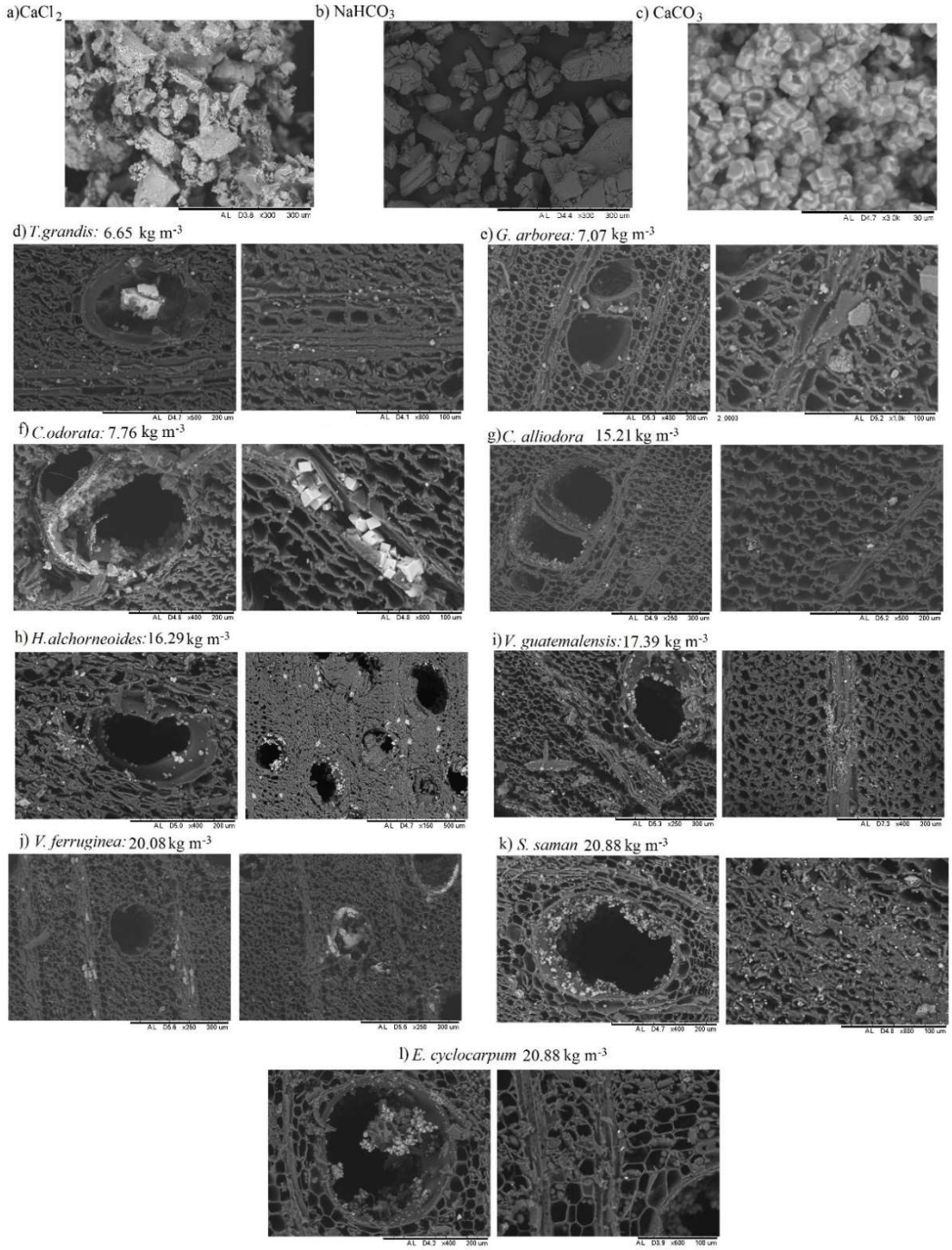

Fig. 3 SEM images of $CaCl_2$ (a), $NaHCO_3$ (b) and $CaCO_3$ (c) salt and SEM images showing in-situ $CaCO_3$ formation in different anatomical features of nine woods from fast growth plantations in Costa Rica.

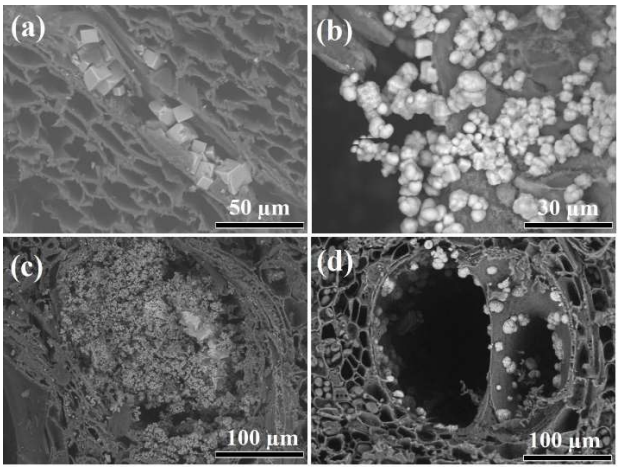

Fig. 4 SEM images of different particle shapes of $CaCO_3$ samples in nine woods from fast growth plantations in Costa Rica (a) calcite particles, (b) vaterite particles, and (c) amorphous particles.

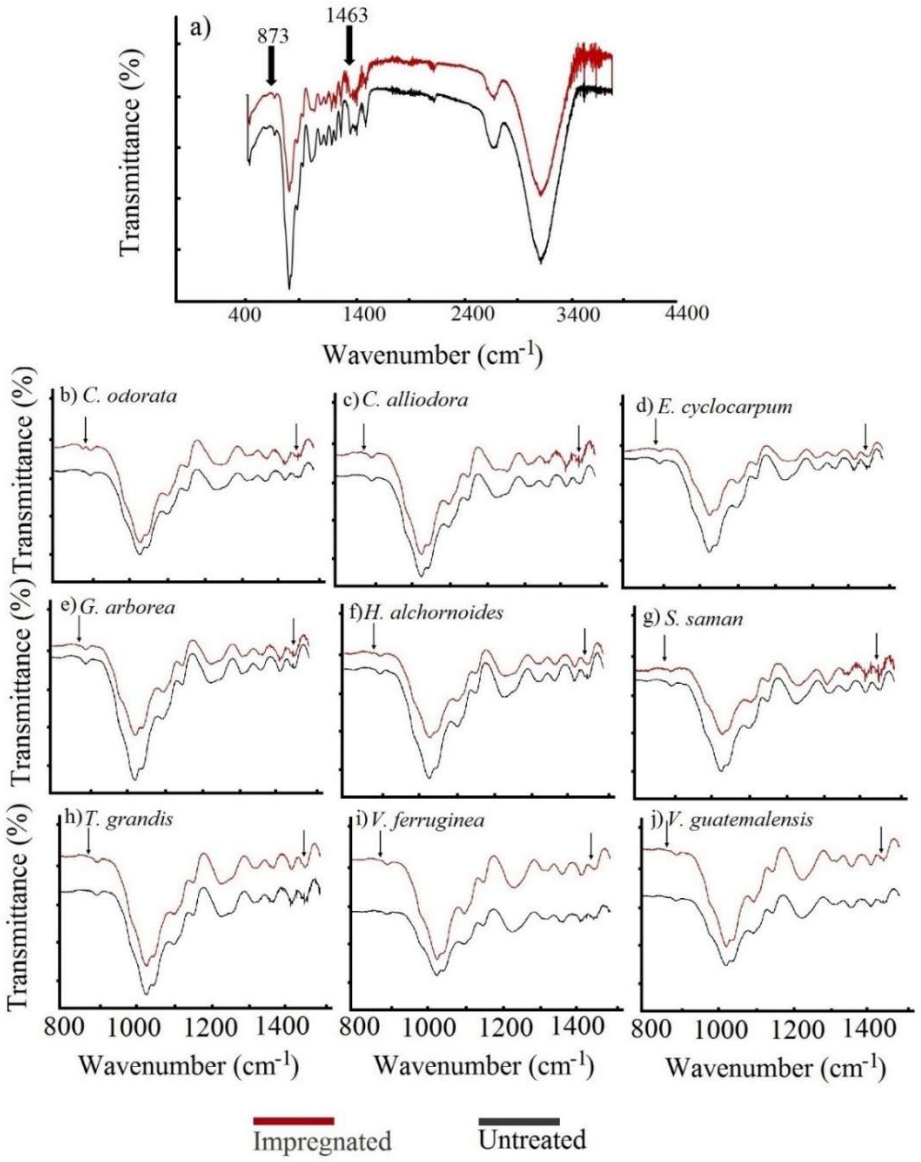

Fig. 5 FTIR spectrum of $CaCO_3$/wood composites (a) and spectrum range from 800 to 1500 cm^{-1} of $CaCO_3$/wood composites of nine fast growth tropical species in Costa Rica (b-j).

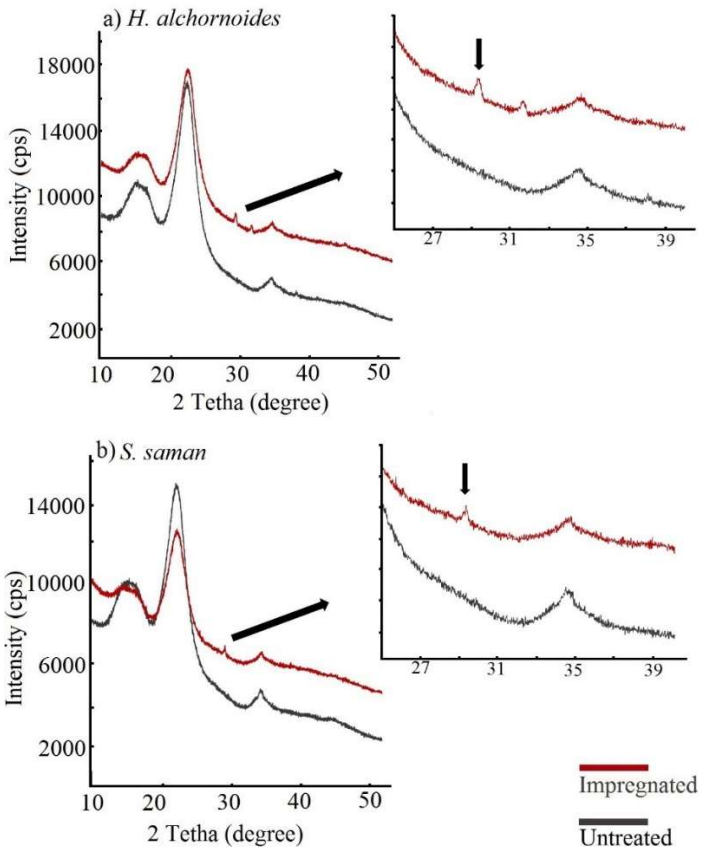

Fig. 6 XDR diffraction of $CaCO_3$/wood composites of nine fast growth tropical species in Costa Rica.

4. Artículo 3. Acetylation of nine tropical hardwood species from forest plantations in Costa Rica - An FTIR spectroscopic analysis.

Acetylation of nine tropical hardwood species from forest plantations in Costa Rica - An FTIR spectroscopic analysis

GAITÁN-ALVAREZ, Johana[1], BERROCAL, Alexander[2], MANTANIS, George I.[3*], MOYA, Roger[4], ARAYA, Fabio[5]

[1]Instituto Tecnológico de Costa Rica, Escuela de Ingeniería Forestal, Apartado 159-7050, Cartago, Costa Rica; Email: jgaitan@itcr.ac.cr, ORCID: 0000-0003-4243-5910

[2]Instituto Tecnológico de Costa Rica, Escuela de Ingeniería Forestal, Apartado 159-7050, Cartago, Costa Rica; Email: aberrocal@itcr.ac.cr, ORCID: 0000-0003-2041-4772

3 University of Thessaly, Dept. of Forestry, Wood Sciences and Design, Lab of Wood Science and Technology, 43100, Karditsa, Greece; Email: mantanis@uth.gr; ORCID: 0000-0002-5715-783X

[4]Instituto Tecnológico de Costa Rica, Escuela de Ingeniería Forestal, Apartado 159-7050, Cartago, Costa Rica; Email: rmoya@itcr.ac.cr; ORCID: 0000-0002-6201-8383

[5]Centro de Investigación y de Servicios Químicos y Microbiológicos (CEQIATEC), Escuela de Química, Instituto Tecnológico de Costa Rica, Cartago 159-7050, Costa Rica; Email: fdaraya@itcr.ac.cr

*Corresponding authors: rmoya@itcr.ac.cr and mantanis@uth.gr

Acetylation of nine tropical hardwood species from forest plantations in Costa Rica - An FTIR spectroscopic analysis

Abstract

Acetylation of softwoods has been broadly investigated in order to increase the dimensional stability and biological resistance of wood. However, the knowledge of this technology has not been applied for tropical hardwood species, up to date. The objective of this work was to study the effect of acetylation on nine tropical hardwood species, from forest plantations in Costa Rica, by applying acetic anhydride in three different treatment times (1h, 2.5h, 4h), as well as to evaluate this by Fourier-transform infrared spectroscopy (FTIR) analysis. Results showed that weight percentage gain (WPG) of wood varied from 2.2% to 16.8%, with *Vochysia ferruginea* wood showing the highest value, and *Gmelina arborea* and *Tectona grandis* species showing the lowest WPGs. Tropical woods such as *Enterolobium cyclocarpum*, *Hieronyma alchorneoides* and *Samanea saman* exhibited statistical differences among treatment times, whereas the rest of the species studied exhibited no significant differences. In general, the most effective acetylation time was 2.5 h, for all the species. The ratio of intensity (RI) from the FTIR spectra was greater at the 1732, 1372 and 1228 cm^{-1} peaks for all species, associated with lignin. A good correlation between the RI of those peaks and WPG was found; the same was also found between all RIs and each other. Meanwhile, RI associated to hemicelluloses and lignin (1592 and 1334 cm^{-1} peaks, respectively) showed no correlation with WPG, nor between each other or with the other RIs. Furthermore, it is suggested that the RI at 1732 cm^{-1} (associated to acetyl groups C=O) can be considered as a reliable indicator of the degree of acetylation for the tropical hardwood species.

Keywords: wood; acetylation; tropical hardwoods; acetic anhydride; hydroxyl group; FTIR spectroscopy.

Introduction

Wood has been used by the humans for centuries, since it is a natural material, easy-to-work, renewable, widely abundant and sustainable [1, 2]. As a lignocellulosic complex, wood does have a structure of cellular walls made of biopolymers such as cellulose and hemicelluloses as well as phenolic polymers like lignin [1, 3, 4]. Despite its positive characteristics, wood can easily be affected by the increasing presence of moisture in its hierarchical structure, which can lead to dimensional instability and/or biological deterioration, or degradation by fungi, insects and bacteria [1, 4]. Polymeric constituents of wood, e.g., lignin, cellulose and hemicelluloses, contain a large amount of free hydroxyl groups [1, 2]. Hemicelluloses, accessible or non-crystalline cellulose, and lignin are mainly responsible for moisture uptake [3, 5]. In these polymers, free hydroxyl groups (OH^- anions) adsorb and release water depending on the changes in temperature and relative humidity causing cell walls -and all of the structure of wood- to adjust to the presence (or absence) of other OH^- anions, such as those of water, thus giving way to changes in dimensional stability of wood, or to potential biological attacks by microorganisms [1, 3, 6].

The presence and amount of hydroxyl groups, capable of forming hydrogen bonds with water molecules, is crucial for dimensional stability. This takes place in sorption sites (as they are commonly termed) which are mainly present in hemicelluloses, followed by cellulose and lignin [7]. Accessibility of these sorption sites in wood has gained much interest as methods to improve wood performance by chemical treatments have been implemented [8]. In the case of cellulose, its configuration in microfibril aggregates makes hydroxyl groups on the surface the only possible sorption sites [9], whereas the amount of sorption sites is much greater in hemicelluloses and lignin [7]. During adsorption in these sites, the water molecule with two full-strength covalent bonds can become bound by two relatively strong H-bonds with a pair of nearby -OH groups of the amorphous polysaccharide polymers, in low moisture content. In meanwhile, conjunction in the H-bond network increases with increasing moisture content, gradually allowing the coalescence of water vapour molecules with already adsorbed water molecules to form water dimers [8]. Thus, this gain in moisture makes the wood dimensionally unstable.

It is due to the dimensional instability that current research sets the objective of implementing chemical modification to wood for lower water uptake, aiming at achieving

higher dimensional stability and increased biological resistance [1, 10–14]. Among these chemical modification techniques, a typical one is that of acetic anhydride [5, 15–18], wherein the OH^- anion group in wood polymeric components becomes chemically bound to a residue of the acetate (CH_3COO) of an acetic anhydride molecule [$(CH_3CO)_2$]; this is well known as, acetylation of wood [1]. In this process, the OH^- anion group is reduced, decreasing hygroscopicity of the wood and thus, increasing its dimensional stability and biological resistance to fungi [4, 19–21]. Markedly, Thybring [19] has clearly stated that decay of acetylated wood cannot progress below 25% moisture content.

As a matter of fact, the composition and distribution of the polymeric constituents in hardwoods differ from those of softwoods, which cause species groups to vary in their sorption sites. Besides these variances, it is true that hardwood species have their own proportion of structural polymeric constituents; therefore, hydroxyl groups are present in different amounts. In hardwood species, hydroxyl groups were reported to be present at percentages of 2.0% to 4.5%, whereas in softwoods, these vary from 0.5% to 1.7% (Rowell, 2016). This difference is attributed to hemicelluloses and lignin compositions: in hardwood species, hemicelluloses contain mostly xylans, while hemicelluloses of softwoods contain mostly glucomannans as well as lignin in a lesser amount [10, 22]. Thus, they possess sorption sites at varying proportions [21, 23].

Studies on wood acetylation have indicated that acetylated softwoods achieve a much higher weight gain, as compared with hardwood species [1], despite the fact they are more abundant in hemicelluloses. Nonetheless, hardwoods contain a higher amount of xylans, which do not have a primary hydroxyl group in which to react [24]. Moreover, softwood species contain a higher percentage of lignin, the polymeric component in which the higher percentage of acetylation typically takes place [1, 3].

In addition to the differences in the type and proportion of hemicelluloses, the anatomical structure differs considerably between wood groups: hardwoods are characterized by the presence of conducting elements such as vessels, whereas softwoods are made of tracheids [25]. This distinction causes the flow of liquids to vary largely, between the wood groups [26], thus affecting the acetylation reaction (associated with the liquid flow in wood) as well as other processes performed in the wood cell walls. In fact, most of the research on

acetylated wood has been focused on softwoods [4], primarily on pine species [16, 17, 27–29].

In spite of these differences, some research work on hardwood species has been carried out. Though, the tropical species remain scarcely known concerning the processes that can be employed in order to improve their physical and biological properties. One of the few studies is that of Matsunaga *et al.* [30] on wood species like *Paraserianthes falcata, Alstonia macrophylla, Pinus caribaea* and *Hevea brasiliensis* which confirmed that acetylation can increase the dimensional stability of wood, up to 60%. Because of the lack of knowledge on the effects of acetylation on tropical hardwoods, there must be a focusing effort to expand the knowledge of the acetylation on such woods, thus widening their potential applications [31], especially for hardwood species of forest plantations.

In Central America, Costa Rica has been implementing reforestation programs with fast-growing plantations that utilize a variety of tropical hardwood species for lumber production [32]. In these programs, early-age tree harvesting yields juvenile wood [4], which is characterized by dimensional instability. Therefore, acetylation provides a way to improve dimensional stability, increase durability and advance other material properties of tropical hardwood species [4, 5, 20, 33, 34]. Given that plantation species in the tropical regions are valuable, research efforts to upgrade the quality of wood and wood products are very important [35].

However, because of the variations in the anatomical structure of tropical hardwoods, which differ from that of softwoods [36], there is insufficient technical information respecting the potential of tropical species for chemical modification, e.g., acetylation [4, 20, 34, 37]. Hence, the aim of this study was to evaluate the effects of acetylation, by using acetic anhydride in liquid phase, on nine tropical hardwood species, commonly cultivated in forest plantations in Costa Rica (*Cedrela odorata, Cordia alliodora, Enterolobium cyclocarpum, Gmelina arborea, Hieronyma alchorneoides, Samanea saman, Tectona grandis, Vochysia ferruginea* and *Vochysia guatemalensis*), and the analysis of key parameters such as solution uptake and weight percentage gain by Fourier-transform infrared spectroscopy (FTIR).

Methodology

Materials

Sapwood, originating from nine Costa Rican fast-growing plantation species, was utilized in the work. It is well established, that only sapwood of these tropical hardwood species has a good permeability [26, 38, 39]. Species used included *Cedrela odorata, Cordia alliodora, Enterolobium cyclocarpum, Gmelina arborea, Hieronyma alchorneoides, Samanea saman, Tectona grandis, Vochysia ferruginea* and *Vochysia guatemalensis*. The wood materials came from plantations varying from 4-8 year-old trees. Once sawn, planks were dried to a moisture content of approx. 12%, and afterwards, 60 samples, measuring 50 mm x 50 mm x 20 mm (radial x tangential x longitudinal) were prepared. The chemical reagents used were: acetic anhydride [$(CH_3CO)_2O$], at 98% concentration (J.T. Baker, Madrid, Spain), and glacial acetic acid [CH_3COOH], at 99% concentration (Químicos Holanda S.A., Costa Rica).

Acetylation process

The acetylation process was carried out in a vacuum-pressure reactor, measuring 10cm in diameter and 31cm in length, with a 2.5 l capacity. The process started by introducing fifteen samples in the reactor, then applying a vacuum for 15 min at -70 kPa (gauge mark), after which, the acetic anhydride and glacial acetic acid solution was introduced in a 92:8 volume ratio, respectively. Once inside, the materials were subjected to a 690 kPa pressure for 30 min, then the excess liquid solution was removed, and nitrogen gas was injected in, to serve as the inert medium to control the internal temperature of the wood. For the reaction, temperature was fixed at 120°C and three different acetylation times were applied for each species, that is, 1h, 2.5h and 4h, labelled as: 1h-acetylation-time, 2.5h-acetylation-time and 4h-acetylation-time, respectively. At the end, the treated samples were rinsed, kept in acetone for 1h, and subsequently left to dry in ambient conditions for one week. Following, they were introduced in a conditioning chamber (for two weeks), at climatic conditions 20ºC and 65% relative humidity, after which, they were weighed up.

Evaluation of the acetylation process

Per each acetylation time, 15 samples, each measuring 50 mm x 50 mm x 20 mm (radial x tangential x longitudinal), were tested. Another set of 15 samples were left untreated

(controls) to be compared with the acetylated materials. For weight measurement, samples were placed into an oven for 24 h, before and after the acetylation process, in order to determine the oven-dry weights. The acetylation process was evaluated by determining the uptake of the solution (uptake) (see Equation 1) and weight percentage gain (WPG), once the process was finished (see Equation 2), considering the weight of the sample in oven-dry condition as the initial weight.

$$Uptake\ \left(\frac{liters}{m^3}\right) = \left(\frac{Weig\quad before\ acetylation(g) - Weig\quad after\ acetylation(g)}{Volumen\ of\ cample\ (cm^3)}\right) x\ \frac{1\ liters}{1000} \quad (1)$$

$$Weight\ percentage\ gain\ (WPG) = \frac{Weig\quad after\ acetylation(g) - Weig\quad before\ acetylation(g)}{Weig\quad before\ acetylation(g)} x100 \quad (2)$$

Fourier Transform Infrared Spectroscopy (FTIR)

One sample per treatment interval as well as one untreated sample was taken per each species and ground to a size of 420 µm and 250 µm, 40 and 60 mesh, respectively. These samples were oven-dried at 105°C until reaching a constant weight. This was followed by a FTIR scan using a Nicolet 380 FTIR spectrometer (Thermo Scientific, Mundelein, Illinois, USA) with a single reflecting cell, equipped with a diamond prism. The equipment was configured to perform readings accumulating 32 explorations, with a 1 cm^{-1} resolution, with background correction before each measurement. The obtained FTIR spectra were processed with Spotlight 1.5.1, HyperView 3.2 and Spectrum 6.2.0 software, developed by Perkin Elmer Inc (Waltham, Massachusetts, USA).

The main vibrations, where the biggest changes occurred in the wood, were identified (Fig. 1); present in the peaks at 1034 cm^{-1} (carbon–oxygen (C–O) stretching), at 1228 cm^{-1} (carbon–hydrogen (C–H) stretching), at 1372 cm^{-1} (methyl group (of the acetyl unit) stretching in cellulose and hemicelluloses), at 1592 cm^{-1} (conjugated carbonyl (C=O) stretching), and at 1732 cm^{-1} (non-conjugated carbonyl (C=O) stretching). Then, the ratio of the intensity transmission of those groups at 1034, 1228, 1372, 1592 and 1732 cm^{1} was assessed between the control (untreated) samples and the acetylated samples (Equation 3).

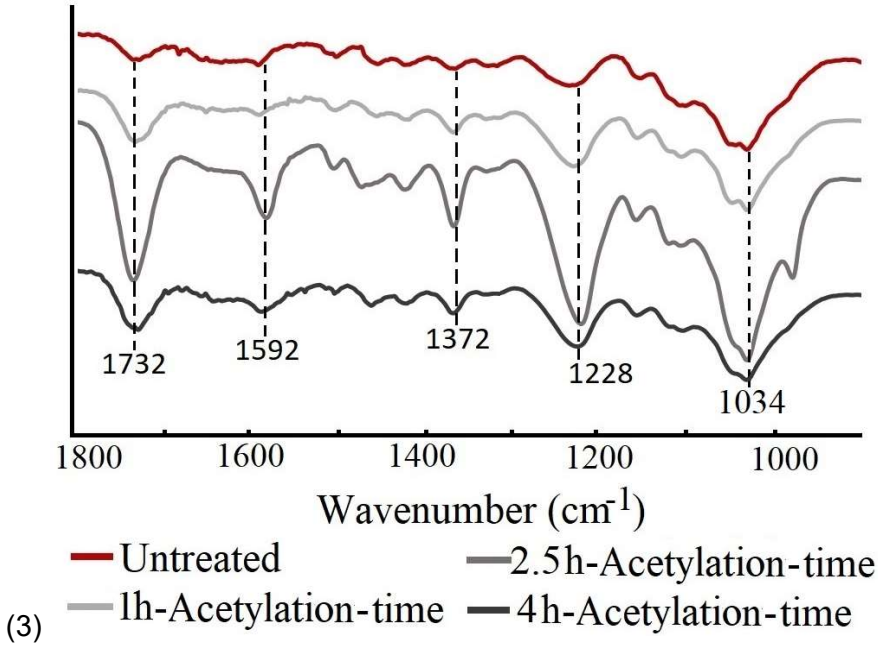

(3)

Fig. 1. FTIR spectra of *V. ferruginea* wood treated with acetic anhydride at three different acetylation times.

Statistical analysis

First, the data were tested for normality and homogeneity, and strange data or outliers of the variables evaluated were eliminated. Then, a descriptive analysis was carried out: the mean and the standard deviation (SD) were determined for each variable studied. A variance analysis (ANOVA) with a statistical significance level at $p<0.05$ was applied to determine the effect of acetylation time (independent variable) on the uptake and WPG (response variables). Tukey's test was used to determine the statistical significance of the difference between the means of the variables. A second analysis was carried out to establish correlations between the WPG and the IR of the peaks affected by acetylation (1034, 1228, 1372, 1592 and 1732 cm^{-1}). This analysis was performed with the software SAS 9.4 (SAS Institute Inc., Cary, NC, USA).

Results

Evaluation of the acetylation process

The uptake of the acetylation solution (uptake) varied from 98.8 l/m^3 to 591.1 l/m^3, with *V. ferruginea* showing the highest values, and *G. arborea* showing the lowest ones (Table 1). In *V. ferruginea, V. guatemalensis, C. alliodora, G. arborea, C. odorata* and *T. grandis* no statistical differences appeared for both parameters (uptake and WPG) among the acetylation times (Table 1). No statistically significant differences were observed between the acetylation times for *E. cyclocarpum*, *S. saman* and *H. alchorneoides* (Table 1). In *H. alchorneoides*, the highest uptake occurred in 1h-acetylation-time, then in 2.5h-acetylation-time, while the lowest one occurred in 4h-acetylation-time. The WPG varied from 2.2% to 16.8%; the highest values exhibited by *V. ferruginea* and the lowest ones shown by *G. arborea* (Table 1). Wood samples of *E. cyclocarpum*, *H. alchorneoides* and *S. saman* exhibited statistically significant differences among the different acetylation times, unlike the other species. Specifically, for *E. cyclocarpum* and *H. alchorneoides* woods, the lowest WPGs were observed at the 4h-acetylation-time (Table 1). Also, *S. saman* wood showed differences, but its lowest WPG was observed in 1h-acetylation-time, whereas its highest WPG was observed in 2.5h-acetylation-time (Table 1). The very low WPG values obtained at the prolonged reaction time (4 h) may be attributed to the thermal degradation of wood polymers.

Table 1. Uptake and weight percentage gain of wood from nine tropical woods treated with acetic anhydride at three different acetylation times.

Wood species	Acetylation time (h)	Uptake (l/m^3)	Weight percentage gain
Vochysia ferruginea	1.0	591.1 (58.2)^{A*}	16.8 (0.7)**^{A}
	2.5	538.8 (56.3)^{A}	16.3 (1.5)^{A}
	4.0	574.4 (63.8)^{A}	16.4 (1.5)^{A}
Vochysia guatemalensis	1.0	562.2 (80.4)^{A}	17.4 (1.6)^{A}
	2.5	547.1 (62.0)^{A}	17.3 (1.8)^{A}
	4.0	535.6 (32.2)^{A}	15.4 (1.6)^{A}
Enterolobium cyclocarpum	1.0	564.3 (89.6)^{B}	11.9 (2.4)^{AB}
	2.5	587.3 (47.0)^{B}	13.5 (2.4)^{B}
	4.0	479.1 (53.7)^{A}	9.7 (0.9)^{A}
Cordia alliodora	1.0	448.3 (94.0)^{A}	10.9 (1.4)^{A}
	2.5	289.6 (22.5)^{A}	8.3 (0.7)^{A}
	4.0	309.8 (17.0)^{A}	7.8 (0.7)^{A}
S-amanea saman	1.0	356.9 (19.2)^{A}	4.5 (0.3)^{A}
	2.5	441.7 (12.0)^{C}	8.5 (0.4)^{C}
	4.0	282.8 (16.8)^{B}	6.8 (0.3)^{B}
Hieronyma alchorneoides	1.0	457.3 (41.0)^{B}	6.6 (0.4)^{B}
	2.5	340.6 (43.3)^{A}	5.2 (0.3)^{A}
	4.0	286.3 (79.0)^{A}	4.8 (0.2)^{A}
Gmelina arborea	1.0	98.8 (12.1)^{A}	2.2 (0.7)^{A}
	2.5	127.4 (12.6)^{A}	2.6 (1.0)^{A}
	4.0	117.3 (64.9)^{A}	2.7 (1.6)^{A}
Cedrela odorata	1.0	159.2 (36.3)^{A}	5.1 (1.3)^{A}
	2.5	159.6 (32.6)^{A}	4.9 (0.9)^{A}
	4.0	140.3 (27.0)^{A}	4.5 (1.0)^{A}
Tectona grandis	1.0	156.7 (13.1)^{A}	2.6 (0.4)^{A}
	2.5	149.5 (20.4)^{A}	2.5 (0.4)^{A}
	4.0	160.4 (20.1)^{A}	2.6 (0.2)^{A}

*Different letters between acetylation times for a given parameter indicate statistical differences at 99%. **Values in the parentheses represent the standard deviations (SD).

Fourier-transform Infrared Spectroscopy (FTIR) analysis

The FTIR spectra showed that in the esterification of the hydroxyl groups by acetic anhydride, the signal intensity of acetyl groups increased at 1732, 1592, 1372, 1228 and 1034 cm^{-1} (Fig. 1). The calculation of the ratio of intensity (RI) of these signals revealed greater intensity in signals at 1732, 1372 and 1228 cm^{-1} for all the tropical species studied (Fig. 2). The highest WPGs, after acetylation, occurred in *V. ferruginea, V. guatemalensis*, *E. cyclocarpum, C. alliodora* and *S. saman* woods (Table 1), which showed the highest intensities in the 1732, 1372 and 1228 cm^{-1} peaks (Fig. 2a-e). On the contrary, species with lower uptakes, for instance, *H. alchorneoides, G. arborea*, *C. odorata* and *T. grandis* species (Table 1) presented the lowest RIs in such signals (Fig. 2f-i). This behavior was confirmed upon establishing the coefficients of correlation, between the WPG and RI (Table 2), which indicated a positive and significant correlation between the 1732, 1372 and 1228 cm^{-1} peaks and the WPG values.

Also, the other RIs that were influenced by acetylation (1592 and 1034 cm^{-1} peaks) did not present a statistically significant correlation with the WPG of the tropical species tested (Table 2). Markedly, upon establishing correlation between the signal intensities affected by acetylation, the signals with greater RIs (1732, 1372 and 1228 cm^{-1} peaks) were correlated with each other (Table 2). Signals with the lower RIs (1592 and 1034 cm^{-1} peaks), on the other hand, did not show correlation with each other, nor did they present any relation with signals of greater RI (Table 2).

Table 2. Pearson correlation matrix of WPG and ratios of intensity of the transmittance in FTIR spectra of acetylated Costa Rican tropical hardwoods.

	WPG	**Peak at 1034 cm^{-1}**	**Peak at 1228 cm^{-1}**	**Peak at 1372 cm^{-1}**	**Peak at 1592 cm^{-1}**	**Peak at 1732 cm^{-1}**
WPG	1					
Peak at 1034 cm^{-1}	0.40^{NS**}	1				
Peak at 1228 cm^{-1}	0.60*	0.06^{NS}	1			
Peak at 1372 cm^{-1}	0.71*	0.13^{NS}	0.92*	1		
Peak at 1590 cm^{-1}	0.24^{NS}	0.17^{NS}	0.36^{NS}	0.21^{NS}	1	
Peak at 1732 cm^{-1}	0.79*	0.12^{NS}	0.91*	0.93*	0.30^{NS}	1

Indicates a statistical significance at level $p<0.05$; **NS: Not statistically significant.

For all species, there was an increase in intensity of the bands at the 1h- and 2.5h-acetylation-time, whereas, at the 4h-acetylation-time a decrease was noted (Fig. 2 a-i). The only exceptions were observed for the wood species *S. saman* and *H. alchorneoides* which presented an increase in RI values at the 1h-acetylation-time, then a noticeable decrease at the 2.5h-acetylation-time, and finally, a slight increase at the 4h-acetylation-time (Fig. 2e-f).

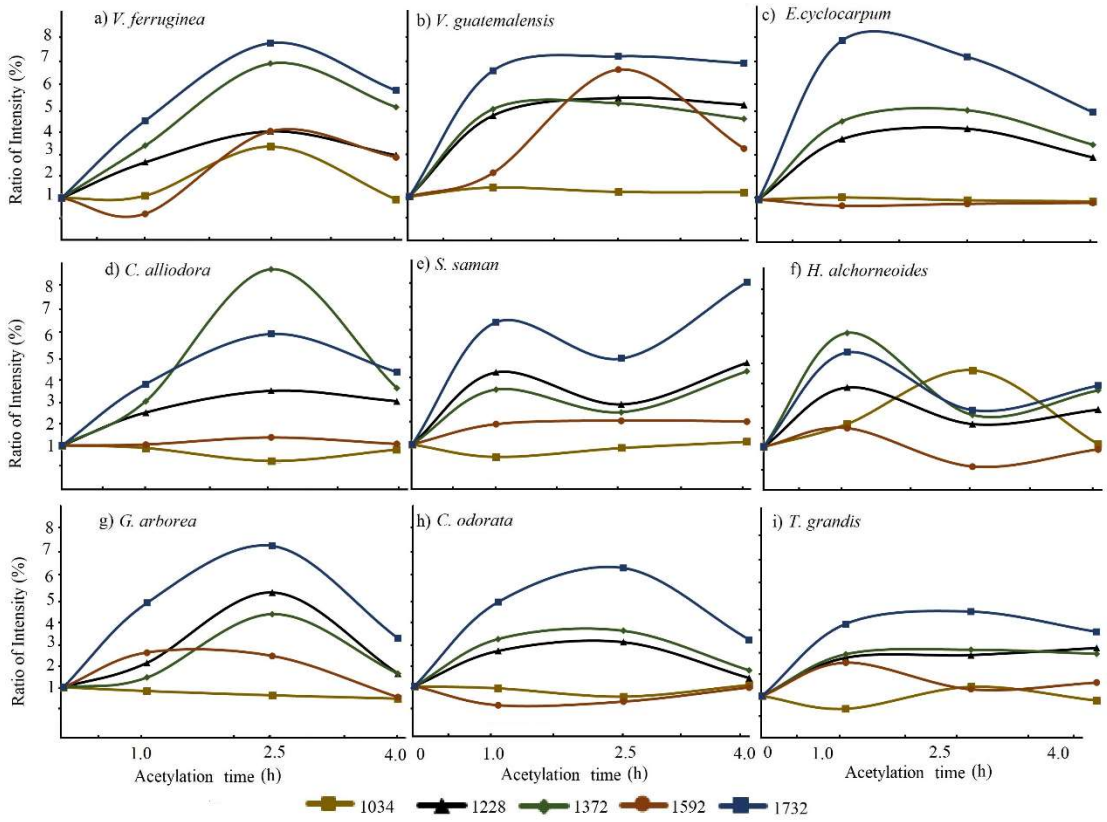

Fig. 2. Ratio of intensity of the transmittance in FTIR spectra of acetylated tropical hardwoods modified in different acetylation times.

Discussion

WPG values of wood, after acetylation, were quite lower than these reported for some softwood species, since WPG values around 20% have been reported [1, 5, 16, 28, 40]. This discrepancy may be attributed to the much lower permeability of the tropical species used in this study, since the uptake ranged from 98.8 to 591.1 l/m^3 in treated wood (Table 1). Liquid uptake in hardwoods is largely related with the permeability of the wood species [41,

42]. That varies as a function of the anatomical characteristics of each species. Even after wood is formed in the trees, its porosity can be changed by biological deterioration and/or by thermal modification in different mediums.

In hardwood species, liquid flow chiefly occurs along the vessel lumina in longitudinal orientation [42], but this flow can be interrupted by the presence of tyloses and gums into the vessels [42]. Vessels connect longitudinal and radial parenchyma across wall pits, so liquids can then flow through the radial lumina [42]. This flow is favored when the rays are composed of over 3 series in width, and of more abundant parenchyma [42]. Variations in the anatomy of the tropical species, tested in this work, were presented and discussed by Moya *et al.*[26]. These authors mentioned that the species *E. cyclocarpum*, *H. alchorneoides*, *S. saman*, *V. ferruginea* and *V. guatemalensis* have anatomical features of larger dimensions, that is: vessels' diameter (over 120 µm), rays' width (from 2 to 10 series of cells or over 252 µm) and rays frequency (over 5 rays per tangential mm), as well as some types of parenchyma [26]. Hence, such anatomical features favor the flow of acetic anhydride and acetic acid solutions. This is in accordance with the results of the present work, in which, the above-mentioned wood species, indeed, exhibited higher uptake and WPG values (Table 1). Quite the opposite, wood species like *C. odorata*, *G. arborea* and *T. grandis* resulted in greatly lower uptake and WPG (Table 1). This is because, as postulated in here, their anatomical features are very unfavorable to liquid flow (e.g., smaller and less-frequent rays, plenty of gums and tyloses in the vessels, fewer vessel-associated axial parenchyma) [26].

The WPGs obtained by the tropical species tested are due to the fact that these species present dissimilar degrees of permeability in their anatomical structures, which in turns influences the acetylation of functional groups. According to Rowell [2], when WPG is close to 4%, due to wood permeability, there is more bonded acetyl in the S2 layer than in the middle lamella; at a WPG of about 10%, acetyl is equally distributed throughout the S2 layer and middle lamella; and with WPG at 20%, there is a slightly higher concentration of acetyl in the middle lamella than in the rest of the cell wall. Then, acetylation of the acetyl groups is expected to be as follows: higher for *V. guatemalensis* and *V. ferruginea*, in all the wood structure, with special emphasis in the middle lamella; uniform for *E. cyclocarpum*, *C. alliodora* and *S. saman* in all the wood structure; and lower for *H. alchorneoides*, *G. arborea*, *C. odorata* and *T. grandis*, since acetylation occurs mainly on the S2 layer of the cellular

wall, probably over acetyl groups from lignin, which presents the highest degree of acetylation [43].

In most species, reaction time did not have a significant effect on the uptake, except for *E. cyclocarpum*, *S. saman* and *H. alchorneoides*, for which the 4h-acetylation-time treatment yielded a significantly lower uptake (Table 1). This large decrease may be attributed to the completion of the acetylation reaction well before the time limit. After some time, the reaction slows and levels off, indicating that the reaction is 'complete' [43]. Then, once acetylation is fulfilled, degradation of the acetic anhydride may have been taken place, since the temperature used for the process (120°C) was close to boiling temperature of this compound (139°C). This suggests that prolonged reaction time is not suitable for species like *E. cyclocarpum*, *S. saman* and *H. alchorneoides*, as the wood and the compound itself appeared to be affected negatively.

The main changes undergone in acetylated wood can be observed in the peaks at 1228, 1372 and 1732 cm^{-1} in all species (Fig. 2), which are in agreement with other studies. In fact, according to Stefke *et al.* [44] and Schwanninger *et al.* [45], these bands are assigned to valence vibrations of acetyl C=O groups (1745 cm^{-1}), aliphatic C–H deformation vibrations in CH_3 (1374 cm^{-1}), the asymmetric C–O stretching vibration from the ester group grafted (C–O–C=O at 1240 cm^{-1}) and C–C plus C–O stretching plus aromatic =C–H in plane deformation vibrations (1265 cm^{-1} from lignin, which is overlapped by the latter, with an increasing number of acetyl groups) as well as the C–O valence vibration (1034 cm^{-1}) from cellulose, hemicelluloses and lignin. Nonetheless, the other two signals (1034 and 1592 cm^{-1}) are important in those species with a higher uptake value, specifically in *V. ferruginea* and *V. guatemalensis* (Fig. 2a-b). This result evidences that acetylation is scarce in the methyl group (of the acetyl unit) stretch (1372 cm^{-1}) and the conjugated carbonyl (C=O) stretch (1592 cm^{-1}) in cellulose and hemicelluloses; in fact, it showed no relation with WPG (Table 2). According to Rowell [33], acetylation occurs mostly in lignin, by 82%, and to a much lesser extent in hemicelluloses and cellulose; therefore, a low signal is to be expected in 1372 and 1592 cm^{-1} intensities. This outcome is in agreement with the very low acetylation of the acetyl groups occurring in the hemicelluloses and cellulose of the tropical woods tested in this work.

Regarding the main signals in acetylation intervals, the maximum acetylation signal occurs within 1 h for *S. saman and H. alchorneoides* (Fig. 2c, 2f), whereas for most species the most efficient acetylation time seemed to be within 2.5 h, as from then on, a decline in the signal takes place, probably due to a thermal degradation of wood upon continued exposure to temperature [43].

Moreover, the RI of peaks associated to acetylation of lignin (1228, 1372 and 1732 cm^{-1}) was related to WPG (Table 2). As for WPG variation (Table 1), and considering all signals are associated to lignin, it is likely that acetyl groups are the same in all species [46], indicating that acetylation of the tropical wood species is almost exclusively associated with the permeability of each species. The variation present in the anatomical structure of the samples is associated to permeability of the hardwood species [41, 42]. Consequently, conductive elements control whether adsorbed acetic anhydride can reach hydroxyl groups in lignin or not: the higher the uptake, the greater the possibility for acetic anhydride to access more bonded acetyl in the S2 layer of the cell wall, or else the acetyl groups in the middle lamella [33] where lignin is present in larger proportion [23]. Accessibility of lignin in tropical species is also evidenced by the correlation between RI associated to it (1732, 1372 and 1228 cm^{-1} peaks), which showed high correlation with each other and presented correlation with the WPG as well (Table 2). However, considering the different coefficients of correlation, it is clear that the highest value comes at 1732 cm^{-1} intensity (associated to acetyl C=O groups), which registers a coefficient of 0.79 (Table 2). Consequently, this RI may be suggested as a good indicator for measuring the degree of acetylation of such tropical hardwood species.

In the acetylation of acetyl groups associated to hemicelluloses and cellulose (1372 and 1592 cm^{-1}, respectively), the biggest variation presented among the species (Fig. 2) was associated with the large variety of types and amount of hemicelluloses present in wood [22]. Each one of the species shows different proportions of the various types of monomers conforming wood hemicelluloses [43], resulting in varying degrees of acetylation and different signals per species. Correspondingly, in this work, this behavior became evident upon observing that the 1372 and 1592 cm^{-1} peaks of RI did not show any correlation with the WPG (Table 2).

Conclusions

Wood samples from nine tropical hardwood species, from forest plantations in Costa Rica, were chemically modified with acetic anhydride, using three different treatment times, namely, 1h, 2.5h and 4h. Analysis of the acetylation was carried out by the Fourier-transform infrared spectroscopy technique. Results showed that WPGs varied from 2.2% to 16.8%, with *Vochysia ferruginea* species exhibiting the highest WPG, whilst *Gmelina arborea* wood exhibited the lowest WPG value.

Other tropical woods like *Enterolobium cyclocarpum*, *Hieronyma alchorneoides* and *Samanea saman* showed to have statistical differences among treatment times, whereas the rest of the species studied exhibited no significant differences. In general, the most effective acetylation time was 2.5 h, for all the tropical hardwood species tested.

Besides, as shown by Gaitán-Álvarez *et al.* (2020), tropical woods with less suitable anatomical features for liquid flow, e.g., smaller and less-frequent radii, large amounts of deposits in the vessels, such as gums and tyloses, and fewer parenchyma associated to vessels, can have lower WPG values in modification or impregnation treatments. As a matter of fact, this was proved to be true, as speculated, for wood species with such unfavorable structural features, like the species *Cedrela odorata*, *Gmelina arborea* and *Tectona grandis.*

In addition, it was found that the ratio of intensity (RI) from the FTIR spectra was greater at the 1732, 1372 and 1228 cm^{-1} peaks for all species, associated with lignin. A positive correlation between the RI of those peaks and WPGs was found. Tropical wood species, as shown, tend to present a substantial variability in the degree of acetylation, considering the WPG and the ratios of intensity at 1732, 1592, 1372, 1228 and 1334 cm^{-1} peaks of the FTIR spectrum.

Conclusively, it was found that the RI of peaks associated to acetylation (1228, 1372 and 1732 cm^{-1}) can be considered as a reliable indicator of the degree of acetylation for the tropical hardwoods tested. These RIs increased with an increment in WPG, leaving the IR at 1732 cm^{-1} (associated to C=O, acetyl groups) as a good index for measuring the degree of acetylation in tropical hardwood species.

Acknowledgements

The authors wish to thank the *Vicerrectoría de Investigación y Extensión*, of the Instituto Tecnológico de Costa Rica (TEC - Cartago, Costa Rica) for the project financial support. This research project was carried out in cooperation with Lab of Wood Science and Technology, of the University of Thessaly (Dept. of Forestry, Wood Sciences and Design), Karditsa, Greece. Prof. G.I. Mantanis would like to acknowledge the contribution of program *Erasmus+ KA107 (International Credit Mobility)* for enabling this type of academic interaction, between TEC and Univ. of Thessaly.

Conflict of interest: The authors declare absolutely no conflict of interest.

Availability of data and materials: the data are disposition

Funding: the funding was provided by *Vicerrectoría de Investigación y Extensión*, of the Instituto Tecnológico de Costa Rica

Authors' contributions: GAITÁN-ALVAREZ, Johana contributed with tree sampling, determining wood properties and running the data analysis. BERROCAL, Alexander and coordinating the research project and running the data analysis. MANTANIS, George I, contributed with designing the experiment and writing the paper. MOYA, Roger contributed with designing the experiment, tree sampling, writing the paper and coordinating the research project. ARAYA, Fabio. Contributed with contributed with designing the experiment.

References

1. Hill CAS (2006) Wood Modification. John Wiley & Sons, Ltd, Chichester, UK, UK

2. Rowell RM (2006) Acetylation of wood: journey from analytical technique to commercial reality. For Prod J 56:4–12

3. Rowell RM (2004) Solid Wood Processing - Chemical Modification. In: Encyclopedia of Forest Sciences. Elsevier, pp 1269–1274

4. Adebawo FG, Naithani V, Sadeghifar H, et al (2016) Morphological and interfacial properties of chemically-modified tropical hardwood. RSC Adv 6:6571–6576. https://doi.org/10.1039/C5RA19409A

5. Rowell RM (2006) Chemical modification of wood: A short review. Wood Mater Sci Eng

1:29–33. https://doi.org/10.1080/17480270600670923

6. Giridhar BN, Pandey KK, Prasad BE, et al (2017) Dimensional stabilization of wood by chemical modification using isopropenyl acetate. Maderas Cienc y Tecnol 19:15–20. https://doi.org/10.4067/S0718-221X2017005000002

7. Engelund ET, Thygesen LG, Svensson S, Hill CAS (2013) A critical discussion of the physics of wood–water interactions. Wood Sci Technol 47:141–161. https://doi.org/10.1007/s00226-012-0514-7

8. Willems W (2018) Hygroscopic wood moisture: single and dimerized water molecules at hydroxyl-pair sites? Wood Sci Technol 52:777–791. https://doi.org/10.1007/s00226-018-0998-x

9. Hofstetter K, Hinterstoisser B, Salmén L (2006) Moisture uptake in native cellulose - The roles of different hydrogen bonds: A dynamic FT-IR study using Deuterium exchange. Cellulose 13:131–145. https://doi.org/10.1007/s10570-006-9055-2

10. Hill CAS, Forster SC, Farahani MRM, et al (2005) An investigation of cell wall micropore blocking as a possible mechanism for the decay resistance of anhydride modified wood. Int Biodeter Biodegr 55:69–76. https://doi.org/10.1016/j.ibiod.2004.07.003

11. Rowell R (2016) Dimensional stability and fungal durability of acetylated wood. Drewno 59:139–150. https://doi.org/10.12841/wood.1644-3985.C14.04

12. Lykidis C, Bak M, Mantanis G, Németh R (2016) Biological resistance of pine wood treated with nano-sized zinc oxide and zinc borate against brown-rot fungi. Eur J Wood Wood Prod 74:909–911. https://doi.org/10.1007/s00107-016-1093-3

13. Mantanis GI (2017) Chemical modification of wood by acetylation or furfurylation: A review of the present scaled-up technologies. BioResources 12:4478–4489

14. Taghiyari HR, Bayani S, Militz H, Papadopoulos AN (2020) Heat Treatment of Pine Wood: Possible Effect of Impregnation with Silver Nanosuspension. Forests 11:466. https://doi.org/10.3390/f11040466

15. Papadopoulos AN, Bikiaris DN, Mitropoulos AC, Kyzas GZ (2019) Nanomaterials and Chemical Modifications for Enhanced Key Wood Properties: A Review. Nanomaterials 9:607. https://doi.org/10.3390/nano9040607

16. Papadopoulos AN, Hill CAS (2002) The biological effectiveness of wood modified with linear chain carboxylic acid anhydrides against Coniophora puteana. Holz Roh-Werkst 60:329–332. https://doi.org/10.1007/s00107-002-0327-8

17. Papadopoulos AN, Hill CAS (2003) The sorption of water vapour by anhydride modified softwood. Wood Sci Technol 37:221–231. https://doi.org/10.1007/s00226-003-0192-6

18. Papadopoulos AN (2006) Chemical modification of pine wood with propionic anhydride: Effect on decay resistance and sorption of water vapour. BioResources 1:67–74.

https://doi.org/10.15376/biores.1.1.67-74

19. Thybring EE (2013) The decay resistance of modified wood influenced by moisture exclusion and swelling reduction. Int Biodeter Biodegr 82:87–95. https://doi.org/10.1016/j.ibiod.2013.02.004

20. Adebawo F, Sadeghifar H, Tilotta D, et al (2019) Spectroscopic interrogation of the acetylation selectivity of hardwood biopolymers. Starch - Stärke 71:1900086. https://doi.org/10.1002/star.201900086

21. Ringman R, Beck G, Pilgård A (2019) The Importance of moisture for brown rot degradation of modified wood: A critical discussion. Forests 10:522. https://doi.org/10.3390/f10060522

22. Wang S, Dai G, Yang H, Luo Z (2017) Lignocellulosic biomass pyrolysis mechanism: A state-of-the-art review. Prog Energy Combust Sci 62:33–86. https://doi.org/10.1016/j.pecs.2017.05.004

23. Engelund ET, Thygesen LG, Svensson S, Hill CAS (2013) A critical discussion of the physics of wood–water interactions. Wood Sci Technol 47:141–161. https://doi.org/10.1007/s00226-012-0514-7

24. Rowell RM (2014) Acetylation of wood - A review. International Journal of Lignocellulosic Products 1(1):1-27. doi:10.22069/ijlp.2014.1920

25. Gibson LJ (2012) The hierarchical structure and mechanics of plant materials. J R Soc Interface 9:2749–2766. https://doi.org/10.1098/rsif.2012.0341

26. Moya R, Gaitan-Alvarez J, Berrocal A, Araya F (2020) Effect of CaCO3 in the wood properties of tropical hardwood species from fast-grown plantation in Costa Rica. BioResources (in press)

27. Larsson Brelid P, Simonson R, Bergman Ö, Nilsson T (2000) Resistance of acetylated wood to biological degradation. Holz Roh-Werkst 58:331–337. https://doi.org/10.1007/s001070050439

28. Passarini L, Zelinka SL, Glass S V., Hunt CG (2017) Effect of weight percent gain and experimental method on fiber saturation point of acetylated wood determined by differential scanning calorimetry. Wood Sci Technol 51:1291–1305. https://doi.org/10.1007/s00226-017-0963-0

29. Huang X, Kocaefe D, Kocaefe Y, Pichette A (2018) Combined effect of acetylation and heat treatment on the physical, mechanical and biological behavior of jack pine (Pinus banksiana) wood. Eur J Wood Wood Prod 76:525–540. https://doi.org/10.1007/s00107-017-1232-5

30. Matsunaga M, Hewage DC, Kataoka Y, et al (2016) Acetylation of wood using supercritical carbon dioxide. J Trop For Sci 28:132–138

31. Bollmus S, Bongers F, Gellerich A, et al (2015) Acetylation of German

Hardwoods. In: Proc of 8th European conference on wood modification. Helsini, Finland., pp 164–173

32. Moya R (2018) La producción de madera de especies nativas en plantaciones comerciales: una opción real. Ambientico 267:32–36

33. Rowell R (2016) Dimensional stability and fungal durability of acetylated wood. Drewno 59:139–150. https://doi.org/10.12841/wood.1644-3985.C14.04

34. Ozmen N (2007) Dimensional Stabilisation of Fast Growing Forest Species by Acetylation. J Appl Sci 7:710–714. https://doi.org/10.3923/jas.2007.710.714

35. Kojima M, Yamamoto H, Okumura K, et al (2009) Effect of the lateral growth rate on wood properties in fast-growing hardwood species. J Wood Sci 55:417–424. https://doi.org/10.1007/s10086-009-1057-x

36. Rowell R (2012) Handbook of Wood Chemistry and Wood Composites. CRC Press

37. Pardo T, Alfaro J (2014) White-rot fungal decay resistance of teak and melina wood treated with acetic anhydride. Int Biodeter Biodegr 88:44–47. https://doi.org/10.1016/j.ibiod.2013.12.001

38. Moya R, Salas C, Berrocal A, Valverde JC (2015) Evaluation of chemical compositions, air-dry, preservation and workability of eight fastgrowing plantation species in Costa Rica. Madera Bosques 21:31-47. doi: 10.21829/myb.2015.210424

39. Tenorio C, Moya R, Salas C, Berrocal A (2016) Evaluation of wood properties from six native species of forest plantations in Costa Rica. Bosque 37:71-84. https://doi.org/10.4067/S0717-92002016000100008

40. Ramsden MJ, Blake FSR, Fey NJ (1997) The effect of acetylation on the mechanical properties, hydrophobicity, and dimensional stability of Pinus sylvestris. Wood Sci Technol 31:97–104. https://doi.org/10.1007/s002260050019

41. Thomas RJ (1976) anatomical features affecting liquid penetrability in three hardwood species. Wood Fiber Sci 4:256–263

42. Ahmed SA, Chun SK (2009) Observation of liquid permeability related to anatomical characteristics in Samanea saman. Turkish J Agric For 33:155–163. https://doi.org/10.3906/tar-0807-13

43. Rowell R, Ibach R (2018) Stable and durable wood products based on molecular modification. J Trop For Sci 30:488–495

44. Stefke B, Windeisen E, Schwanninger M, Hinterstoisser B (2008) Determination of the weight percentage gain and of the acetyl group content of acetylated wood by means of different infrared spectroscopic methods. Anal Chem 80:1272–1279. https://doi.org/10.1021/ac7020823

45. Schwanninger M, Stefke B, Hinterstoisser B (2011) Qualitative Assessment of

Acetylated Wood with Infrared Spectroscopic Methods. J Near Infrared Spectrosc 19:349–357. https://doi.org/10.1255/jnirs.942

46. Ohkoshi M (2002) FTIR-PAS study of light-induced changes in the surface of acetylated or polyethylene glycol-impregnated wood. J Wood Sci 48:394–401. https://doi.org/10.1007/BF00770699

5. Artículo 4. Wood properties of nine acetylated tropical woods from fast-growth plantations in Costa Rica.

Wood properties of nine acetylated tropical woods from fast-growth plantations in Costa Rica

Johana GAITAN-ALVAREZ

Instituto Tecnológico de Costa Rica, Escuela de Ingeniería Forestal, Apartado 159-7050, Cartago, Costa Rica. Email: jgaitan@tcr.ac.cr https://orcid.org/0000-0003-4243-5910

Róger MOYA*

Instituto Tecnológico de Costa Rica, Escuela de Ingeniería Forestal, Apartado 159-7050, Cartago, Costa Rica. E-mail: rmoya@itcr.ac.cr https://orcid.org/0000-0002-6201-8383

Alexander BERROCAL

Instituto Tecnológico de Costa Rica, Escuela de Ingeniería Forestal, Apartado 159-7050, Cartago, Costa Rica. Email: aberrocal@itcr.ac.cr https://orcid.org/0000-0003-2041-4772

Fabio ARAYA

Instituto Tecnológico de Costa Rica, Escuela de Química, Instituto Tecnológico de Costa Rica, Cartago 159-7050, Costa Rica. Email: fdaraya@itcr.ac.cr

*Authors correspondence, Email: rmoya@itcr.ac.cr

Wood properties of nine acetylated tropical woods from fast-growth plantations in Costa Rica

Abstract

The effect of acetylation on tropical wood is limited, due to its diverse levels of permeability and how these alter the weight percentage gain (WPG) in acetylated wood. The object of this work was to know the effect of acetylation on the thermal stability, colour, physical properties, dimensional stability, angle of contact and durability of nine tropical species used in commercial reforestation practices in Costa Rica. Results showed that weight percentage gain (WPG) varied from 2.2 % to 16.8 %. A positive statistical correlation was observed between WPG, pre-exponential factors in TGA analysis and the initial angle of contact, whereas a negative statistical correlation was found between moisture variation due to changes in equilibrium moisture conditions, water absorption and weight loss due to fungal attack. In those species with a WPG over 10% (*Vochysia ferruginea*, *V. guatemalensis*, *Cordia alliodora* and *Enterolobium cyclocarpum*), thermal stability, the angle of contact and resistance to biological attack increased, while swelling, absorption and moisture content variation decreased. For these species, the best behaviours were obtained with an acetylation time of 2.5 hours. The properties of wood in species with a WPG under 5% were scarcely affected by the different acetylation times and showed little difference in relation to untreated wood.

- **Keywords:** moisture absorption, wood properties, tropical wood, fast-growth plantation, dimensional stability

Introduction

Wood has multiple uses (Rowell 2016; Mantanis 2017), but it is easily degraded or affected in presence of moisture (Adebawo et al. 2016). Components of wood (lignin, cellulose and hemicellulose) contain free hydroxyl radicals (Rowell 2012) that adsorb and release water depending on changes in temperature and relative humidity conditions, causing cell walls —and all of the structure of wood, in general—to adjust to the presence (or absence) of moisture, thus giving way to changes in the dimensional stability of lumber (Rowell 2004; Giridhar et al. 2017).

Recent research has implemented chemical modifications to wood in order to acquire lower water absorption and, thus, greater dimensional stability (Mantanis 2017), without altering

wood properties (Rowell 2006a). Among these chemical alterations, a typical one is the use of acetic anhydride (Papadopoulos 2006; Hill 2006; Rowell 2006b), wherein the OH^- anion group of the wood components becomes chemically bound to a residue of the acetate (CH_3COO) of an acetic anhydride molecule ($(CH_3CO)_2$; this is known as acetylation (Mantanis 2017). In this process, the OH^- anion group is reduced, decreasing hygroscopicity of the wood and increasing its dimensional stability as a result (Adebawo et al. 2016). Other important wood properties take benefit from acetylation (Gérardin 2016; Mantanis 2017), notably: natural resistance to fungi and insects (Fojutowski et al. 2014; Rowell 2016); resistance to marine conditions; reduced wettability (Wålinder et al. 2013; Bongers et al. 2016), swellings of wood (Kozarić et al. 2016; Chai et al. 2016); increased wood hardness (Rowell 2006a). In general terms, reduction of the mechanical properties of the wood has not been reported (Mantanis 2017).

Polymer composition and distribution in hardwood species differ from those of softwood species (Engelund et al. 2013), therefore acetylation produces varied effects (Rowell 2016; Rowell and Ibach 2018). In hardwood species, hydroxyl groups are reported to be present at percentages of 2.0 to 4.5%, whereas in softwoods these vary from 0.5 to 1.7% (Rowell 2016). This difference is attributed to hemicellulose and lignin compositions: in hardwood species, hemicelluloses include glucuronoxylan, xyloglucan and glucomannan, while softwood hemicellulose is primarily composed of xyloglucan, arabinoglucuronoxylan and galacto-glucomannan, as well as lignin in a lesser proportion (Wang et al. 2017).

Studies on wood acetylation have indicated that acetylated hardwoods achieve lesser weight percentage gain (WPG) compared with acetylated softwood species (Rowell 2016; Rowell and Ibach 2018). Nonetheless, compared with softwoods, hardwoods contain a higher content of xylans, which do not have a primary hydroxyl group in which to react (Rowell 2014). Moreover, softwood species contain a greater percentage of lignin, the component where the higher percentage of acetylation has been shown to take place (Rowell 2016).

In addition to the difference in the type and proportion of hemicellulose, the anatomical structure differs significantly between both wood species groups: hardwoods are characterised by the presence of conducting elements such as vessels, whereas softwoods are made of tracheids (Gibson 2012). This distinction causes the flow of liquid to vary between both groups (Gaitán-Álvarez et al. 2020), therefore affecting the acetylation process (associated to liquid flow in wood) as well as other processes performed on lumber (Kozarić *et al.*, 2016).

In spite of these differences and the studies conducted on softwoods, some research on hardwood species have been carried out (Matsunaga et al. 2016) (Gaitan-Álvarez *et al.*, 2021).

Weight percentage gain (WPG) for tropical hardwood species ranges from 4% to 18%, values that are inferior to those found in softwood species (Gaitán-Álvarez *et al.*, 2021). This difference can be attributed mostly to the flow of liquid in wood, regulated by its permeability, which is determined by the anatomical elements appropriate for liquid flow (Emaminasab et al. 2017). In these first studies the change in wood properties due to acetylation remains unknown, which has not allowed expanding the uses of hardwood species (Bollmus et al. 2015).

In Central America, Costa Rica has implemented reforestation programs with fast-growth plantations that use a variety of tropical hardwood species for lumber production (Moya 2018). In these programs, early-age tree harvesting yields juvenile wood (Adebawo et al. 2016), which is characterized by dimensional instability (Adebawo et al. 2019). Therefore, a series of treatments have been implemented to improve lumber properties (Gaitán-Álvarez et al. 2020; Tenorio and Moya 2021) and reduce the durability and dimensional stability problems of these species (Moya et al. 2017a; Gaitán-Álvarez et al. 2020). In situations like this, acetylation provides an opportunity to improve dimensional stability, durability and other wood properties of tropical hardwood species (Mantanis and Young 1997; Rowell 2006b, 2016; Ozmen 2007; Adebawo et al. 2016). Given that plantation species in tropical regions represent a great opportunity for production, it is of utmost importance to increase the quality of wood to give added value to the products (Kojima et al. 2009).

In face of this lack of information regarding the change in properties of hardwood species caused by acetylation, the object of the present study was to evaluate the effect of acetylation with acetic anhydride in liquid phase on nine hardwood species commonly used in commercial reforestation in Costa Rica (*Cedrela odorata, Cordia alliodora, Enterolobium cyclocarpum, Gmelina arborea, Hieronima alchorneoides, Samanea saman, Tectona grandis, Vochysia ferruginea* and *Vochysia guatemalensis*). The effects on thermal stability by thermogravimetric analysis (TGA), wood colour, physical properties, dimensional stability, angle of contact and durability were thus evaluated.

Methodology

Materials

Species used were *Cedrela odorata, Cordia alliodora, Enterolobium cyclocarpum, Gmelina arborea, Hieronyma alchorneoides, Samanea saman, Tectona grandis, Vochysia ferruginea* and *Vochysia guatemalensis*, as they present good permeability (Moya et al. 2015; Tenorio et al. 2016) and have previously reported susceptibility to acetylation (Gaitán-Álvarez

et al., 2021). Gaitán-Álvarez *et al.* (2021) present the characteristics and origin of these woods in great detail. The lumber was dried to moisture content of 12% to 15% and comprised mostly sapwood. The reagents used were: acetic anhydride $(CH_3CO)_2O$ at 98% concentration, commercial brand J.T. Baker (Madrid, Spain) (https://www.fishersci.es/es/es/brands/IPF8MGDA/jt-baker.html); and glacial acetic acid CH_3COOH at 99% concentration, distributed by Químicos Holanda Costa Rica S.A. (Costa Rica). (https://www.brenntag.com/locations/en/brenntag-locations/loc-809-qu%C3%ADmicos-holanda-costa-rica-s-a.jsp).

Acetylation process

A detailed description of the acetylation process is given in Gaitán-Álvarez *et al.* (2021). The process consisted in applying vacuum to the samples for 15 minutes at -70 kPa (gauge mark), after which the solution of acetic anhydride and glacial acetic acid was introduced, in a 92:8 proportion respectively. Once inside, the contents were subjected to a 690 kPa pressure for 30 minutes, then the excess liquid solution was extracted and nitrogen gas was injected to serve as the inert medium to control internal temperature of the wood. For the reaction, temperature was fixed at 120 °C and three different acetylation times were applied per species: 1.0, 2.5 and 4.0 hours, labelled 1h-acetylation-time, 2.5h-acetylation-time and 4h-acetylation-time respectively. Last, the samples were introduced in a conditioning chamber (for two weeks), at climatic conditions of 20°C and 65% relative humidity, after which, they were weighed up.

Evaluation of the acetylation process

Per each acetylation time, 15 samples were tested, each measuring 2 cm thick, 5 cm wide and 5 cm long. Parallel to this, 15 other samples were extracted and left untreated to be compared with the acetylated wood. These samples were labelled as untreated-wood. Samples for acetylation were measured in length, width and depth before and after the acetylation process. For weight measurement, samples were placed into an oven for 24 h before and after the acetylation process in order to determine the weight in dry conditions. The acetylation impregnation process was evaluated by determining absorption of the solution and weight percentage gain (WPG) once the acetylation process was finished, considering the weight of the sample in oven-dried condition as the initial weight.

Thermogravimetric Analysis (TGA)

The TGA was performed in an ultra-high purity nitrogen ambient at 100 ml min^{-1} flux. A 5 mg dry sample was used and the heating rate chosen was 20 °C min^{-1} from 50 °C up to 800 °C. The analyses were carried out in a brand TA Instruments, model SDT Q600 thermogravimetric analyser (TA Instruments, New Castle, DE, USA). The TGA provided values for loss of mass in relation to temperature, from which the derivative thermogravimetry (DTG) was obtained; this allowed to determine the position and temperature at which sample degradation took place. The TGA and DTG data were analysed in the TA Instruments Universal Analysis 2000 software (TA Instruments, New Castle, DE, USA).

By using the DTG data, the thermal stability curve (Equation 1) was obtained by derivation of the linearized model of the equation according to Sbirrazzuoli *et al.* (2003), where the Friedman conversion method is employed. The model was established for the range between 200 °C and 400 °C, with the purpose of calculating the energy of activation (Ea) required to decompose the material.

$$In\left(\frac{d\alpha}{dt}\right) = lnk_0 + \left(\frac{-Ea}{RT}\right) + nln(1-\alpha) \quad (1)$$

$$K = A\ x\ e^{\left(\frac{-Ea}{RT}\right)} \quad (2)$$

Where: α: degraded mass, dα/dt: percentage of the degraded sample per unit time, A: pre-exponential factor, Ea: energy of activation and T: temperature.

Evaluation of colour

Colour was determined for all 15 samples in each acetylation time. Colour measurement was performed before and after the acetylation process in the same site. A HunterLab miniSkan XE Plus spectrophotometer was used for colour measurement, with standardised CIEL*a*b* chromatographic system. The CIEL*a*b* colour system allows three-dimensional colour measurement. The total colour change (ΔE*) was then quantified according to ASTM D-2244 (ASTM 2005) and was established by difference between colour parameters after and before acetylation.

Measurement of the contact angle

Contact angle was measured with an FTA˚ D200 imaging goniometer (Folio Instruments Inc., Ontario, Canada) at 20 °C. One drop (6 mL) of pure water was added to wood surfaces with an injection microsyringe. Measurements were carried out in the longitudinal direction. Contact angle was calculated as a mean of both sides of the drop to compensate for any

horizontal variations; the procedure used by Cool and Hernández (2011) was followed. Two contact angles were measured: initial contact angle ($\theta_{initial}$) and the stabilisation contact angle ($\theta_{stabilization}$). In addition, the final time of the test (T_{final}) was recorded, which corresponded to the moment when the angle showed no change. This procedure was performed on 5 samples per treatment, for every species studied.

Physical properties

The moisture content (MC), moisture content variation (MCV) and width swelling (WS) of wood samples were determined by the change in equilibrium moisture content (EMC) conditions, rising from 10 % to 18 % (Equation 3), while water absorption (WA) was determined by immersion in cold water for 24 h. The MC of these prepared samples was determined as indicated in the ASTMD4442-42 (Astm 2007) norm. For determination of MCV and WS, 15 prepared samples per acetylation time and 15 untreated wood samples, all measuring 2 cm thick, 5 cm wide and 5 cm long, were weighed and measured at 10 % moisture. Then, for a period of 3-4 weeks, the samples were climatized at 18% humidity. After climatization, they were weighed and measured once again, based on the ASTM D4933-99 standard (ASTM 1999), with adaptations to conditions in Costa Rica, where ambient humidity is approximately 18 % in critical conditions. For calculation of MCV, Equation 4 was used, while Equation 3 was used to calculate WS. For determination of WA by immersion in cold water, Equation 5 was used following the ASTM D4446–13 standard (ASTM 1985). For this, 15 samples per species and treatment were weighed before and after submersion in water for 24 h.

$$Swelling\ \ (mm) = (g)\frac{measurement 12\%\,(mm) - measurement 1\ \%\,(mm)}{measurement\ 12\%\,(mm)} * 100 \quad (3)$$

$$Moisture\ variation = Moisture\ content_{18\%} - Moisture\ content_{12\%} \quad (4)$$

$$Water\ absorption = \frac{Wei\quad_{MC}\ (g) - Weig\quad_{oven\ dried}\ (g)}{Weigt\ _{oven\ dried}\ (g)} * 100 \quad (5)$$

Durability

The accelerated laboratory test of natural decay resistance was carried out according to the ASTM D-2017-81 standard (2014) For each treatment and each species, 30 samples measuring 2 cm wide, 2 cm long and 2 cm thick were prepared. The two types of fungi used in this test were *Trametes versicolor* and *Lenzites acuta*, which correspond to white-rot and brown-rot fungi respectively. For each type of fungus, 15 samples in total were subjected to fungal

degradation per species and treatment. Decay resistance was reported as weight loss (percentage) after 12 weeks of fungal exposure.

Statistical analysis

Data were tested for normality and homogeneity, and strange data or outliers of the variables evaluated were eliminated. For each species and treatment, the mean, standard deviation and coefficient of variation were determined for every variable studied. A variance analysis (ANOVA) with a statistical significance level of $p<0.05$ was applied to determine the effect of mineralisation time. Tukey's test was used to determine the statistical significance of the difference between the means of the variables. This analysis was performed with the SAS 9.4 program (SAS Institute Inc., Cary, N.C.).

Results

Evaluation of the acetylation process

The WPG varied from 2.2% to 16.8%, the highest values were recorded from *V. ferruginea* while the lowest were from *G. arborea* and *T. grandis* (Figure 1). No statistical differences were present in the WPG between acetylation times for *V. ferruginea, V. guatemalensis, C. alliodora, C. odorata, G. arborea* and *T. grandis*. On the other hand, significant statistical differences between acetylation times were observed in *E. cyclocarpum*, *S. saman* and *H. alchorneoides*: in *E. cyclocarpum* and *H. alchorneoides* woods the WPG was lower for 4h-acetylation-time, whereas in *S. saman* wood the lesser value in WPG was present in 1h-acetylation-time and the greatest was observed in 2.5h-acetylation-time (Figure 1).

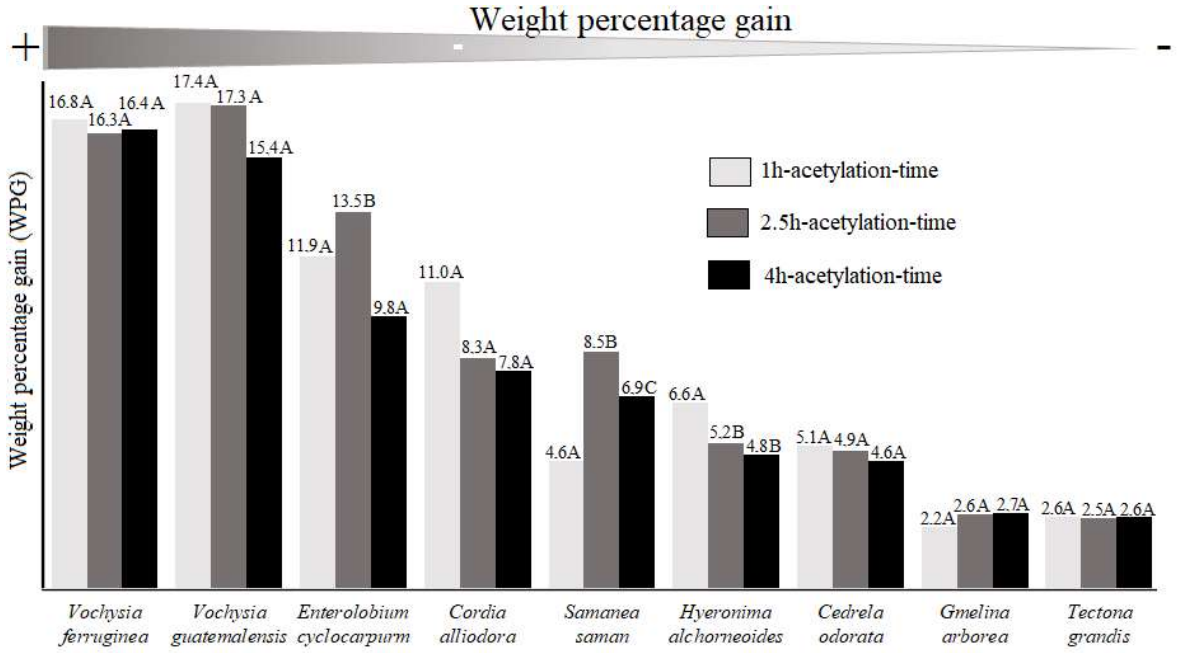

Figure 1. Weight percentage gain (WPG) of wood with different acetylation times from 9 fast-growth tropical species in Costa Rica

Legend: Different letters between acetylation times for a given parameter indicate statistical differences at 99%

Thermogravimetric analysis (TGA)

The behavioural pattern of thermal decomposition from the TGA is the same for the nine acetylated woods and the untreated wood; however, the differences in decomposition of each species can be observed from the DTG curve (Figure 2). In all nine species, for both acetylated and untreated wood the DTG curve reveals a peak after 200 °C, then a maximum decomposition peak in the 320–360 °C range, and a third decomposition beyond the 380 °C (Figure 2a). The DTG curves show that the maximum decomposition peak (320–360 °C) is similar for both acetylated and untreated wood in most species, this peak is where differences in the intensity of maximum decomposition can be observed. A greater intensity of the maximum decomposition peak can be observed for 1h-acetylation-time and 2.5h-acetylation-time in *V. ferruginea*, *C. odorata*, *E. cyclocarpum*, *G. arborea*, *V. guatemalensis* and *T. grandis* woods (Figure 2a, c-d, f, h-i). In *S. saman*, *C. alliodora* and *H. alchorneoides* wood samples, the maximum decomposition peak is higher for untreated wood than for acetylated wood; additionally, a lower decomposition peak is observed for 1h-acetylation-time samples (Figure 2b, e, g).

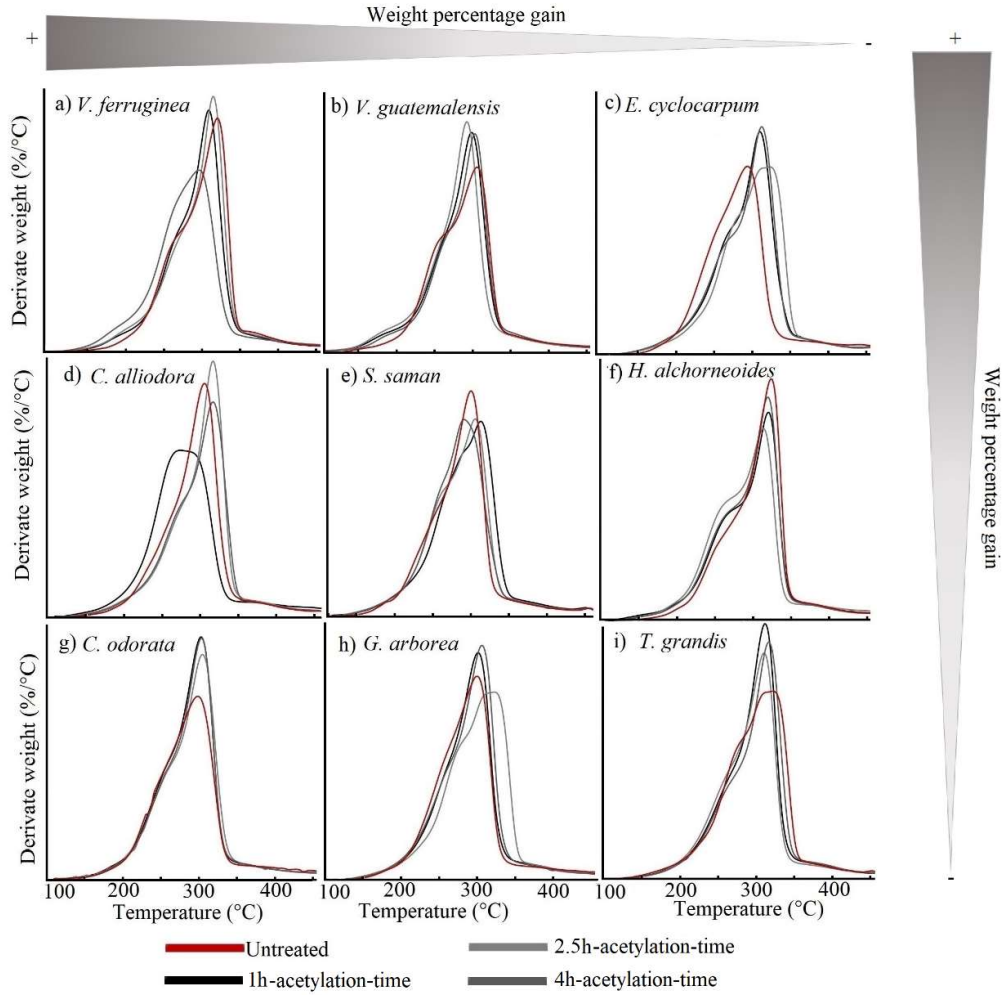

Figure 2. DTG curves of wood from nine fast-growth tropical species in Costa Rica with different acetylation times.

The coefficients of determination (R^2) obtained for the thermal stability models of all species were between 0.74 and 0.93 (Table 1). The pre-exponential factor (A) increased with acetylation in all wood species, with the exception of *T. grandis*. In relation to energy of activation (Ea), an increase was observed in acetylated samples as compared to untreated samples in *E. cyclocarpum*, *S. saman*, *H. alchorneoides*, *C. odorata*, *G. arborea* and *T. grandis*. In *V. guatemalensis* and *T. grandis*, the Ea value was the same in acetylated samples and untreated samples, whereas in *C. odorata* samples acetylation decreased this value (Table 1). Regarding acetylation times, a proportional increase in Ea with time was seen in *V. ferruginea*, *E. cyclocarpum*, *H. alchorneoides*, *C. odorata* and *G. arborea* woods. In *V. guatemalensis* and *C. alliodora* woods, the Ea value did not vary with time, whereas in *S. saman* and *T. grandis* lumbers there was variation between acetylation times (Table 1).

Table 1. Activation energies and pre-exponential factors for thermal decomposition of wood from nine fast-growth tropical species in Costa Rica with different acetylation times.

Species	Acetylation time (hours)	Correlation coefficient (R^2)	Pre-exponential factors (A)	Activation energies (Ea) (kJ/mol)
Vochysia ferruginea	Untreated	0.85	3.84×10^{06}	49.69
	1.0	0.92	2.93×10^{07}	60.44
	2.5	0.93	2.92×10^{07}	66.20
	4.0	0.92	2.68×10^{07}	58.58
Vochysia guatemalensis	Untreated	0.79	8.97×10^{05}	42.69
	1.0	0.88	2.23×10^{07}	42.89
	2.5	0.88	2.24×10^{07}	42.93
	4.0	0.87	2.45×10^{07}	42.16
Enterolobium cyclocarpum	Untreated	0.82	3.72×10^{06}	48.81
	1.0	0.93	1.43×10^{07}	54.53
	2.5	0.93	1.32×10^{07}	54.50
	4.0	0.93	2.44×10^{07}	56.82
Cordia alliodora	Untreated	0.88	1.11×10^{06}	54.55
	1.0	0.88	6.64×10^{06}	50.76
	2.5	0.91	4.89×10^{06}	50.81
	4.0	0.90	4.50×10^{06}	50.65
Samanea saman	Untreated	0.86	5.16×10^{06}	50.30
	1.0	0.92	8.30×10^{06}	52.17
	2.5	0.74	8.02×10^{06}	50.98
	4.0	0.74	8.35×10^{06}	51.38
Hieronyma alchorneoides	Untreated	0.81	2.15×10^{06}	48.21
	1.0	0.90	7.19×10^{06}	52.12
	2.5	0.87	7.31×10^{06}	52.08
	4.0	0.89	1.14×10^{07}	54.41
Cedrella odorata	Untreated	0.80	2.72×10^{06}	48.00
	1.0	0.85	7.75×10^{06}	51.94
	2.5	0.85	1.50×10^{07}	57.81
	4.0	0.88	1.02×10^{07}	56.52
Gmelina arborea	Untreated	0.80	3.67×10^{06}	49.30
	1.0	0.88	1.07×10^{07}	53.71
	2.5	0.93	1.27×10^{07}	54.27
	4.0	0.89	1.76×10^{07}	55.73
Tectona grandis	Untreated	0.93	1.34×10^{07}	54.73
	1.0	0.91	1.15×10^{07}	59.61
	2.5	0.87	1.35×10^{07}	55.24
	4.0	0.89	1.19×10^{07}	55.11

Evaluation of colour

Evaluation of ΔE* revealed changes as follows: *T. grandis* showed a major change in 1h-acetylation-time and 4h-acetylation-time; *V. ferruginea* showed changes in 2.5h-acetylation-time; *C. alliodora* presented the least ΔE* in 1h-acetylation-time and 4h-acetylation-time; and *V. guatemalensis* lumber increased the ΔE* value with acetylation time, being statistically higher in the 4h-acetylation-time (Table 2). The ΔE* in *T. grandis*, *G. arborea*, *S. saman*, *V. ferruginea* and *C. odorata* lumbers was not affected by acetylation in any of the times. In *E. cyclocarpum* lumber, the greater ΔE* value was present in 1h-acetylation-time, the same as in 4h-acetylation-time. In *H. alchorneoides* wood the ΔE* value was statistically higher in 4h-acetylation-time (Table 2).

Table 2. Colour change of wood from nine fast-growth tropical species in Costa Rica with different acetylation times.

	Species	Colour change (ΔE*)		
		1h-acetylation-time	2.5h-acetylation-time	4h-acetylation-time
+ Weight percentage gain −	*Vochysia ferruginea*	11.8 (48.9)^{A}	12.1 (37.8)^{A}	14.7 (31.1)^{A}
	Vochysia guatemalensis	16.7 (47.2)^{A}	23.1 (67.6)^{AB}	33.7 (44.2)^{B}
	Enterolobium cyclocarpum	24.8 (15.2)^{A}	21.01 (14.3)^{B}	22.9 (23.7)^{AB}
	Cordia alliodora	7.3 (67.0)^{A}	19.6 (39.9)^{C}	13.5 (42.0)^{B}
	Samanea saman	15.6 (54.9)^{A}	16.8 (34.0)^{A}	13.8 (53.8)^{A}
	Hieronyma alchorneoides	8.9 (30.5)^{A}	6.7 (37.0)^{A}	13.9 (54.2)^{B}
	Cedrela odorata	10.9 (57.5)^{A}	8.7 (34.0)^{A}	13.4 (53.8)^{A}
	Gmelina arborea	19.7 (23.2)^{A}	19.9 (33.7)^{A}	21.4 (41.4)^{A}
	Tectona grandis	25.0 (70.2)^{A}	17.1 (81.8)^{A}	23.5 (63.7)^{A}

Legend: Different letters between acetylation times indicate statistical differences at 99% and values in parentheses represent coefficient of variation.

Measurement of the contact angle

The angles of contact sampled were affected by acetylation of wood in all species. In the case of $\theta_{initial}$, the value increased for all acetylation times in *V. ferruginea*, *C. alliodora* and *G. arborea* as compared to their untreated samples; these species did not show differences between acetylation times (Figure 3a, 3d, 3g). Meanwhile, the $\theta_{stabilization}$ increased as follows: for all acetylation times in *V. ferruginea* (Figure 3a); for 2.5h-acetylation-time and 4h-acetylation-

time in *C. alliodora* (Figure 3d); and for 1h-acetylation-time in *G. arborea* (Figure 3g). Acetylation increased the $\theta_{initial}$ only for 1h-acetylation-time in *V. guatemalensis* (Figure 3b) and *S. saman* (Figure 3e) lumbers, while the $\theta_{stabilization}$ was increased for all acetylation times in these species (Figure 3b and 3e). In *H. alchorneoides* lumber the $\theta_{initial}$ increased for 1h-acetylation-time, but the $\theta_{stabilization}$ remained unaffected by acetylation (Figure 3f). In lumber from *E. cyclocarpum*, *C. odorata* and *T. grandis* the $\theta_{initial}$ was not affected by any of the acetylation times (Figure 3c, h, i); the $\theta_{stabilization}$, on the other hand, increased for 1h-acetylation-time and 2.5h-acetylation-time in *E. cyclocarpum* and *T. grandis* lumbers (Figure 3c, i), but in *C. odorata* the $\theta_{stabilization}$ remained unaffected by acetylation (Figure 3h).

Regarding T_{final}, this value was increased by acetylation in *V. ferruginea*, *V. guatemalensis*. *C. alliodora*, *S. Saman*, *H. alchorneoides* and *T. grandis* (Figure 3a-b, 3d-f, 3i); however, T_{final} was greater for 1h-acetylation-time in *V. guatemalensis* and *S. saman* (Figure 3b, c) and 4h-acetylation-time in *T. grandis* lumber (Figure 3i). In *V. ferruginea*, *C. alliodora* and *H. alchorneoides* lumbers, T_{final} values were statistically equivalent for all acetylation times (Figure 3a, 3d and 3f). In *E. cyclocarpum* lumber, acetylation increased T_{final} values for 1h-acetylation-time and 2.5h-acetylation-time (Figure 3c). In *G. arborea* samples, acetylation time did not affect T_{final} value statistically (Figure 3g). In *C. odorata* wood the T_{final} value was unaffected only for 1h-acetylation-time and 2.5h-acetylation-time, while it decreased for 4h-acetylation-time (Figure 3h).

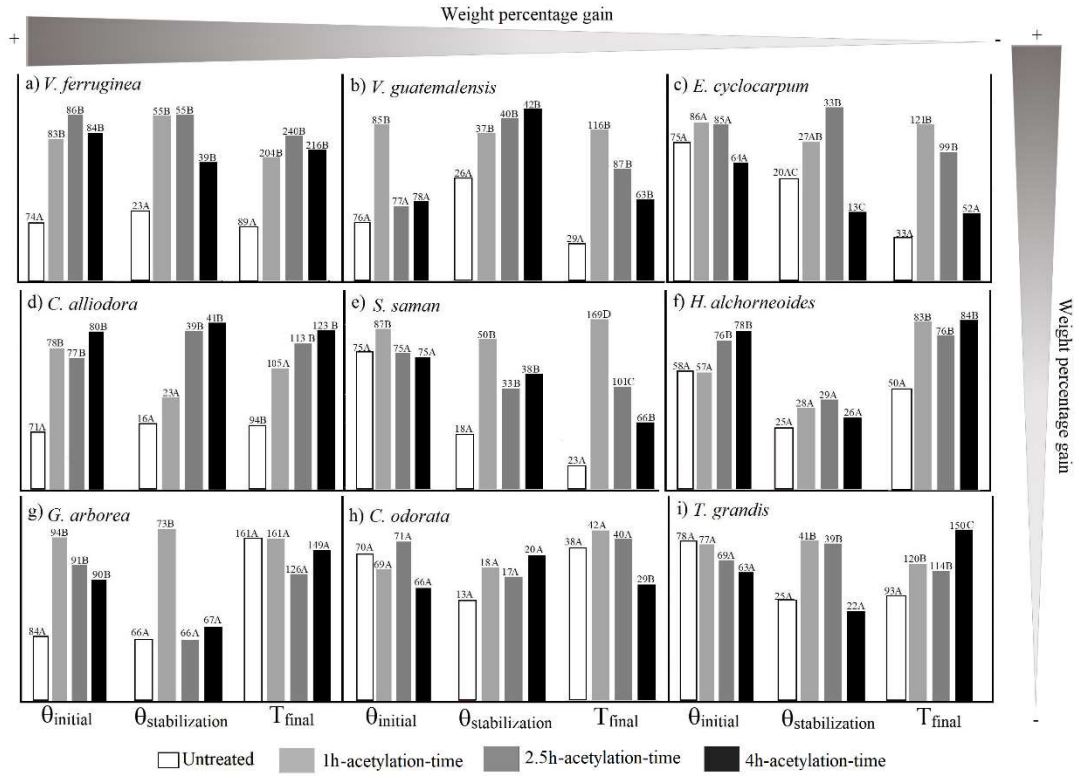

Legend: Different letters between acetylation times indicate statistical differences at 99% for each variable.

Figure 3. Initial and final angles and final time for wood from nine fast-growth tropical species in Costa Rica with different acetylation times.

Physical properties

In general, wood acetylation decreased MC, then stabilisation took place in *H. alchorneoides*, *T. grandis*, *V. guatemalensis* and *V. ferruginea* lumbers. In *H. alchorneoides*, *T. grandis* and *V. ferruginea* lumbers there was no difference in MC between acetylation times, but *V. guatemalensis* wood showed its lowest MC for 1h-acetylation-time and 2.5h-acetylation-time (Table 3). In *C. odorata*, acetylation decreased the MC for 1h-acetylation-time and 4h-acetylation-time, but the 2.5h-acetylation-time treatment was statistically equivalent to the untreated samples. The lowest MC in *G. arborea* wood was present in 4h-acetylation-time, while the other times and the untreated samples showed no differences. *E. cyclocarpum* showed its lowest MC for 2.5h-acetylation-time, while the other times and the untreated samples were equivalent regarding MC. In *S. saman* lumber, the lower MC value came with 1h-acetylation-time, while the other times were different from each other. Acetylation decreased the MC in *C.*

alliodora wood for 2.5h-acetylation-time and 4h-acetylation-time, but the 1h-acetylation-time was statistically equivalent to the untreated samples.

Variation in MCV due to the change in EMC conditions was between 2.80% and 7.86%. This variable was statistically lower for acetylated wood than for untreated wood in all species (Table 3). As for the various acetylation times, no significant differences appeared in *C. odorata*, *G. arborea*, *H. alchorneoides*, *T. grandis*, *V. ferruginea* and *V. guatemalensis* woods. The remaining species showed differences in the MCV value: *E. cyclocarpum* had a lower value for 2.5h-acetylation-time than for the other two times; *S. saman* showed the lower value for 1h-acetylation-time; and *C. alliodora* lumber had a lower value for 2.5h-acetylation-time and 4h-acetylation-time (Table 3).

Width swelling (WS) varied in all species and for all treatments. The values were between 1.79 mm and 0.43 mm and all species studied showed statistical differences between acetylation times. The lower WS values among all 9 species appeared for 1h-acetylation-time and 2.5h-acetylation-time (Table 3).

The WA value varied between 17.11% and 67.16% in all species. The species that presented the highest values were *C. odorata* (Table 3). Lumber samples from *C. odorata*, *V. ferruginea*, *E. cyclocarpum*, *S. saman* and *C. alliodora* presented statistical differences between acetylation times, with the lower WA values obtained from 1h-acetylation-time and 2.5h-acetylation-time. Meanwhile, *T. grandis* and *V. guatemalensis* also presented statistical differences, but the lowest percentage was obtained from the 4h-acetylation-time treatment (Table 3).

Table 3. Moisture content, moisture content variation, dimensional swelling and water absorption after 24 hours of wood from nine fast-growth tropical species in Costa Rica with different acetylation times.

Species	Acetylation time (hours)	Moisture content (%)	Moisture content variation (%)	Wide swelling (mm)	Water absorption after 24 hours (%)
Vochysia ferruginea	Untreated	10.2 (2.0)^{A}	6.9 (10.1)^{A}	1.87 (41.4)^{A}	67.2 (11.6)^{A}
	1.0	9.1 (12.0)^{B}	3.5 (7.4)^{B}	0.47 (47.9)^{B}	40.8 (7.5)^{B}
	2.5	9.0 (6.7)^{B}	3.3 (7.7)^{B}	0.37 (58.0)^{B}	40.4 (7.0)^{B}
	4.0	9.6 (10.4)^{AB}	3.6 (8.0)^{B}	0.80 (54.6)^{B}	47.4 (16.2)^{C}
Vochysia guatemalensis	Untreated	10.8 (6.3)^{A}	7.6 (15.8)^{A}	1.31 (48.0)^{A}	62.8 (19.8)^{A}
	1.0	8.8 (9.2)^{BC}	4.3 (11.6)^{B}	0.76 (49.1)^{B}	48.8 (10.8)^{B}
	2.5	8.3 (5.3)^{B}	3.9 (8.6)^{B}	0.82 (31.8)^{B}	50.3 (8.6)^{B}
	4.0	9.2 (9.9)^{C}	4.3 (7.8)^{B}	0.66 (34.3)^{B}	49.5 (10.5)^{B}
Enterolobium cyclocarpum	Untreated	10.7 (3.5)^{A}	6.4 (4.2)^{A}	1.19 (29.2)^{A}	30.8 (11.2)^{AB}
	1.0	10.2 (9.7)^{A}	3.6 (9.6)^{A}	0.28 (60.5)^{B}	29.9 (12.5)^{AB}
	2.5	9.3 (8.1)^{B}	2.9 (9.7)^{B}	0.24 (71.5)^{B}	26.6 (10.1)^{B}
	4.0	10.1 (6.8)^{A}	3.7 (6.9)^{A}	0.58 (85.9)^{B}	30.9 (12.1)^{A}
Cordia alliodora	Untreated	10.6 (3.9)^{A}	6.3 (1.4)^{A}	1.68 (15.9)^{A}	51.9 (13.5)^{A}
	1.0	10.5 (3.3)^{A}	3.7 (9.2)^{B}	0.65 (73.6)^{B}	35.8 (11.1)^{B}
	2.5	8.9 (6.1)^{B}	3.5 (7.5)^{BC}	0.61 (54.0)^{B}	25.5 (8.9)^{C}
	4.0	9.1 (5.1)^{B}	3.3 (6.8)^{C}	0.65 (93.2)^{B}	30.6 (7.6)^{D}
Samanea saman	Untreated	11.6 (2.6)^{A}	6.5 (3.9)^{A}	1.63(13.2)^{A}	35.1 (10.1)^{A}
	1.0	9.4 (6.5)^{B}	2.8 (6.2)^{B}	0.32 (170.9)^{B}	20.3 (23.0)^{B}
	2.5	10.8 (3.1)^{C}	3.9 (6.6)^{C}	0.41 (60.2)^{B}	39.4(12.0)^{B}
	4.0	10.2 (6.6)^{D}	3.6 (9.3)^{D}	0.65 (30.0)^{B}	33.4 (10.0)^{C}
Hieronyma alchorneoides	Untreated	10.9 (1.6)^{A}	6.2 (4.7)^{A}	1.86 (32.7)^{A}	28.1 (8.9)^{A}
	1.0	9.1 (5.3)^{B}	3.7 (7.3)^{B}	0.57 (55.5)^{B}	25.1 (12.9)^{A}
	2.5	9.0 (3.0)^{B}	3.9 (10.3)^{BC}	0.56 (23.0)^{AB}	26.1 (10.0)^{A}
	4.0	9.4 (2.8)^{B}	4.3 (10.3)^{C}	0.69 (34.1)^{B}	25.4 (16.3)^{A}
Gmelina arborea	Untreated	10.4 (1.8)^{A}	6.1 (10.6)^{A}	1.40 (23.7)^{A}	18.3 (53.4)^{A}
	1.0	10.3 (7.6)^{A}	5.1 (6.9)^{B}	0.70 (39.8)^{B}	24.1 (16.9)^{A}
	2.5	10.1 (9.8)^{A}	4.5 (11.8)^{B}	0.73 (51.4)^{B}	22.7 (44.1)^{A}
	4.0	9.2 (5.9)^{B}	4.9 (21.9)^{B}	0.88 (48.3)^{B}	25.9 (38.4)^{A}
Cedrela odorata	Untreated	10.6 (3.6)^{A}	7.9 (2.8)^{A}	1.49 (37.6)^{A}	56.8 (13.4)^{A}
	1.0	9.8 (7.4)^{B}	5.9 (5.7)^{B}	0.99 (36.6)^{B}	53.3 (8.1)^{A}
	2.5	10.1 (4.0)^{AB}	5.4 (3.9)^{C}	0.77 (49.2)^{B}	40.6 (9.9)^{B}
	4.0	9.7 (8.4)^{B}	5.4 (6.5)^{C}	0.86 (35.9)^{B}	41.2 (10.1)^{B}
Tectona grandis	Untreated	10.4 (3.2)^{A}	5.9 (4.9)^{A}	1.20 (22.2)^{A}	35.6 (18.2)^{A}
	1.0	9.2 (11.6)^{B}	4.7 (6.6)^{B}	0.64 (52.8)^{BC}	22.6 (10.6)^{B}
	2.5	8.7 (4.1)^{B}	4.5 (7.3)^{B}	0.62 (42.0)^{BC}	21.2 (13.5)^{B}
	4.0	9.3 (7.7)^{B}	4.4 (9.9)^{B}	0.85 (50.6)^{C}	17.1 (18.0)^{C}

Weight percentage gain +

Legend: Different letters between acetylation times indicate statistical differences at 99% and values in parentheses represent coefficients of variation

Decay resistance

Weight loss due to fugal decay varied from 3.9% to 14.2% with *Lenzites acuta* and from 3.6% to 15.2% with *Trametes versicolor* in all species studied (Figure 4a-i). As for resistance to

decay from *Lenzites acuta*, acetylated wood presented less weight loss in relation to untreated wood; however, a significant difference was only observed in *V. ferruginea*, *S. saman*, *E. cyclocarpum* and *V. guatemalensis* (Figure 5a, c-e). In the remaining species there was no difference between untreated lumber samples and those treated with various acetylation times (Figure 4b, 4f, 4g y 4h). Weight loss was statistically equivalent among all species in the three acetylation times, (Figure 4). Regarding fungal decay by *Trametes versicolor*, weight loss was statistically lower in acetylated wood than in untreated wood, with an exception in *H. alchorneoides* and *T. grandis*, which did not present statistical differences (Figure 4h-i). Among the three acetylation times it was observed that the lowest weight loss percentages appeared for 2.5h-acetylation-time in *S. saman* and *T. grandis* (Figure 4c, 4i).

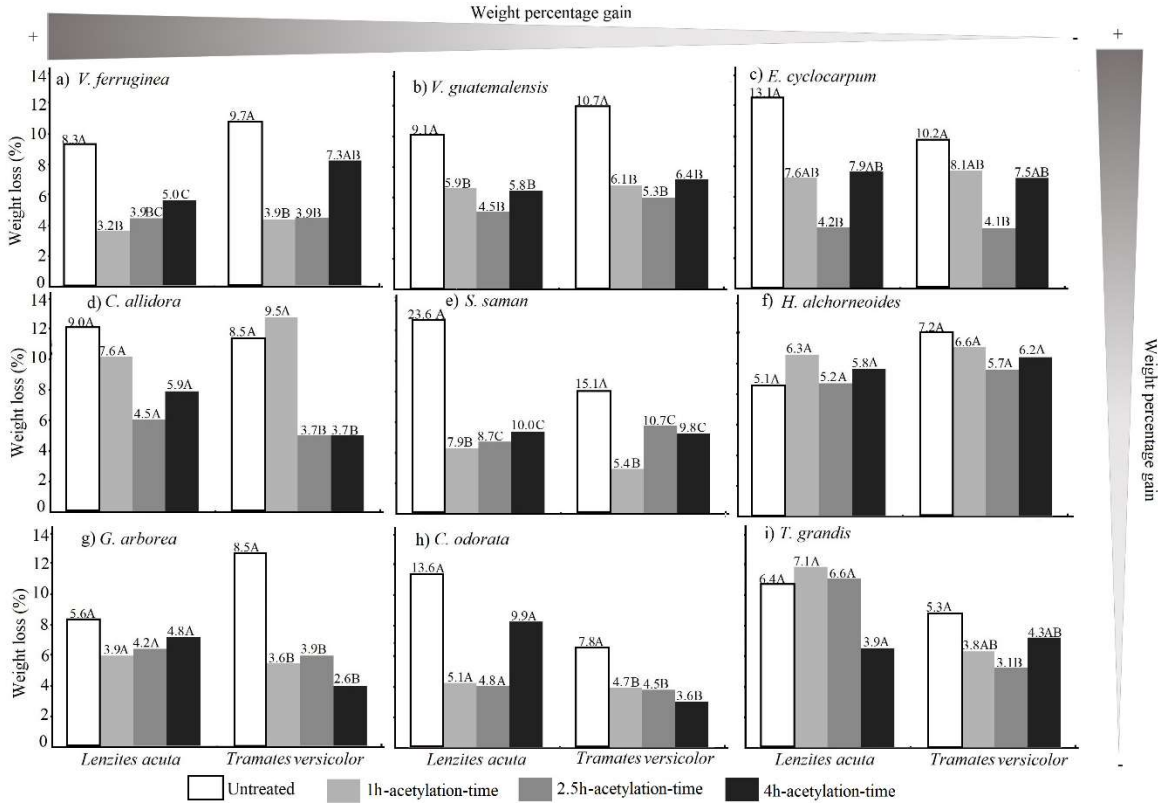

Legend: Different letters between acetylation times for a given fungal decay indicate statistical differences at 99%.

Figure 4. Weight loss due to fungal decay by *Lenzites acuta* and *Trametes versicolor* in wood from nine fast-growth tropical species in Costa Rica with different acetylation times.

Correlation between weight percentage gain and wood properties of acetylated wood

A statistically positive correlation was observed between the WPG, pre-exponential factors (A) and $\theta_{initial}$, while a statistically negative correlation appeared between MCV and WA. Conversely, no correlation was seen between Ea, ΔE^*, $\theta_{stalization}$, T_{final}, MC and weight loss by *L. acuta* and *T. versicolor* (Table 4).

Table 4. Pearson correlation of weight percentage gain (WPG) with different properties of acetylated wood from nine fast-growth tropical species in Costa Rica.

Wood properties	Correlation coefficient
Pre-exponential factors (A)	0.68**
Energy of activation (Ea)	0.31 ^{NS}
Wood colour change (ΔE^*)	0.10 ^{NS}
$\theta_{initial}$	0.42 *
$\theta_{stalization}$	0.08 ^{NS}
T_{final}	0.20 ^{NS}
Moisture content	-0.31 ^{NS}
Moisture content variation	-0.58**
Wide swelling (mm)	-0.27 ^{NS}
Water absorption	-0.83**
Weight loss by *L. acuta*	0.04 ^{NS}
Weight loss by *T. versicolor*	0.16 ^{NS}

Legend: ** statistically significant at significance level 0.05; * statistically significant at significance level 0.01; and NS: not statically significant.

Discussion

Liquid absorption in hardwood is related to permeability of the wood species (Thomas 1976; Ahmed and Chun 2009), which varies as a function of the anatomical elements of the wood. In hardwood species, liquid flow occurs chiefly along lumina vessels in the longitudinal orientation (Ahmed and Chun 2009), but this flow can be interrupted by the presence of tyloses or gum in the vessels (Ahmed and Chun 2009). Vessels connect longitudinal and radial parenchyma across wall pits, so liquids can then flow through the ray lumina (Ahmed *et al.*,

2011). This flow is favoured when the rays are composed of either over 3 series in width, or a greater abundance of parenchyma (Ahmed and Chun 2011). Variations in the anatomy of the species tested in acetylation are presented and extensively discussed by Gaitán-Álvarez *et al.* (Gaitán-Álvarez et al. 2020). These authors mention that *E. cyclocarpum*, *H. alchorneoides*, *S. saman*, *V. ferruginea* and *V. guatemalensis* present anatomical features of greater dimensions, specifically vessels' diameter (over 120 µm), rays' width (from 2 to 10 series of cells or over 252 µm) and their frequency (over 5 rays/mm^2), as well as various types of parenchyma (Gaitán-Álvarez et al. 2020). These anatomical features favour the flow of acetic anhydride and glacial acetic acid solutions, in accordance with the present study, in which these species present higher absorption and WPG values (Figure 1). Contrastingly, species showing the lower absorption and WPG values were *C. odorata*, *G. arborea* and *T. grandis* (Figure 1), due to anatomical elements less favourable to liquid flow, such as smaller and less-frequent rays, deposits in vessels such as gum and tyloses, as well as few vessel-associated parenchyma (Gaitán-Álvarez et al. 2020).

In most species, acetylation times did not have an effect on the absorption except for *E. cyclocarpum*, *S. saman* and *H. alchorneoides*, for which the 4h-acetylation-time treatment yielded a significantly lower absorption (Figure 1).This decrease, for these species, may be attributed to completion of the acetylation reaction well before the time limit. After some time, the reaction slows and levels off, indicating that the reaction is 'complete' (Rowell and Ibach 2018). Then, once acetylation is fulfilled, degradation of the acetic anhydride may have taken place, since the temperature used for the process (120°C) was close to boiling temperature of this compound (139°C). This result suggests that a longer acetylation time may not be appropriate for *E. cyclocarpum*, *S. saman* and *H. alchorneoides*.

In untreated lumber samples, thermal decomposition had relative similarity among the 9 species (Tenorio and Moya 2013; Moya et al. 2017b) and, indeed, the values of A and Ea varied from 8.97x10^5 to 5.16x10^6 and from 42,65 to 54.73 kJ/mol, respectively (Table 1). Nevertheless, the effect of acetylation varies with every species and acetylation time, therefore this behaviour is not clear. This result agrees with Hung *et al.* (2017), who indicate that thermogravimetric behaviour of acetylated wood is barely known and the real effects are not well determined, which is likely influenced by the type of chemical compound used in the acetylation process (Özmen et al. 2013).

The greater intensity of the maximum decomposition peak (is observed for 1h-acetylation-time and 2.5h-acetylation-time in *V. ferruginea*, *C. odorata*, *E. cyclocarpum*, *G.*

arborea, *V. guatemalensis* and *T. grandis* samples (Figure 2a, c-d, f, h, i), whereas for *S. saman*, *C. alliodora* and *H. alchorneoides* it is observed in untreated samples. These results show there is no relation between decomposition and WPG, which is confirmed by the non-significant statistical relation between the Ea and WPG values (Table 4). The increase in thermal stability by acetylation was addressed by Hung *et al.* (2017), which agrees with results obtained for acetylated samples in *V. ferruginea*, *E. cyclocarpum*, *H. alchorneoides*, *C. odorata* and *G. arborea* lumbers, as an increase in Ea can be seen with acetylation (Table 1). However, in acetylated samples from *E. cyclocarpum*, *S. saman*, *H. alchorneoides*, *C. odorata*, *G. arborea* and *T. grandis* no increase in thermal stability is observed, which is consistent with results by Rowell (2006a, 2014) and Shen (2016), who reported that acetylation does not affect thermal stability.

Thermal stability is determined by accessibility to carbon, oxygen and other elements in the wood matrix (Pawar et al. 2013). Acetylation of tropical species depends on permeability of the lumber, which in turn is influenced by its anatomy and capacity to let liquids pass (Emaminasab *et al.*, 2017), so it is not possible to define a clear relation between WPG and thermal stability of acetylated wood for these species, as studies on components and anatomical parts where acetylation actually occurs are necessary to establish the relationship between the process and the resulting thermal stability. An example is the work by Özmen *et al.* (2013), which shows the relationship between thermal stability and the infiltration of the chemical component at different sites of the wood structure.

Acetylation of the various tropical species studied induced a significant change in wood colour compared to colour prior to treatment. Cui *et al.* (2004) established five colour change levels that can be perceived by the human eye and depend on the ΔE^* value. Of these categories, those in which the human eye perceives the most cover the ΔE^* variation of values between 6.0 and 12.0, which is classified as quite noticeable by the human eye and, if ΔE^* is higher than 12.0, then there is a total colour change. After acetylation, most of the species presented total wood colour change, except for *C. alliodora* in 1h-acetylation-time, *H. alchorneoides* in 1h-acetylation-time and 2.5h-acetylation-time and *C. odorata*, for which the colour change is classified as quite noticeable (Table 2).

Remarkably, there was no relation between ΔE^* and WPG (Table 4), hence the little differences present in ΔE^* in relation to acetylation times. Although this study did not evaluate the effect of acetylation on colour stability by testing ultraviolet resistance of wood under outdoor conditions, a considerable amount of studies indicate that the increase in WPG in acetylated

wood improves wood colour behaviour against ultraviolet rays (Hon, 1995; Moya and Perez, 2008; Mitsui, 2010; Mantanis, 2017; Sadatnezhad *et al.*, 2017; Sandberg *et al.*, 2017). Therefore, it is to be expected that those species with greater WPG values preserve wood colour better, even when ΔE* values indicate change with respect to colour prior to treatment.

The contact angle determines surface tension and surface tension parameters. On a given solid surface, it is the common way of obtaining the surface energy of the solid material (Gindl *et al.*, 2001) and, in the case of wood, the contact angle influences surface-related processes such as water adsorption, wetting and adhesion (Collett, 1972). In this way, in some species, namely *V. ferruginea*, *C. alliodora* and *G. arborea*, these properties were favoured with acetylation in relation to untreated samples, because $\theta_{initial}$, $\theta_{stabilization}$ and T_{final} values increased. In addition, the increase in the contact angles studied and the final time indicate a change in polarity of the surface for the different tropical wood species (Adebawo *et al.*, 2016b). This is especially true in species with a high degree of acetylation (high WPG), as a positive correlation was revealed between $\theta_{initial}$ and WPG (Table 4). This result agrees with those obtained by Adebawo *et al.* (2016b) for other tropical species, as they indicate that upon acetylation there comes incorporation of acetyl groups into the cell walls, thereby making the wood surface hydrophobic (Sandberg *et al.*, 2017). Another aspect of this relation between $\theta_{initial}$ and WPG is that there are less differences between untreated and acetylated wood in species with low WPG, such as *C. odorata* or *T. grandis* (Figure 3e-f); conversely, these differences increase in those species with greater WPG values, as is the case with *V ferruginea* or *V. guatemalensis* (Figure 3a-b).

Concerning the correlation established between different parameters of the contact angle and WPG, significant correlation was found only for $\theta_{initial}$ (Table 4), indicating that in these species $\theta_{initial}$ was a more appropriate indicator of the degree of acetylation in wood.

Each acetylation time yields different values of WPG (Figure 1) and, of course, different surface effects which may or may not be compatible with water molecules (Gindl *et al.*, 2001). Among the different tropical species presented in this study, in those with a high WPG value, specifically *V. ferruginea*, *V. guatemalensis* and *E. cyclocarpum* (Figure 3a-c), the 4h-acetylation-time yields similar values of contact angles and T_{final} compared to untreated samples, suggesting better acetylation in 1h-acetylation-time and 2.5h-acetylation-time for those species. Meanwhile, in species with a lower WPG value, acetylation time from 1 to 4 hours will not produce variation in contact angles and their final stabilisation time (Figure 3d-i).

As expected, physical properties related to water absorption (MC, MCV, WS and WA) in most species decreased in value after acetylation, except for *H. alchorneoides*, *G. arborea* and *C. odorata* which, as previously indicated, have low permeability and thus lower degree of acetylation (Thomas, 1976; Ahmed and Chun, 2009), which affects WPG directly. In fact, the lower acetylation and its effect on physical properties related to water absorption can also be observed in the correlation analysis shown for MC, MCV, WS and WA, in which these presented negative correlation with WPG (a decrease in each parameter with increasing WPG); however, only for MCV and WA showed statistical significance (Table 4). The presence and amount of hydroxyl groups, capable of forming hydrogen bonds with water molecules, is important to dimensional stability and they are mainly present in hemicelluloses, followed by cellulose and lignin (Engelund *et al.*, 2013). During water absorption in these sites, the water molecule with two full-strength covalent bonds may become bound by two relatively strong H-bonds with a pair of nearby OH groups of the amorphous polysaccharide polymers in low moisture content. Meanwhile, the cooperativity in the H-bond network increases with increasing moisture content, gradually allowing the coalescence of water vapour molecules with already adsorbed water molecules to form water dimer (Willems, 2018). Thus, this gain in moisture makes wood dimensionally unstable as the lumber gains weight. With acetylation, however, the OH^- anion group in wood components becomes chemically bound to a residue of the acetate (CH_3COO) of an acetic anhydride molecule $(CH_3CO)_2$ (Mantanis, 2017). In this process, the OH^- anion group is reduced, decreasing hygroscopicity of the wood and increasing its dimensional stability as a result (Adebawo et al. 2016).

According to Rowell (2016), acetylation of lumber prevents its biological degradation by three possible mechanisms: the first one consists in modifying the composition and physical configuration of the substrate where the specific enzymatic attack may take place; the second one where the acetyl group forms a covalent bond, therefore it is no longer available for an enzymatic attack; and a third theory based on the physical blockage of micropores of the cellular wall, rendering enzymatic penetration impossible. As confirmed in the present study, susceptibility to fungal attack is related to WPG (Rowell 2014, 2016); however, this is a negative correlation, indicating that an increasing WPG decreases loss of mass by the two fungi tested (Table 4). Therefore, differences between acetylated and untreated samples were less or almost null in those species with lower WPG (Figure 4b, 4f-h). This effect owes to low acetylation, which eases fungal enzymes' access to hydroxyl groups (Rowell 2014, 2016). There were no effects on resistance to decay related to length of acetylation times, indicating that in shorter times

acetyl groups have already been taken by the acetate group (CH_3COO), leaving little opportunity for fungal attack (Pawar et al. 2013).

Conclusions

Acetylation of tropical lumbers is achieved with varying levels of WPG, which is more directly related to the type of species and less to the length of the acetylation time. This clearly evidences that differences from one species to another are attributed to liquid flow inside the wood, or permeability. This variation in WPG per species produces various effects on the properties of lumber. When species present WPG values over 10%, for example *V. ferruginea*, *V. guatemalensis*, *C. alliodora* or *E. cyclocarpum*, thermal stability and the contact angles increase, with the advantage that there is a decrease in the value of parameters related to water absorption (swelling, moisture content and moisture content variation) and a favourable increase in resistance to biological degradation. Additionally, for such species, results show that the 2.5 h time is an appropriate acetylation time. Meanwhile, despite the effects on the physical properties of their lumber, species with a low WPG value (under 5%) such as *C. odorata*, *G. arborea* and *T. grandis* do not benefit as effectively as species with a higher WPG.

References

Adebawo F, Sadeghifar H, Tilotta D, et al (2019) Spectroscopic interrogation of the acetylation selectivity of hardwood biopolymers. Starch - Stärke 71:1900086. doi: 10.1002/star.201900086

Adebawo FG, Naithani V, Sadeghifar H, et al (2016) Morphological and interfacial properties of chemically-modified tropical hardwood. RSC Adv 6:6571–6576. doi: 10.1039/C5RA19409A

Ahmed SA, Chun SK (2009) Observation of liquid permeability related to anatomical characteristics in Samanea saman. Turkish J Agric For 33:155–163. doi: 10.3906/tar-0807-13

Ahmed SA, Chun SK (2011) Permeability of Tectona grandis L. as affected by wood structure. Wood Sci Technol 45:487–500. doi: 10.1007/s00226-010-0335-5

Astm (2007) Standard test methods for direct moisture content measurement of wood and wood-base materials. Annu B ASTM Stand 92:1–6. doi: 10.1520/D4442-07.

ASTM (2005) Standard Practice for Calculation of Color Tolerances and Color Differences from Instrumentally Measured Color Coordinates 1. Annu B ASTM Stand i:1–10. doi: 10.1520/D2244-16

ASTM (1999) Standard Guide for Moisture Conditioning of Wood and Wood-Based Materials 1. Current i:1–8. doi: 10.1520/D4933-99R10.2

ASTM (1985) Standard test method for anti-swelling effectiveness of water-repellent formulations and differential swelling of untreated wood when exposed to liquid water environments. Annu B ASTM Stand Sect 4, Constr Vol 0409, Wood 702–706. doi: 10.1520/D4446-08R12.when

ASTM (2014) Standard test method of accelerated laboratory test of natural decay resistance of woods. Annu B ASTM Stand Vol 410 ASTM D2014:5

Bollmus S, Bongers F, Gellerich A, et al (2015) Acetylation of German Hardwoods. In: Proc of 8th European conference on wood modification. Helsini, Finland., pp 164–173

Bongers F, Meijerink T, Lütkemeier B, et al (2016) Bonding of acetylated wood. Int Wood Prod J 7:102–106. doi: 10.1080/20426445.2016.1161944

Chai Y, Liu J, Wang Z, Zhao Y (2016) Dimensional stability and mechanical properties of plantation poplar wood esterified using acetic anhydride. BioResources 12:. doi: 10.15376/biores.12.1.912-922

Collett BM (1972) A review of surface and interfacial adhesion in wood science and related fields. Wood Sci. Technol. 6:1–42

Cool J, Hernández RE (2011) Performance of three alternative surfacing processes on black spruce wood and their effects on water-based coating adhesion. Wood Fiber Sci 43:365–378

Cui W, Kamdem DP, Rypstra T (2004) Diffuse reflectance infrared fourier transform spectroscopy (DRIFT) and color changes of artificial weathered wood. Wood Fiber Sci 36:291–301

Emaminasab M, Tarmian A, Oladi R, et al (2017) Fluid permeability in poplar tension and normal wood in relation to ray and vessel properties. Wood Sci Technol 51:261–272. doi: 10.1007/s00226-016-0860-y

Engelund ET, Thygesen LG, Svensson S, Hill CAS (2013) A critical discussion of the physics of wood–water interactions. Wood Sci Technol 47:141–161. doi: 10.1007/s00226-012-0514-7

Fojutowski A, Koziróg A, Kropacz A, Noskowiak A (2014) The susceptibility of some acetylated hardwood species to mould fungi attack – An attempt to objectify the assessment. Int Biodeterior Biodegradation 86:60–65. doi: 10.1016/j.ibiod.2013.08.007

Gaitán-Álvarez J, Moya R, Berrocal A, Araya F (2020) In-situ mineralization of calcium carbonate of tropical hardwood species from fast-grown plantations in Costa Rica. Carbonates and Evaporites submited:

Gérardin P (2016) New alternatives for wood preservation based on thermal and chemical modification of wood— a review. Ann For Sci 73:559–570. doi: 10.1007/s13595-015-0531-

4

Gibson LJ (2012) The hierarchical structure and mechanics of plant materials. J R Soc Interface 9:2749–2766. doi: 10.1098/rsif.2012.0341

Gindl M, Sinn G, Gindl W, et al (2001) A comparison of different methods to calculate the surface free energy of wood using contact angle measurements. Colloids Surfaces A Physicochem Eng Asp 181:279–287. doi: 10.1016/S0927-7757(00)00795-0

Giridhar BN, Pandey KK, Prasad BE, et al (2017) Dimensional stabilization of wood by chemical modification using isopropenyl acetate. Maderas Cienc y Tecnol 19:15–20. doi: 10.4067/S0718-221X2017005000002

Hill CAS (2006) Wood Modification. John Wiley & Sons, Ltd, Chichester, UK, UK

Hon D (1995) Stabilization of wood color : is acetylation blocking effective ? Wood fiber Sci 27:360–367

Hung K-C, Yang C-N, Yang T-C, et al (2017) Characterization and thermal stability of acetylated slicewood production by alkali-catalyzed esterification. Materials (Basel) 10:393. doi: 10.3390/ma10040393

Kojima M, Yamamoto H, Okumura K, et al (2009) Effect of the lateral growth rate on wood properties in fast-growing hardwood species. J Wood Sci 55:417–424. doi: 10.1007/s10086-009-1057-x

Kozarić L, Kukaras D, Bešević M, et al (2016) Acetylated wood in constructions. Transilv. Univ. Braşov 9:81–86

Mantanis GI (2017) Chemical Modification of Wood by Acetylation or Furfurylation: A Review of the Present Scaled-up Technologies George. BioResources 12:4478–4489

Mantanis GI, Young RA (1997) Wetting of wood. Springer-Verlag

Matsunaga M, Hewage DC, Kataoka Y, et al (2016) Acetylation of wood using supercritical carbon dioxide. J Trop For Sci 28:132–138

Mitsui K (2010) Acetylation of wood causes photobleaching. J Photochem Photobiol B Biol 101:210–214. doi: 10.1016/j.jphotobiol.2010.07.005

Moya R (2018) La producción de madera de especies nativas en plantaciones comerciales: una opción real. Ambientico 267:32–36

Moya R, Perez D (2008) Effects of physical and chemical soil properties on physical wood characteristics of tectona grandis plantations in Costa Rica. J Trop For Sci 20:

Moya R, Rodriguez-Zuñiga A, Berrocal A, Vega-Baudrit J (2017a) Effect of silver nanoparticles synthetized with NPsAg- ethylene glycol (C2H6O2) on brown decay and white decay fungi of nine tropical woods. J Nanosci Nanotechnol 17:. doi: 10.1166/jnn.2017.13814

Moya R, Rodríguez-Zúñiga A, Puente-Urbina A (2017b) Thermogravimetric and devolatilisation analysis for five plantation species: Effect of extractives, ash compositions, chemical

compositions and energy parameters. Thermochim Acta 647:. doi: 10.1016/j.tca.2016.11.014

Moya R, Salas C, Berrocal A, Valverde JC (2015) Evaluation of chemical compositions, air-dry, preservation and workability of eight fastgrowing plantation species in costa rica. Madera Bosques 21:

Ozmen N (2007) Dimensional Stabilisation of Fast Growing Forest Species by Acetylation. J Appl Sci 7:710–714. doi: 10.3923/jas.2007.710.714

Özmen N, Çetin NS, Mengeloğlu F, et al (2013) Effect of wood acetylation with vinyl acetate and acetic anhydride on the properties of wood-plastic composites. BioResources 8:753–767. doi: 10.15376/biores.8.1.753-767

Papadopoulos AN (2006) Chemical modification of pine wood with propionic anhydride: Effect on decay resistance and sorption of water vapour. BioResources 1:67–74. doi: 10.15376/biores.1.1.67-74

Pawar PMA, Koutaniemi S, Tenkanen M, Mellerowicz EJ (2013) Acetylation of woody lignocellulose: Significance and regulation. Front. Plant Sci. 4:118

Rowell R (2012) Handbook of Wood Chemistry and Wood Composites. CRC Press

Rowell R (2016) Dimensional stability and fungal durability of acetylated wood. Drewno 59:139–150. doi: 10.12841/wood.1644-3985.C14.04

Rowell R, Ibach R (2018) Stable and durable wood products based on molecular modification. J. Trop. For. Sci. 30:488–495

Rowell RM (2004) Solid Wood Processing| Chemical Modification. In: Encyclopedia of Forest Sciences. Elsevier, pp 1269–1274

Rowell RM (2006a) Acetylation of wood: journey from analytical technique to commercial reality. For Prod J 56:4–12

Rowell RM (2006b) Chemical modification of wood: A short review. Wood Mater Sci Eng 1:29–33. doi: 10.1080/17480270600670923

Rowell RM (2014) Acetylation of wood-A review

Sadatnezhad SH, Khazaeian A, Sandberg D, Tabarsa T (2017) Continuous surface densification of wood: A new concept for large-scale industrial processing. BioResources 12:3122–3132. doi: 10.15376/biores.12.2.3122-3132

Sandberg D, Kutnar A, Mantanis G (2017) Wood modification technologies - A review. IForest 10:895–908

Sbirrazzuoli N, Vyazovkin S, Mititelu A, et al (2003) A Study of Epoxy-Amine Cure Kinetics by Combining Isoconversional Analysis with Temperature Modulated DSC and Dynamic Rheometry. Macromol Chem Phys 204:1815–1821. doi: 10.1002/macp.200350051

Shen X, Xie Y, Wang Q (2016) Improved acetylation efficacy of wood fibers by ionic liquid

pretreatment. BioResources 12:. doi: 10.15376/biores.12.1.684-695

Tenorio C, Moya R (2021) Development of a thermo-hydro-mechanical device for wood densification adaptable to universal testing machines and its evaluation in a tropical species. J Test Eval 49:. doi: 10.1520/JTE20180760

Tenorio C, Moya R (2013) Thermogravimetric characteristics, its relation with extractives and chemical properties and combustion characteristics of ten fast-growth species in Costa Rica. Thermochim Acta 563:. doi: 10.1016/j.tca.2013.04.005

Tenorio C, Moya R, Salas C, Berrocal A (2016) Evaluation of wood properties from six native species of forest plantations in Costa Rica. Bosque 37:. doi: 10.4067/S0717-92002016000100008

Thomas RJ (1976) anatomical features affecting liquid penetrability in three hardwood species. Wood Fiber Sci 4:256–263

Wålinder M, Brelid PL, Segerholm K, et al (2013) Wettability of acetylated Southern yellow pine. Int Wood Prod J 4:197–203. doi: 10.1179/2042645313Y.0000000045

Wang S, Dai G, Yang H, Luo Z (2017) Lignocellulosic biomass pyrolysis mechanism: A state-of-the-art review. Prog Energy Combust Sci 62:33–86. doi: 10.1016/j.pecs.2017.05.004

Willems W (2018) Hygroscopic wood moisture: single and dimerized water molecules at hydroxyl-pair sites? Wood Sci Technol 52:777–791. doi: 10.1007/s00226-018-0998-x

6. Artículo 5. Propiedades de la madera furfurilada de nueve especies tropicales de rápido crecimiento en Costa Rica

Propiedades de la madera furfurilada de nueve especies tropicales de rápido crecimiento en Costa Rica

Alexander BERROCAL

Instituto Tecnológico de Costa Rica, Escuela de Ingeniería Forestal, Apartado 159-7050, Cartago, Costa Rica. Email: aberrocal@itcr.ac.cr https://orcid.org/0000-0003-2041-4772

Johana GAITAN-ALVAREZ

Instituto Tecnológico de Costa Rica, Escuela de Ingeniería Forestal, Apartado 159-7050, Cartago, Costa Rica. Email: jgaitan@tcr.ac.cr https://orcid.org/0000-0003-4243-5910

Róger MOYA*

Instituto Tecnológico de Costa Rica, Escuela de Ingeniería Forestal, Apartado 159-7050, Cartago, Costa Rica. E-mail: rmoya@itcr.ac.cr https://orcid.org/0000-0002-6201-8383

Fabio ARAYA

Instituto Tecnológico de Costa Rica, Escuela de Química, Instituto Tecnológico de Costa Rica, Cartago 159-7050, Costa Rica. Email: fdaraya@itcr.ac.cr

Propiedades de la madera furfurilada de nueve especies tropicales de rápido crecimiento en Costa Rica

Resumen

El conocimiento del efecto de la furfurilación en maderas tropicales es limitado, por tal motivo el objetivo de este trabajo fue determinar la influencia de los tratamientos de furfurilación en las propiedades físicas, mecánicas y durabilidad de la madera de nueve especies utilizadas en la reforestación comercial en Costa Rica. Los resultados mostraron que la absorción de la disolución FA varió entre 90.8 y 308.7 (l m^{-3}) y en la disolución FA-NPs Ag varió entre 77.0 y 306.4 l m^{-3}. Para las propiedades de color se obtuvo que, en todas las especies en los parámetros L* y a* antes y después en ambos tratamientos, se presentaron diferencias estadísticas significativas; mientras que en el parámetro b* los resultados variaron dependiendo de la especie y el tratamiento. Con respecto al ΔE del cambio de color se obtuvo que en todas las especies este valor fue mayor en el tratamiento FA-NPs Ag. La densidad de todas las especies, en los diferentes tratamientos, varió entre 335.65 y 848.91 (kg m^{-3}). La propiedad hinchamiento a lo ancho varió entre 0.26 a 1.00 mm y en espesor varió entre 0.21 a 1.11 mm. En cuanto a la absorción de agua por inmersión se obtuvo menor absorción de agua en las muestras previamente furfuriladas. La pérdida de peso por biodeterioro causado por el hongo de pudrición café *Lenzites acuta* varió entre 3.98% a 15.06%, mientras que por efecto del hongo de pudrición blanca *Tramates versicolor* varió entre 3.14% y 15.06%. Para el esfuerzo de dureza se observó que los valores en todas las especies y tratamientos varió entre 1089.60 N y 5505.61 N. En la mayoría de especies el valor de dureza incrementó en los tratamientos de furfurilación (FA y FA-NPs Ag). Al evaluar el desempeño de los tratamientos, mediante los espectros del análisis rayos-X FTIR, se observó la existencia de 4 señales importantes en los tratamientos FA y FA-NPs Ag que no se presentan en las muestras no tratadas, estas señales se logran observar en 899, 1562, 1652 y 1711 cm^{-1}. El comportamiento de descomposición térmica en el TGA de las nueve maderas furfuriladas presentó el mismo patrón que la madera sin tratar, sin embargo, se logró observar las diferencias en la descomposición de las especies a través de la curva de DTG. A través del análisis de microscopía de escaneo de láser confocal se logró observar una mayor cantidad de fluorescencia en la especie de mayor absorción, principalmente alrededor de los vasos en el tratamiento de FA, mientras que el tratamiento con FA-NPs sólo se observó en las fibras y en la no tratada no se presentó fluorescencia. De la

misma forma, pero en menor cantidad, se observa fluorescencia en la especie de media absorción, principalmente en el tratameinto FA-NPs. Finalmente, en la especie de ligera absorción la fluorescencia es mínima y poco visible en los tratamientos de furfurilación.

Palabras clave: propiedades de la madera, maderas tropicales, plantaciones de rápido crecimiento, densificación, absorción de humedad.

Introducción

La madera tiene excelentes propiedades físicas y mecánicas, así como también texturas únicas, que le permiten desempeñar un papel destacado en el campo de la construcción, obtención de productos derivados y la mueblería (Li et al., 2016). Como material, la madera se considera fácil de trabajar, renovable, altamente disponible y sostenible (Mantanis, 2017). En su mayor parte, se ha utilizado sin ninguna modificación (Rowell, 2016; Rowell, 2014).

Sin embargo, algunas de sus características inherentes la hacen susceptible, por ejemplo, la afinidad con el agua y la biodegradabilidad, reducen su calidad. La modificación de la madera es una forma de mejorar estas características, para aumentar el uso de los productos de madera (Lahtela y Kärki, 2015), mejorando la durabilidad de la madera, sin el uso de sustancias tóxicas (Mantanis, 2017). La modificación de la madera con alcohol furfurílico (FA), conocida como furfurilación, se ha estado desarrollando en las últimas décadas. El FA es un derivado del furfural, obtenido a través del proceso de hidrogenación (Sejati et al., 2017). El propósito de la furfurilación es mejorar propiedades de la madera, tales como la resistencia a la descomposición y disminuir la absorción de humedad (Lande, Westin, et al., 2004a; Lande et al., 2008). La polimerización del alcohol furfurílico en la madera es una reacción química bastante compleja. El cuestionamiento de si la furfurilación de la madera es una verdadera modificación química de la pared cellular, sigue sin respuesta por parte de la comunidad científica (Mantanis, 2017). Algunos científicos creen que sí corresponde a proceso de modificación química, ya que alcohol furfurílico (polímero) reacciona consigo mismo y posiblemente también lo hace con la lignina en las paredes celulares (Gérardin, 2016; Li et al., 2016; Nordstierna et al., 2008).

Por lo tanto, los complejos de alcohol furfurílico son depositados predominantemente en las cavidades de la madera, y también en las paredes celulares y se polimerizan in situ (Mantanis y Lykidis, 2015). La polimerización se lleva a cabo en las cavidades microscópicas de las

células, lo que se detecta fácilmente mediante varias técnicas microscópicas (Barsberg y Thygesen, 2009). Estudios recientes de nanoindentación han indicado que las mejoras en el módulo de indentación y la dureza de las células de madera furfuriladas demuestran indirectamente, pero significativamente, que el alcohol furfurílico penetra en las células de madera durante el proceso de modificación (Li et al., 2016).

La furfurilación de la madera brinda una alta protección contra la biodegradación por hongos (Esteves et al., 2011; Kumari et al., 2016) termitas (Gascón-Garrido et al., 2013; Hadi et al., 2005), bacterias y barrenadores marinos (Westin et al., 2006) y envejecmiento (Temiz et al., nd), así como también aumenta la dureza, disminuye el contenido de humedad de equilibrio y mejora en gran medida la estabilidad dimensional de la madera (Lande, Westin, et al., 2004a; Mantanis y Lykidis, 2015). Los cambios en las propiedades mecánicas dependen de características medibles (Lahtela y Kärki, 2015). Mientras que algunas propiedades muestran cambios insignificantes, otras como por ejemplo la dureza, pueden aumentar aproximadamente un 50% (Esteves et al., 2011).

Sejati et al., (2017) determinaron que la furfurilación conduce a una mejora de varias propiedades de la madera, tal y como lo ratifican otros estudios. Por ejemplo Esteves et al. (2011) informaron que la furfurilación de la madera puede reducir el contenido de humedad de equilibrio (EMC) de 17.3 a 9%. Baysal et al. (2004) encontraron una mejora en la eficiencia anti hinchamiento (ASE) y una disminución en la absorción de agua (WA) de la madera furfurilada. Si bien el FA no tiene del todo o tiene un efecto ligeramente positivo en las propiedades mecánicas (Xie et al., 2013), algunos de esos efectos positivos son el aumento del módulo de ruptura y la elasticidad (Lande et al. 2004b) y la dureza Brinell (Epmeier et al., 2004). Sin embargo, uno de los inconvenientes de este tratamiento es la disminución de la resistencia al impacto (Lande, Eikenes, et al., 2004).

A pesar de que múltiples estudios muestran que la madera furfurilada es un material excelente y ecológico, debido a que la madera furfurilada no es dañina para el medio ambiente o los usuarios durante y después de la vida útil, e incluso cuando se quema, la madera furfurilada no libera más materia orgánica volátil. compuestos (VOC) e hidrocarburos aromáticos policíclicos (HAP) que la madera no tratada (Lande, Westin, et al., 2004a; Pilgård et al., 2010), y en consecuencia, se ha comercializado con éxito (Dong et al. 2014); la madera se vuelve más oscura después de la furfurilación (Herold et al., 2013), lo que también limita la aplicación del proceso. Por lo tanto, es importante investigar cómo mejorar la resistencia de la madera con

una baja ganancia porcentual en peso, para reducir el efecto de oscurecimiento, especialmente en maderas de rápido crecimiento.

El objetivo principal de este estudio fue determinar el efecto de los tratamientos de furfurilación en las propiedades físicas, mecánicas y durabilidad de la madera de nueve especies utilizadas en la reforestación comercial en Costa Rica (*Cedrela odorata, Cordia alliodora, Enterolobium cyclocarpum, Gmelina arborea, Hieronyma alchornoides, Samanea saman, Tectona grandis, Vochysia ferruginea* y *Vochysia guatemalensis*) y evaluar el desempeño del proceso.

Metodología

Materiales

Madera de albura de nueve especies, que presentan buena permeabilidad (Moya et al., 2015; Tenorio et al., 2016), provenientes de plantaciones forestales de rápido crecimiento en Costa Rica, fue utilizada. Las especies seleccionadas fueron *Cedrela odorata (C.o), Cordia alliodora (C.a), Enterolobium cyclocarpum (E.c), Gmelina arborea (G.a), Hieronyma alchorneoides (H.a), Samanea saman (S.s), Tectona grandis (T.g), Vochysia ferruginea (V.f)* y *Vochysia guatemalensis (V.g)*. La edad de las plantaciones donde se recolectó el material varió entre los 4 y los 8 años de edad. En el muestreo fueron cortados tres árboles por especie en trozas de 1 metro de largo y luego fue aserrada en tablas de 7,5 cm de ancho x 2,5 cm de espesor. Estás tablas se dejaron secar al aire hasta que llegaran a un contenido de humedad entre 12-15% y luego se extrajeron piezas de dimensiones de 46 cm de largo x 7.5 cm de ancho y 2 cm de espesor, garantizando que la madera se compusiera de madera de albura.

Los reactivos utilizados fueron alcohol furfurílico al 98% de la marca comercial Sigma Aldrich Chemistry (Belgium) distribuido en Costa Rica por CASJIM (https://www.sigmaaldrich.com/catalog/product/aldrich/w249106?lang=en&region=CR&gclid=CjwKCAiA1rPyBRAREiwA1UIy8NjvSgcHZkXmW9fkShf7iDe0jclqE1aJQUYqQd0sxyWSY1aJwYkoXxoC0sAQAvD_BwE). Borato de sodio 10-hidrato de la marca comercial J.T. Baker (Madrid, España) distribuido por Fisher Scientific (https://www.fishersci.es/es/es/brands/IPF8MGDA/jt-baker.html). Ácido cítrico de la marca comercial Central Drug House (New Delhi, India), distribuido en Costa Rica por PreLab (https://www.prelab.com/). Acido oxálico dihidratado extra puro de la marca comercial Oxforf

Lab Fine Chem LLP (Maharastra, India) distribuido en Costa Rica por PreLab (https://www.prelab.com/).

Proceso de furfurilación

El proceso de furfurilación se llevó a cabo en un reactor de vacío-presión de dimensiones de 10 cm de diámetro y 31 cm de largo con capacidad de 2.5 litros. Se utilizaron 15 muestras por tratamiento de cada especie. Se probaron dos disoluciones, una con nanopartículas de plata, y otra sin nanopartículas de plata. El proceso consistió en la introducción de las 15 muestras en el reactor para luego aplicar vacío por 45 minutos a -70 kPa (gauge), para luego introducir solución de alcohol furfulirico (FA), la primera estaba constituida de una proporción de FA (50%), agua destilada (46.25%), borato de sodio utilizado como agente buffer (2%), y ácido orgánico como catalizador compuesto de ácido oxálico y ácido cítrico (1.75%) identificada como solución FA, y la segunda estaba constituida por una proporción de FA (50%), agua destilada (46.25%), borato de sodio utilizado como agente buffer (2%), y ácido orgánico como catalizador compuesto de ácido oxálico y ácido cítrico (1.75%), y 50 ppm de nanopartículas de plata, identificada como FA-NPs Ag. Una vez colocada la solución adentro del reactor, se aplicó presión 690 kPa por 2 horas, luego de esto se extrajo el excedente de la solución líquida y se limpiaron las muestras para eliminar excedente de la solución en la superficie. Luego se fijó la temperatura del reactor a 40°C por 4 horas aplicando vacíos de presión a -70 kPa (gauge) cada hora por 20 minutos. Transcurridas las 4 horas se extrajeron las muestras del reactor se envolvieron en papel aluminio y se introdujeron en un horno por 16 horas a 103°C.

Características iniciales

La característica inicial evaluadas en el proceso de furfurilación fue el cambio de color del material. El color fue determinado en la totalidad de muestras antes y después del proceso de furfurilación en los dos tratamientos. Un espectrofotómetro marca HunterLab miniSkan XE Plus fue utilizado para medir el color, con sistema cromatográfico estandarizado CIE L * a * b *. El sistema de color CIE L* a * b * permite la medición tridimensional del color. El cambio total de color (ΔE*) se cuantificó de acuerdo con la norma ASTM D-2244 (ASTM, 2005) y se esTablació por diferencia entre los parámetros de color antes y después de la furfulización.

Evaluación del proceso de furfurilación

En el proceso de furfurilación fueron testeadas 15 muestras de cada uno de los tratamientos, de 2 cm de espesor, 5 cm de ancho y 5 cm de largo. Paralelamente, fueron extraídas 15

muestras que no fueron tratadas para su comparación con los tratamientos de furfurilación, en todas las especies estudiadas. Las muestras tratadas fueron pesadas y medidas sus dimensiones de largo, ancho y espesor; antes y después del proceso de furfurilación. El proceso de impregnación de la furfurilación se evaluó mediante la absorción de la solución (Ecuación 1), en tres distintos momentos del proceso. La absorción 1, la cual corresponde a la cantidad de material impregnado después del proceso de vacío-presión con la solución. La absorción 2, la cual corresponde a la cantidad de material después de aplicar 40°C de temperatura en el reactor por 4 horas. Y la absorción 3, corresponde al valor después de las muestras ser llevadas al horno por 16 horas a una temperatura de 103°C.

$$Absorción\ \left(\frac{litros}{m^3}\right) = \left(\frac{Peso\ _{antes}(g) - Peso_{después}(g)}{Volumen\ de\ la\ muestra\ (cm^3)}\right) x \frac{1\ litros}{1000} \qquad (1)$$

Propiedades físicas

Se determinaron las propiedades físicas de densidad, contenido de humedad, absorción de agua de la madera por inmersión, hinchamiento de la madera en sentido tangencial y radial y absorción de humedad por el cambio de condición en contenido de humedad en equilibrio (de 12% a 18%). La densidad de las muestras fue determinada en las 15 muestras impregnadas con y sin nanopartículas de plata y en las 10 no tratadas, se midió el volumen por las dimensiones de largo, ancho, espesor y el peso de la muestra para luego determinar la densidad (peso /volumen). El contenido de humedad a su vez fue calculado igualmente en todas las muestras impregnadas con y sin nanopartículas de plata y 10 no impregnadas, siguiendo el procedimiento de la norma ASTMD4442-42 (ASTM, 2007). Para determinar el hinchamiento tangencial, radial y el porcentaje de absorción de agua, 15 muestras de cada tratamiento por especie de 5x5x2 cm fueron acondicionadas y pesadas al 12% y luego por un periodo de 3-4 semanas fueron acondicionadas al 18% de humedad. Después de acondicionadas nuevamente fueron pesadas y medidas sus dimensiones. Este procedimiento es basado en la norma ASTM D4933-99 (ASTM, 1999) pero modificada a las condiciones de Costa Rica, donde las condiciones ambientales de humedad son de aproximadamente 18%. Para el cálculo de hinchamiento tangencial y radial se utilizó la ecuación 2. La absorción de humedad fue calculada con la ecuación 3, obteniendo primero el contenido de humedad 12% y al 18% con respecto al peso seco (Ecuación 3), y la diferencia de ambos contenidos de humedad fue la absorción de humedad de las muestras (Ecuación 4). Para la ganancia de peso

por inmersión en agua, 15 muestras cada especie/tratamiento previamente pesadas fueron sumergidas en agua por 24 horas, después de las 24 horas se registró el peso y siguiendo la ecuación 4, se obtuvo la ganancia en peso, este procedimiento fue seguido según la norma ASTM D4446 –13 (ASTM, 1985).

$$Hinchamiento\ \ (mm) = (g)\frac{medición12\%\ (mm) - medición18\%\ (mm)}{medición\ 12\%\ (mm)} * 100 \quad (2)$$

$$Contenido\ de\ humedad_{MC} = \frac{Peso_{CH}\ \ (g) - Peso_{seco\ al\ horno}\ (g)}{Peso_{seco\ al\ hor}\ \ \ (g)} * 100 \quad (3)$$

$$Absorción\ de\ humedad = Contenido\ de\ humedad_{18\%} - Contenido\ de\ humedad_{12\%} \quad (4)$$

Propiedades mecánicas

La propiedad mecánica evaluada fue la dureza de la madera. Para este análisis la prueba se realizó en 20 muestras furfulizadas con y sin nanopartículas de plata y 20 muestras sin tratar, en todas las especies estudiadas. La dureza Janka fue determinada siguiendo los estándares ASTM D143-14 (2000).

Durabilidad

Para llevar a cabo el ensayo de resistencia a la descomposición natural se utilizó la metodología expuesta en la norma ASTM D-2017-81 (1994). En cada tratamiento (sin furfurilación, furfurilada sin nano partículas y furfurilada con nanopartículas) y para cada especie se prepararon 15 muestras de 2 cm de ancho x 2 cm de largo x 2 cm de espesor de tamaño. Se utilizaron dos tipos de hongos para esta prueba, los cuales fueron *Trametes versicolor* y *Lenzites acuta*, correspondiente a pudrición blanca y café, respectivamente. En cada tipo de hongo fueron sometidos a la degradación del hongo un total de 15 muestras por especie/tratamiento.

Espectroscopia de rayos-X FTIR

De cada especie fue tomada muestras de madera furfurilizada con y sin nanopartículas de plata y no tratadas, estas fueron molidas a un tamaño de 420 µm 250 µm (40 y 60 mesh, respectivamente). Las muestras fueron secadas al horno a 105°C hasta peso constante. Luego fue realizado el barrido de espectroscopia infrarroja de transformada de Fournier (FTIR), utilizando un espectrómetro Nicolet 380 FTIR (Thermo Scientific) con una célula reflectante única (equipada con un cristal de diamante). El equipo se configuró para realizar lecturas acumulando 32 exploraciones con una resolución de 1 cm^{-1}, con una corrección de fondo antes

de cada medición. Los espectros FTIR obtenidos se procesaron con el software Spotlight 1.5.1, HyperView 3.2 y Spectrum 6.2.0 desarrollados por Perkin Elmer. Inc.

Análisis termo gravimétrico TGA

Para obtener las curvas de degradación térmica se realizó un TGA bajo una presión atmosférica inerte en un ambiente de nitrógeno, utilizando de cada tratamiento por especie 5mg de aserrín previamente seco. Se utilizó una velocidad de calentamiento de 20°C min^{-1} desde los 50°C hasta los 800°C, en una atmosfera de nitrógeno de pureza ultra alta en un flujo de 100 ml min^{-1}. Los análisis se realizaron en un analizador termogravimétrico TA Instruments, modelo SDT Q600. El TGA proporciono valores para la pérdida de masa en relación con la temperatura, a partir de la cual se obtuvo la termogravimetría derivada (DTG), lo que permitió determinar la posición y la temperatura a la que se produjo la degradación de la muestra. Los datos TGA y sus derivados (DTG) fueron analizados en el software TA Instruments Universal Analysis 2000.

Microscopía de escaneo láser confocal

El instrumento utilizado fue un microscopio confocal de escaneo láser (TCS SP2, Leica Microsystems, Wetzlar, Alemania) con un objetivo 639 (inmersión en agua). Las dos longitudes de onda de excitación del láser utilizadas fueron 488 y 633 nm, y los rangos del detector fueron 500-550 y 550-600 nm, respectivamente. Se usó el mismo ajuste de ganancia para cada una de las dos longitudes de onda de excitación, permitiendo así la comparación directa de las intensidades de emisión para imágenes obtenidas usando la misma longitud de onda de excitación. Se obtuvieron tres imágenes por especie, una con cada tratamiento (FA y FA-NPs Ag) y otra sin tratamiento.

Análisis estadístico

El análisis estadístico consistió primeramente en comprobar la normalidad y homogeneidad de los datos y la eliminación de datos extraños o “outliers”. Una vez realizado esto, el análisis descriptivo consistió en la determinación de promedio, desviación estándar y coeficiente de variación para cada variable estudiada por cada especie y tratamiento. Posteriormente, para cada variable evaluada se realizó un análisis de varianza ANOVA con un nivel de significancia estadística de $p< 0.05$ para determinar la variabilidad de cada una ante el tratamiento de furfurilación la prueba de Tukey fue usada para determiner la significancia estadística de las diferencias entre las medias de las variables. Este análisis se realizó en el programa SAS 9.4 (SAS Institute Inc., Cary, N.C.).

Resultados y análisis de resultados

Características iniciales del material

El análisis ANOVA para las características iniciales del material mostró, que existen diferencias significativas entre las variables absorción, parámetro de color L* después del tratamiento, parámetro de color a* después del tratamiento, parámetros de color b* después del tratamiento y ΔE* con respecto a la especie, el tratamiento y la interacción especie*tratamiento.

Tabla 1. Valor F del ANOVA para las características iniciales del material de nueve especies tropicales de rápido crecimiento de Costa Rica.

Variable	Especie	Tratamiento	Especie*Tratamiento
Absorción	20.26**	0.30^{NS}	4.15**
Parámetro de color L* después	11.28**	85.46**	5.86**
Parámetro de color a* después	11.85**	10.28**	3.67**
Parámetro de color b* después	7.97**	22.24**	2.46**
ΔE*	15.69**	68.40**	5.97**

Nota: * media estadísticamente significativa al 99%.

En la absorción de las disoluciones de la furfurilación se obtuvo que en la disolución FA la absorción varió entre 90.8 y 308.7 (l m^{-3}) siendo *C.o* la especie con menor absorción y *V.f* la especie con mayor absorción (Figura 1a). En esta primera disolución las especies que presentaron menor absorción y por ende diferencias estadísticas con respecto a los demás fueron *C.o, G.a* y *T.g* (Figura 1a). En la disolución FA-NPs Ag la absorción varió entre 77.0 y 306.4 l m^{-3}, siendo *S.s* la especie con menor absorción y la mayor *V.f* (Figura 1b). En esta disolución las especies que presentaron diferencias estadísticas con respecto a las demás fueron *C.o, S.s, E.c* y *T.g* (Figura 1a y 1b). Con respecto a las diferencias encontradas por especie se tiene que en *S.s* y *E.c* se presentaron diferencias significativas entre ambos tratamientos, siendo mayor la absorción con la disolución de FA, de la misma manera en *G.a* y *H.a* se presentaron diferencias significativas entre los tratamientos, siendo FA-NPs Ag la que presento la mayor absorción (Figura 1c).

La absorción (l m^{-3}) de las disoluciones a partir de FA y FA-NPs Ag, empleadas en la furfurilación de la madera, varió con el tipo de disolución y entre especies. Estas variaciones están en

concordancia con lo obtenido en estudios similares, ya ha sido reportado que la absorción de sustancias hidrosolubles, por métodos vacío presión, se ve influenciada por la variación en la estructura anatómica de la madera. De la misma forma, Keenan y Tejada (1988) encontraron que la absorción de sustancias en la madera está relacionada con su densidad en diferentes especies forestales de bosques naturales en la Región Andina de Colombia, Perú, Bolivia y Venezuela. Así mismo, diferencias en la absorción de sustancias hidrosolubles en las maderas de rápido crecimiento de Costa Rica (Figura 1), adicionadas utilizando el método vacío-presión, ya han sido reportadas por Moya et al 2015 y Tenorio et al 2016.

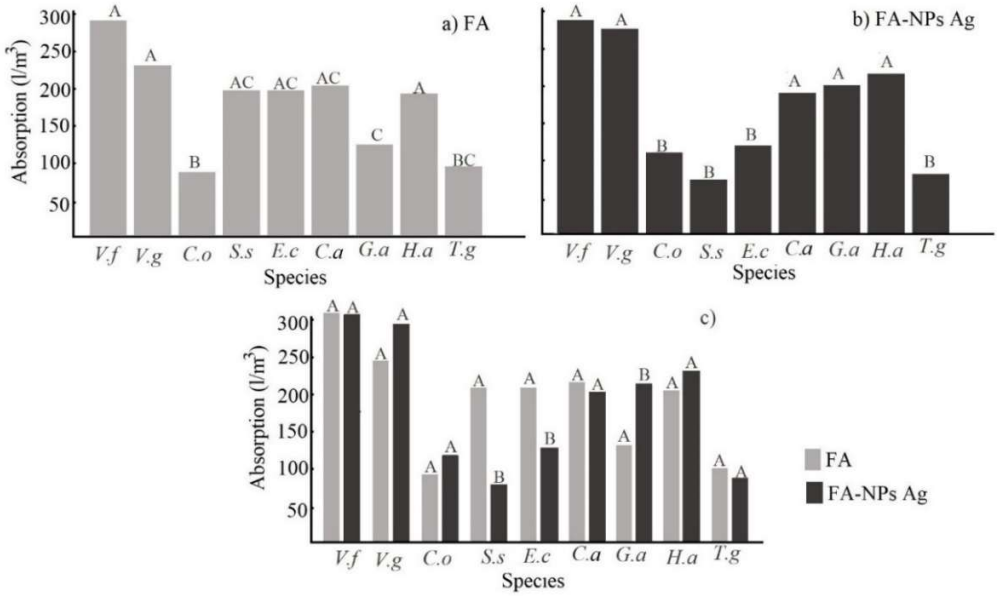

Figura 1. Absorción de alcohol furfurílico (a), y alcohol furfurílico con nano partículas de plata, en nueve especies tropicales de Costa Rica.

Notas: a, b: Diferentes letras entre especies significa estadísticamente diferente al 99%.

c: Diferentes letras entre tratamientos FA y FA-NPs Ag significa estadísticamente diferente al 99%.

En las propiedades de color se obtuvo que en todas las especies en el parámetro L* antes y después (L^*_i and L^*_f) en ambos tratamientos se presentó una disminución del color estadísticamente significativa (Tabla 2). En el parámetro de color a* se presentó que antes y después de los tratamientos (a^*_i and a^*_f) ocurrió un aumento del valor en todas las especies, exceptuando en *H.a* y *T.g* donde se presentó una disminución, sin embargo, en todas las especies y tratamientos se presentaron diferencias estadísticas significativas (Tabla 2).

Tabla 2. Parámetros de color y cambio de color de madera furfurilada de nueve especies tropicales en Costa Rica

Especie	Tratamiento	L_i	L_f	a^*_i	a^*_f	b^*_i	b^*_f	ΔE
Vochysia ferruginea	FA	79,32^A	48,88^B	5,29^A	8,54^B	16,82^A	21,46^B	31,94^A
	FA-NPs Ag	79,82^A	34,61^B	5,2^A	8,02^B	17,19^A	15^A	46,06^A
Vochysia guatemalensis	FA	79,71^A	41,43^B	5,97^A	10,73^B	19,4^A	22,86^B	39,09^A
	FA-NPs Ag	79,99^A	32,37^B	5,92^A	10,3^B	19,31^A	20,63^A	48,35^A
Cedrella odorata	FA	77,57^A	45,54^B	6,87^A	9,53^B	19,96^A	22,78^B	30,46^A
	FA-NPs Ag	76,01^A	45,17^B	7,66^A	9,78^B	22,61^A	20,16^A	31,65^A
Samanea saman	FA	81,45^A	54,28^B	3,94^A	6,48^B	24,97^A	18,59^B	29,41^A
	FA-NPs Ag	81,05^A	31,96^B	4,41^A	9,94^B	25,9^A	17,2^B	50,69^B
Enterolobium cyclocarpoum	FA	79,84^A	53,03^B	4,08^A	8,91^B	21,16^A	25,69^B	29,07^A
	FA-NPs Ag	77,59^A	25,54^B	4,49^A	8,57^B	21,36^A	17,61^B	51,5^B
Cordia allidora	FA	76,38^A	46,14^B	4,35^A	7,4^B	17,73^A	18,38^A	31,1^A
	FA-NPs Ag	75,26^A	23,93^B	4,46^A	9,39^B	17,75^A	15,99^A	52,45^B
Gmelina arborea	FA	76,49^A	66,2^B	4,74^A	7,32^B	21^A	22,97^B	11,35^A
	FA-NPs Ag	74,42^A	53,42^B	5,3^A	9,32^B	22,02^A	21,33^A	21,86^A
Hieronima alchorneoides	FA	71,49^A	39,87^B	11,15^A	9,47^B	19,21^A	20,09^A	32,33^A
	FA-NPs Ag	68,96^A	43,82^B	11,73^A	9,07^B	18,64^A	18,78^A	26,14^A
Tectona grandis	FA	79,8^A	47,99^B	4,83^A	11,43^B	22,47^A	24,42^A	33,18^A
	FA-NPs Ag	79,31^A	34,67^B	4,78^A	12,58^B	24,66^A	25,43^A	46,01^A

Nota: Diferentes letras entre parámetros iniciales y finales de color inicial significan estadísticamente diferentes al 99%

Diferentes letras entre tratamientos FA y FA-NPs Ag en ΔE* significan estadísticamente diferentes al 99%.

En el parámetro de color b* antes y después de los tratamientos (b^*_i y b^*_f), se presentaron cambios de color al aplicar los tratamientos en las especies *S.s* y *E.c* en ambos tratamientos ocurrió un cambio de color presentando diferencias estadísticas significativas; en *V.f, V.g, C.o*, y *G.a* solamente se presentaron diferencias estadísticamente significativas en el cambio de color en el tratamiento FA-NPs Ag; mientras que en *C.a , H.a* y *T.g* no se evidenció cambio del parámetro de color en ninguno de los dos tratamientos (Tabla 1). Con respecto al ΔE del cambio

de color por tratamiento en cada especie se obtuvo que en todas las especies este valor fue mayor en el tratamiento FA-NPs Ag, sin embargo sólo en las especies *S.s, E.c* y *C.a* se presentaron diferencias estadísticas significativas entre el tratamiento FA y FA-NPs Ag (Tabla 2).

Con respecto al cambio color registrado durante el proceso de furfurilación, los resultados obtenidos fueron consistentes con un estudio realizado por Dong et al. (2016) en cuatro especies de rápido crecimiento (poplar, Chinese fir. Eucalyptus y Masson pine). En ambos casos se obtuvo una diminución en el parámetro L*, que está directamente relacionada con la concentración del alcohol furfurílico, además el parámetro a* incrementó en todos los casos, mientras que el parámetro b* varió entre especies. Un incremento en los valores a* y b*, indican que la superficie de la madera tiende a volverse rojiza (Temiz et al. 2007).

De la misma forma, Acosta et al. (2020) encontraron que para *Pinus elliottii* la madera tratada con FA (alcohol furfurílico), presentó menor brillo (L*) para los planos tangencial y radial. Con respecto a las coordenadas verde-rojo (a*), a mayor concentración de FA, mayor incremento en este parámetro, lo que significó una predominancia de tonos rojos en la superficie de la madera tratada. En términos generales el parámetro a* está íntimamente relacionado con los compuestos fenólicos de diferentes maderas (Lima et al. 2005), lo cual parece indicar un cambio químico, que no es totalmente claro, en la lignina o en algún extractivo orgánico que pertenece a la madera. Por otra parte, la coordenada azul-amarillo (b*) de la madera tratada cambió significativamente en ambos planos (Acosta et al. 2020). Teóricamente, el parámetro b* está asociado con cromóforos orgánicos presentes en los extraíbles y la lignina (Pincelli et al. 2012), indicando también una interacción química entre la madera y el alcohol furfurílico.

En el ΔE del cambio de color por tipo de tratamiento entre todas las especies, mostró que, en el tratamiento FA el mayor valor lo obtuvo *V.g* con 39.1 y el menor *G.a* con 11.4, en este tratamiento *C.o, G.a* y *H.a* fueron las especies que presentaron diferentes estadísticas significativas (Figura 2a). En cuanto al tratamiento FA-NPs Ag el mayor valor de cambio de color ΔE* lo presentó *V.g* con 48.4 y el menor *G.a* con 26.1 siendo esta ultima la única especie diferente estadísticamente con respecto a las restantes (Figura 2b).

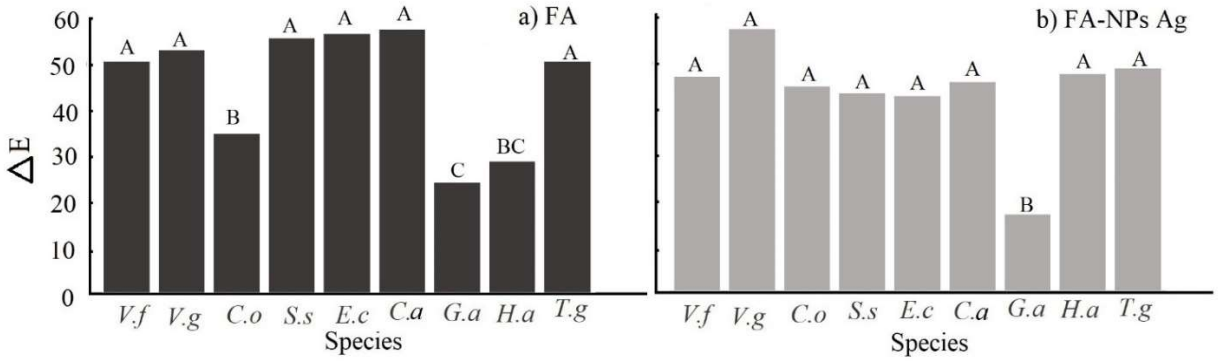

Figura 2. Cambio de color de madera furfurilada de nueve especies tropicales en Costa Rica

Notas: Diferentes letras entre especies significa estadísticamente diferente al 99%.

Estos resultados son consistentes con lo reportado por Acosta et al. (2020), aunque en su estudio solamente se observaron diferencias significativas en el plano tangencial entre las maderas furfuriladas, debido a que los tratamientos causaron niveles de cambio de color especialmente en el plano tangencial, que fue el que cambió de color uniformemente.

Si bien el oscurecimiento de la madera es beneficios para ocultar manchas y decoloraciones (Don et al. 2016). Algunos estudios han reportado que la madera furfurilada exhibe efectos extensivos de tonalidades grisáceas en sus superficies después de un largo tiempo de envejecimiento al exterior (Temiz et al. 2007; Mantanis y Lykidis, 2015). Por lo tanto, la potencial aplicación de maderas de rápido crecimiento furfuriladas, sería para uso en interiores tales como muebles, pisos y usos decorativos, para remplazar maderas valiosas.

Propiedades físicas

En relación a las propiedades físicas, se observaron dos tendencias claramente definidas, la primera donde la furfurilación mejora significativamente las propiedades como fue el caso de la densidad y la disminución en la capacidad para absorber humedad. Por el contrario, el efecto en otras propiedades tales como hinchamiento a lo ancho y en espesor al pasar de un contenido de humedad en equilibrio de 12% a 18% y la absorción de humedad por el cambio de condición en contenido de humedad en equilibrio (de 12% a 18%) varió entre especies y no mostró diferencias significativas entre los tratamientos, factores tales como la anatomía de las especies, concentración, penetración y polimerización del alcohol furfurílico en la madera y sus interacciones, pudieron haber generado este comportamiento para estas propiedades.

La densidad de todas las especies en los diferentes tratamientos varió entre 335.65 y 848.91 (kg m^{-3}), obteniendo el menor valor *V.f* y el mayor valor *H.a* (Tabla 3). Además, se logró observar que en la mayoría de especies el valor de densidad aumenta al comparar sin tratamiento con el tratamiento FA, pero luego disminuye en el tratamiento a FA-NPs Ag (Tabla 3), exceptuando en *C.o* y *H.a* donde el valor densidad se mantuvo en los tratamientos y en *G.a* donde la densidad a FA-NPs Ag fue la mayor (Tabla 3).

El efecto positivo en la densidad obtenido en este estudio, viene dado por la forma en que se lleva a cabo el proceso de furfurilación en la madera. La penetración y polimerización del alcohol furfurílico en las cavidades de la madera y en la pared celular, mejoran la mayoría de las propiedades de la madera modificada (Li et al. 2015). Para *Pinus pinaster*, Esteves et al. (2011) reportaron un incremento en la densidad de 37% en madera furfurilada. La densificación de productos de madera, así como también su mayor estabilidad dimensional y el incremento en otras propiedades, se atribuye al tamaño molecular reducido de los monómeros de alcohol furfurílico, que penetran más fácilmente las paredes celulares de la madera (Westin et al. 2009; Kokaefe et al. 2015). En todas las especies se presentaron diferencias estadísticas entre los tratamientos evaluados, siendo sin tratamiento diferente estadísticamente a FA y FA-NPs Ag (Tabla 3).

La propiedad hinchamiento a lo ancho varió entre 0.26 a 1.00 mm, donde el menor valor lo obtuvo *V.f* y el mayor *E.c* (Tabla 3), se observó a su vez que en *V.f* y *C.o* ocurrió una disminución del valor de hinchamiento a lo ancho en los tratamientos de furfurilación, sin embargo en *V.g, G.a* y *T.g* ocurrió una disminución en el tratamiento con FA pero un aumento en el tratamiento FA-NPs Ag, y en *S.s, E.c, C.o* y *H.a* ocurrió un aumento en el hinchamiento a lo ancho en el tratamiento FA, pero una disminución en el tratamiento FA-NPs Ag (Tabla 3), a pesar de esto solo se presentaron diferencias estadísticas con respecto a la madera no tratada en V.*f, S.s, E.c, Co* y *T.g* (Tabla 3).

El hinchamiento en espesor varió entre 0.21 y 1.11 mm, obteniendo el menor valor en *T.g* y el mayor en *V.g*, en esta propiedad no se evidenciaron tendencias definidas con respecto no tratada, tratamiento FA y tratamiento FA-NPs Ag, y se presentaron diferencias significativas en *V.g, E.c, H.a* y *T.g* (Tabla 3).

Tabla 3. Propiedades físicas de madera furfurilada de nueve especies tropicales en Costa Rica

Especie	Tratamiento	Densidad (kg m^{-3})	Hinchamiento en ancho (mm)	Hinchamiento en espesor (mm)	Variación de humedad (%)	Absorción de agua (%)
Vochysia ferruginea	No tratada	364,04 (8,76)^{A}	0,61 (42,25)^{A}	0,82 (83,58)^{A}	1,75 (12,94)^{A}	41,72 (9,11)^{A}
	FA	662,01 (6,63)^{B}	0,60 (65,85)^{A}	0,97 (87,99)^{A}	2,7 (22,73)^{A}	16,16 (11,27)^{B}
	FA-NPs Ag	527,97 (4,28)^{C}	0,26 (101,59)^{B}	0,56(71,92)^{A}	2,07 (19,36)^{A}	10,39 (38,87)^{C}
Vochysia guatemalensis	No tratada	359,03 (6,01)^{A}	0,71 (29,64)^{A}	0,67 (97,72)^{A}	2,46 (14,93)^{A}	46,59 (11,48)^{A}
	FA	610,69 (5,69)^{B}	0,53 (59,90)^{A}	0,40 (85,18)^{A}	3,45 (37,15)^{AB}	17,64 (14,40)^{B}
	FA-NPs Ag	589,35 (8,17)^{B}	0,64 (85,31)^{A}	1,11 (47,99)^{B}	4,04 (23,98)^{B}	14,17 (11,20)^{B}
Cedrella odorata	No tratada	335,63 (9,23)^{A}	0,44 (42,09)^{A}	0,46 (64,31)^{A}	1,82 (9,58)^{A}	34,68 (9,90)^{A}
	FA	412,15 (8,02)^{B}	0,33 (44,41)^{A}	0,49 (100,60)^{A}	1,59 (18,43)^{A}	28,9 (14,58)^{B}
	FA-NPs Ag	371,97 (6,80)^{AB}	0,19 (71,89)^{A}	0,51 (81,20)^{A}	1,17 (58,78)^{A}	25,92 (11,71)^{B}
Samanea saman	No tratada	604,06 (1,88)^{A}	0,44 (50,24)^{A}	0,32 (84,02)^{A}	2,04 (11,43)^{A}	28,02(6,96)^{A}
	FA	695,24 (5,02)^{B}	0,74 (86,43)^{B}	0,41 (92,34)^{A}	3,11 (65,92)^{A}	24,67 (7,80)^{A}
	FA-NPs Ag	693,12 (4,82)^{B}	0,61 (41,26)^{B}	0,36 (53,17)^{A}	1,97 (11,37)^{A}	10,5 (13,89)^{B}
Enterolobium cyclocarpum	No tratada	517,83 (16,50)^{A}	0,36 (72,48)^{A}	0,44 (101,88)^{A}	1,6 (33,74)^{A}	30,94 (11,62)^{A}
	FA	591,84 (7,13)^{B}	1,00 (48,26)^{B}	0,51 (49,21)^{AB}	5,88 (67,10)^{B}	26,99 (12,44)^{A}
	FA-NPs Ag	557,16 (7,89)^{AB}	0,66 (34,81)^{AB}	0,68 (56,63)^{B}	4,98 (34,28)^{B}	16,75 (22,91)^{B}
Cordia allidora	No tratada	364,72 (7,10)^{A}	0,33 (45,53)^{A}	0,36 (58,28)^{A}	1,55 (17,64)^{A}	35,42 (12,23)^{A}
	FA	539,51 (5,26)^{B}	0,34 (71,84)^{A}	0,41 (95,63)^{A}	1,37 (42,61)^{A}	28,4 (10,37)^{B}
	FA-NPs Ag	539,18 (8.08)^{B}	0,76 (29,53)^{B}	0,51 (89,03)^{A}	3,94 (26,61)^{B}	17,22 (25,13)^{C}
Gmelina arborea	No tratada	486,86 (9,90)^{A}	0,41 (36,25)^{A}	0,4 (114,37)^{A}	1,45 (19,65)^{A}	12,15 (28,41)^{A}
	FA	490,42 (14,20)^{A}	0,38 (69,03)^{A}	0,28 (84,74)^{A}	1,68 (29,54)^{A}	23,1718,24)^{B}
	FA-NPs Ag	576,64 (6,23)^{B}	0,42 (76,93)^{A}	0,29 (71,69)^{A}	1,29 (51,06)^{A}	22,1 (12,01)^{B}
Hieronima alchorneoides	No tratada	643,99 (5,81)^{A}	0,61 (48,35)^{A}	0,7 (71,91)^{A}	1,5 (22,28)^{A}	19,3 (7,64)^{A}
	FA	848,86 (7,37)^{B}	0,83 (31,40)^{A}	0,88 (91,06)^{A}	2,09 (14,60)^{A}	8,51 (5,23)^{B}
	FA-NPs Ag	848,91 (9,81)^{B}	0,78 (83,66)^{A}	0,34 (92,86)^{B}	0,81 (53,92)^{A}	8,73 (22,58)^{B}
Tectona grandis	No tratada	568,17 (5,50)^{A}	0,56 (52,62)^{A}	0,69 (97,05)^{A}	1,4 (19,07)^{A}	23,88 (10,54)^{A}
	FA	659,87 (3,24)^{B}	0,20 (63,88)^{B}	0,21 (117,38)^{B}	1,13 (28,34)^{A}	15,91 (25,68)^{B}
	FA-NPs Ag	652,83 (7,63)^{B}	0,39 (117,19)^{AB}	0,26 (101,00)^{B}	1,45 (17,58)^{A}	11,91 (23,42)^{B}

Nota: Diferentes letras entre tratamientos (No tratada, FA y FA-NPs Ag) significa estadísticamente diferente al 99%.

La absorción de humedad al pasar de un CH de 12% al 18%, varió entre 0.81 y 5.88%, donde el menor valor se registró en *H.a* y el mayor en *E.c* (Tabla 3), en esta propiedad se logra

observar una tendencia en el aumento de variación de la humedad en los tratamiento de furfurilación con respecto a no tratada, sin embargo sólo en *V.g, E.c, H.a* y *T.g* se lograron evidenciar diferencias estadísticas (Tabla 3). Factores tales como la anatomía de las especies, concentración, penetración y polimerización del alcohol furfurílico en la madera y sus interacciones, pudieron haber generado este comportamiento para estas propiedades.

En cuanto a absorción de agua por inmersión se obtuvo que el menor valor se presentó en *H.a* con 8,51 % y el mayor en *V.g* con 46,59 % (Tabla 3), en esta variable se logra evidenciar que existe menor absorción de agua en las muestras previamente furfuriladas ya que en todas las especies la madera no tratada presenta el mayor porcentaje de absorción de agua, a su vez es menor el porcentaje de absorción de agua en el tratamiento FA-NPs Ag que en el tratamiento FA, exceptuando *G.a* donde la madera no tratada presentó el mayor porcentaje, de la misma forma en todas las especies se presentaron diferencias estadísticas significativas entre no tratada y los tratamientos de furfurilación (FA y FA-NPs Ag) (Tabla 3).

Este efecto ya ha sido reportado por otros autores, por ejemplo Dong et al. (2015) encontraron que para madera de albura de *Pupulus* spp modificada con una matriz de alcohol furfurílico con nano partículas de SiO_2, mostró que el porcentaje de absorción de humedad era de 50% en madera tratada a diferentes concentraciones de nanoSiO_2 (0% a 2,0%), mientras que en la madera sin tratamiento el porcentaje de absorción fue cercana al 90%.

Dong et al (2016) encontraron para poplar, Eucalyptus, Chinese fir y pino que la madera furfurilida tiene menor índice de hinchamiento y menor porcentaje de absorción de agua, variando entre 0,64 y 0,44 del valor para la madera sin tratamiento al aumentar la concentración de FA de un 30% a un 70% en el primer caso, para las diferentes especies. Mientras que el porcentaje de absorción de agua también fue menor en madera tratada en comparación con la madera no tratada, con variaciones de 37% y 18% del valor para la madera sin tratamiento, al aumentar la concentración de FA de un 30% a un 70% para las cuatro especies estudiadas. Similar comportamiento fue reportado por Baysal et al (2004) para madera de Japanese cedar y Scots pine, el proceso de furfurilación reduce el porcentaje de absorción de agua de 180 y 123% a 21% y 45%, respectivamente.

La explicación de este comportamiento viene dada porque en el proceso de furfurilación se espera que la resina FA hidrófoba incorporada, ubicada en las cavidades celulares y en los microporos de la pared celular, ocupe el espacio disponible para el agua, disminuyendo así su

absorción por parte de la madera (Kong et al. 2018). Teniendo en cuenta sus pequeñas moléculas y polaridad, los monómeros el FA pueden ingresar a la pared celular y polimerizarse allí después del curado. Se espera que la resina FA hidrofóbica formada se acumule en la pared celular y, por lo tanto, reduzca la capacidad de la pared celular de hincharse tras la inmersión en agua, lo que da como resultado una estabilidad dimensional mejorada de la madera tratada (Kong et al 2018). De hecho, sólo la parte de la resina FA, que ingresa a las paredes celulares, contribuye a la estabilidad dimensional de la madera, mientras que las depositadas en el lumen celular muestra un menor efecto.

Propiedades mecánicas y biodeterioro

La pérdida de peso debido al deterioro causado por el hongo de pudrición café *Lenzites acuta* varió entre 3.98% a 15.06% donde el menor valor se observó en *C.a* y el mayor en *S.s* (Figura 3a), además quedó evidenciado que en la mayoría de las especies ocurre una disminución de la pérdida de peso antes los tratamientos de furfurilación exceptuando en *C.o* donde ocurrió un aumento del porcentaje en el tratamiento FA-NPs Ag (Figura 3a), a su vez se observó que *V.g, C.o, S.s, E.c, C.a* y *T.g* presentaron diferencias estadísticas entre madera no tratada y los tratamientos de furfurilación (FA y FA-NPs Ag) (Figura 3a). Por su parte, la pérdida de peso por efecto del hongo de pudrición blanca *Tramates versicolor* varió entre 3.14% y 15.06% donde el menor valor se observó en *C.o* y el mayor *S.s* (Figura 3b), para este hongo la pérdida de peso fue menor en los tratamientos de furfurilación exceptuando las *especies G.a, H.a* y *T.g* donde se observó mayor pérdida de peso en el tratamiento FA-NPs Ag (Figura 3b), a pesar de la tendencia observada, en estas tres especies no se evidenciaron diferencias estadísticas, mientras que en las restantes especies, la madera no tratada fue estadísticamente diferente a los tratamientos FA y FA-NPs Ag (Figura 3b).

Esta tendencia de menor pérdida de masa en madera furfurilada con respecto a la madera sin tratar, registrada en este estudio, ya ha sido reportada por otros autores (Lande et al. 2004b, Thygesen et al. 2010; Esteves et al. 2011 y Li et al 2015).

Se han propuesto varios mecanismos posibles para explicar esta resistencia al deterioro. Venås (2008) sugirió que la reducción en el volumen vacío, a través del aumento de volumen con FA, fue una posible razón del aumento de la resistencia a la descomposición de la madera furfurilada; a saber, las resinas formadas a base del furfurilo bloquean la vía de acceso de los hongos descomponedores en la madera. La penetración de resina en la pared celular de la

madera y posible la reticulación entre FA y los componentes de la pared celular, cambia la naturaleza química de la pared celular, por lo que no resulta atractivo para los hongos en descomposición (Pilgård y Alfredsen 2009; Lande et al. 2004b). Por su parte, Ringman et al. (2014) creen que la reducción en la absorción de humedad también contribuyó a inhibir el crecimiento de hongos en la madera furfurilada.

Al igual que para hongos de pudrición, la madera furfurilada es resistente a perforadores marinos, terminas subterráneas y de madera seca (Lande et al. 2004; Lande y Westin, 2004; Westin et al. (2016). Existe una relación directa entre retención y niveles de protección para diferentes agentes de biodeterioro (Schneider, 2007). De la misma forma, la pérdida de masa causada por pudrición en madera furfurilada con una WPG media (30%) y alta (50%) fueron menores a las pérdidas de masa de muestras tratadas con CCA a una retención para clase de uso 4, en contacto con el suelo (Lande et al. 2008). En esa misma línea Lande et al. (2004) reportan que la resistencia a la pudrición blanca y café es alta para madera furfurilada, tratada con una WPG de 35%. Los cementerios de estacas confirman la misma tendencia de que la madera furfurilada también tiene potencial de alta resistencia al deterioro, inclusive en contacto con el suelo.

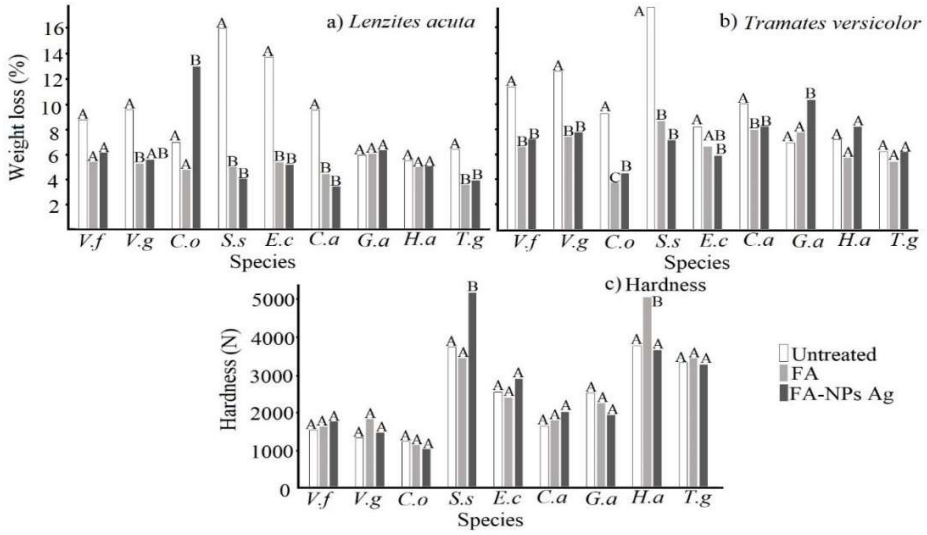

Figura 3. Pérdida de peso causada por el hongo de pudrición café *Lenzites acuta* (a) y el hongo de pudrición blanca *Trametes versicolor* (b) y esfuerzo de dureza (c) de madera furfurilada de nueve especies tropicales en Costa Rica.

Nota: Diferentes letras entre tratamientos (no tratada, FA y FA-NPs Ag) significa estadísticamente al 99%.

Para el esfuerzo de dureza se observó que los valores en todas las especies y tratamientos varió entre 1089.60 (en *C.o*) y 5505.61 N (en *H.a*) (Figura 3c). En la mayoría de especies el valor de dureza incrementa en los tratamientos de furfurilación (FA y FA-NPs Ag), tal es el caso de *V.f, V.g, S.s, E.c, C.a, H.a* y *T.g* (Figura 3c), sin embargo el análisis estadístico mostró que solamente en *S.s* y *H.a* se presentaron diferencias estadísticas (Figura 3c).

El efecto de la furfurilación, en diferentes propiedades mecánicas de la madera, está explicado en parte por su correlación positiva con la densidad de la madera (Van Gelder et al. 2006). En esta misma línea, se infiere que la resina FA llena las cavidades de las células y ayuda a reforzar la estructura de la madera, aumentando así su resistencia al colapso en la compresión. Por el contrario, para las propiedades de flexión el efecto de refuerzo de la resina FA probablemente se ve contrarrestado por la inevitable degradación ácida de las hemicelulosas durante el tratamiento, lo que debilita la integridad de la estructura de la pared celular (Kong et al.2018).

Una mejora en las propiedades de dureza por efecto de la furfurilación y la furfurilación modificada con nanopartículas, como la observada en este estudio para especies tropicales de rápido crecimiento, ya fue reportada para madera de albura de *Populus* spp. de rápido crecimiento, tratada con FA y una mezcla de FA-SiO_2 y donde se obtuvo un incremento en su dureza de 34% y 48%, respectivamente (Dong et al. 2014). De la misma forma, Larsson-Brelid (2013) indicó que la madera furfurilada se caracteriza por una mayor dureza, elasticidad y módulos de ruptura en comparación con la madera no tratada; sin embargo, también es más frágil.

No todas las propiedades mecánicas se ven incrementadas con la furfurilación, Kong et al. (2018) reportan una ligera mejoría del MOE (20%) y una reducción ligeramente menor en el MOR (11%) para la madera furfurilada, a pesar de su alta carga de resina FA. Las diferentes influencias de la furfurilación en la compresión y la resistencia a la flexión de la madera están explicadas por la interacción entre las especies y el proceso de furfurilación (Don et al. 2015, Li et al. 2015). Albura de *Pinus pinaster*, tratada con una mezcla de alcohol furfurílico (70%) mostró un decrecimiento de 40% en el contenido de humedad en equilibrio, un incremento en la estabilidad dimensional del 45%, el MOE se vio ligeramente afectado por el tratamiento, el esfuerzo de flexión incrementó un 6%, a diferencia de la dureza, que aumentó un 50% y la densidad un 37% (Esteves et al. 2011).

Las propiedades de flexión parecen ser más sensibles a la degradación de los componentes de la pared celular. Como consecuencia, la furfurilación da como resultado un MOE ligeramente mejorado e incluso un MOR reducido para la madera tratada (Kong et al.2018).

Espectroscopia de rayos-X FTIR

En los espectros del análisis rayos-X FTIR se logró observar la existencia de 4 señales importantes en los tratamientos FA y FA-NPs Ag que no se presentan en las muestras no tratadas, estas señales se logran observar en 899, 1562, 1652 y 1711 cm^{-1} (Figura 4a-i). A su vez de estas señales las más pronunciadas fueron la 899 y 1711 cm^{-1} (Figura 4a-i), mientras que más leves fueron 1562 y 1652 cm^{-1} (Figura 4a-i). También se logra observar que en *V. f, V. g, S.s, E. c y C. a* (Figura 4 a, b, d, e, f), estas señales son más notorias, y poco notorias o casi nulas en *C. o, G. a, H. a* y *T. g* (Figura 4 c, g, h, i).

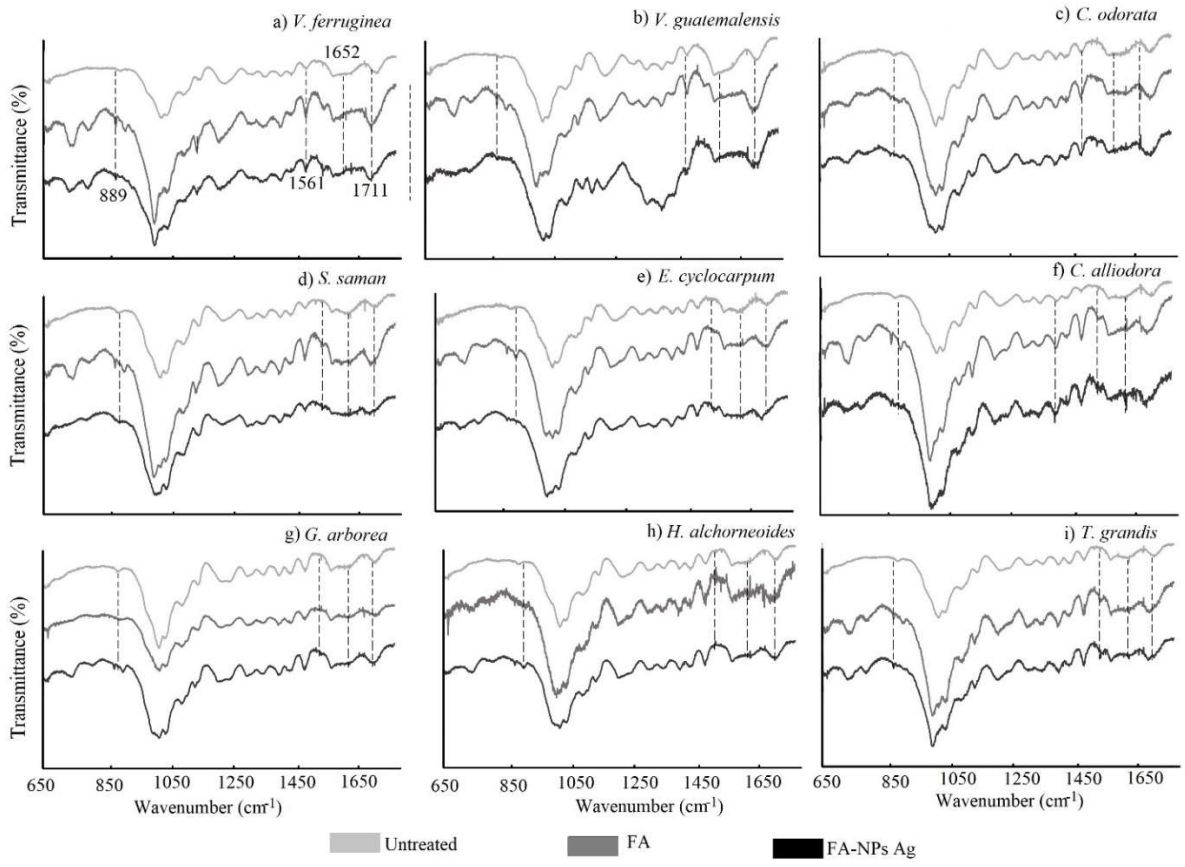

Figura 4. Espectro FT-IR de madera furfurilada con diferentes tratamientos de nueve especies tropicales en Costa Rica.

En cuanto a la caracterización de la madera furfurilada por medio del FTIR las señales encontradas en la madera tratada a 1711 y 1562 cm^{-1} (Figura 4a-i) son atribuidos a una vibración de C=O de la y-dicetona formada a partir de la apertura del anillo hidrolítico de los anillos del furano de las resinas de FA impregnadas y la vibración esquelética de los anillos 2.5-disustituidos de furano respectivamente (Ahmad et al., 2013; Pranger & Tannenbaum, 2008), lo que representa la polimerización del monómero de FA y FA-NPs en la madera (Dong et al., 2014). Las pequeñas señales encontradas a 1652 y 899 cm^{-1} se asignan al estiramiento de carbonilo conjugado y entre los enlaces B-glucosídicos y las unidades de azúcar, respectivamente (Sun, 2001). Este comportamiento, explicado por (Ahmad et al., 2013), lo atribuye a la hidrólisis ácida de la lignina y la hemicelulosa en la madera, producto de la impregnación de las resinas (FA y FA-NPs Ag). A su vez en aquellas especies con mayor absorción de las resinas como V*. ferruginea* (*V.f*)*, V. guatemalensis* (*V.g*)*, S. saman* (*S.s*)*, E. cyclocarpum* (*E.c*), *C. allidora* (*C.a*) y *H. alchorneoides* (*H.a*) (Figura 4) las señales de FTIR mencionadas anteriormente fueron más notables (Figura 4), lo que señala que en estas especies la reacción fue adecuada y las resinas a base de FA se añadieron correctamente a la madera. Lo que concuerda con el estudio de (Gao et al., 2017), en madera de albura de Poplar de rápido crecimiento.

Análisis termo gravimétrico TGA

El comportamiento de descomposición térmica en el TGA de las nueve maderas furfuriladas presenta el mismo patrón que la madera sin tratar, sin embargo, se logra observar las diferencias en la descomposición de las especies a través de la curva de DTG (Figura 5). En la madera furfurilada y la madera no tratada de las nueve especies, se observa un pico en la curva de DTG después de los 200 °C, luego un pico máximo de descomposición en 320-360 °C; y la tercera descomposición después de los 380 °C (Figura 5). Así mismo, se logra observar también que las curvas DTG en todas las especies es menor en la madera no tratada, en comparación con aquellas tratadas (FA y FA-NPs). A su vez se logra observar que la mayoría de especies furfuriladas el pico después de los 200°C disminuye o es casi nulo, con respecto a la madera no tratada, exceptuando *S.s, H. a* y *T. g* (Figura 5 d, h, i).

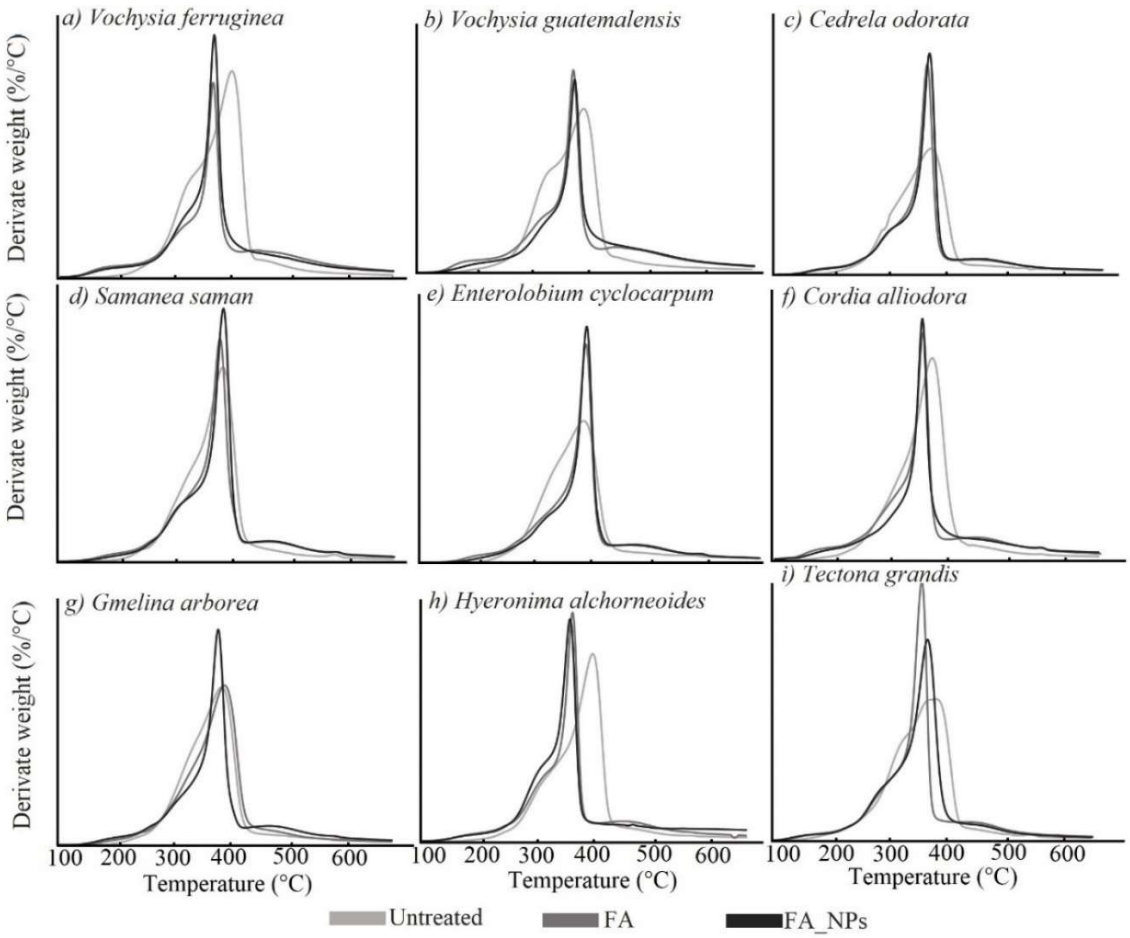

Figura 5. Análisis DTG de madera con diferentes tratamientos de furfurilación de nueve especies tropicales de rápido crecimiento en Costa Rica.

En el análisis de estabilidad térmica (TGA-DTG) comúnmente las hemicelulosas son los primeros componentes en degradarse y el primer hombro visible en la curva DTG (Figura 5) (Yang et al., 2019). El pico máximo de degradación representa la degradación de las celulosas (Sarvaramini y Larachi, 2017). Mientras que lo restante corresponde a las ligninas, las cuales se degradan durante un intervalo de temperatura mayor (Worasuwannarak et al., 2007). Como se logró observar el pico de máxima degradación fue mayor en las muestras tratadas con las resinas de FA (FA y FA-NPs) (Figura 5), lo que explica que los polímeros de FA llenan los poros de la madera, provocando que la interacción entre FA y la celulosa de la madera mejore, dando como resultado una mayor estabilidad térmica (Dong et al., 2020). Este resultado concuerda con otros trabajos (Kong et al., 2018; Shirmohammadli et al., 2019) donde los autores señalan que al agregar resinas con FA aumenta la estabilidad térmica del material.

A su vez también en aquellas especies con mayor absorción de las resinas *V. f, V. g, S. s, E. c*, *C. a* y *H. a* (Figura 1) se observó una menor pérdida de masa entre los 200°C y 300°C (Figura 5) en las muestras tratadas con FA y FA-NPs, lo que puede estar relacionado con el hecho de que la matriz inorgánica podría promover la formación de carbón auto aislante en las superficies de madera furfurilada, lo que inhibe la transferencia de calor a estas temperaturas (Dong et al., 2015). Mientras que su principal pérdida de masa ocurre entre los 320 y 400 °C (Figura 5), rango de temperatura donde se degrada el FA, el cual también se superpone con la degradación del mayor porcentaje de celulosa y parte de la lignina (Bastani et al., 2015b, 2015a; Wang et al., 2019).

Microscopía de escaneo de láser confocal

Para el análisis de microscopía de escaneo de láser confocal se seleccionaron tres especies una primera de absorción alta como *Vochysia ferruginea* (*V.f*), de mediana absorción *Enterolobium cyclocarpum* (*E.c*) y de baja absorción *Tectona grandis* (*T.g*) (Figura 1). Se logró observar mayor cantidad de fluorescencia en la especie de mayor absorción (Figura 6 a,b,c) principalmente alrededor de los vasos en el tratameinto de FA (Figura 6a), mientras que el tratamiento con FA-NPs sólo se observó en las fibras (Figura 6b), y en la no tratada no se presentó fluorescencia (Figura 6c). De la misma forma, pero en menor cantidad, se observa fluorescencia en la especie de media absorción (Figura 6 d,e), principalmente en el tratameinto FA-NPs (Figura 6e). Y en la especie de ligera absorción la fluorescencia es mínima y poco visible en los tratamientos de furfurilación (Figura 6 g,h).

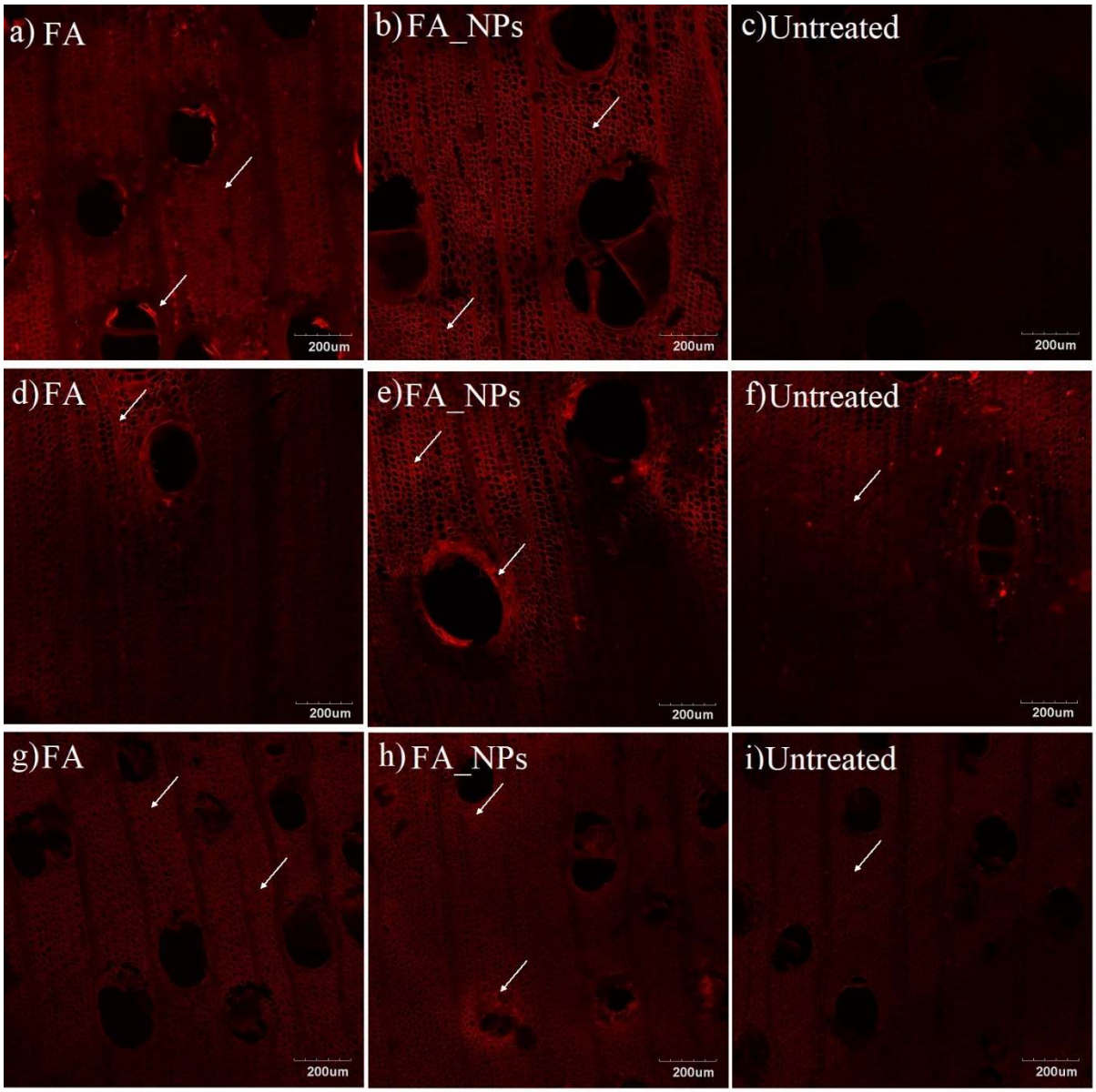

Figura 6. Microscopía de escaneo de láser confocal para muestras de alta absorción de alcohol furfurílico (*Vochysia ferruginea* (a,b,c)), media absorción de alcohol furfurílico (*Enterolobium cyclocarpum* (d, e, f)) y baja absorción de alcohol furfurílico (*Tectona grandis* (g, h, i)) de especies tropicales de rápido crecimiento en Costa Rica.

La micro distribución de las resinas (FA y FA-NPs) en las cavidades de la madera impregnada se lograron observar por medio de imágenes de microscopía de escaneo de láser confocal (Figura 6) en una longitud de onda de 600 nm. Se logró observar que entre mayor sea la absorción de las resinas en *V. f* (Figura 1), mayor es la emisión de fluorescencia (Figura 6 a,b).

Esta emisión se da principalmente en las paredes de los vasos y los lúmenes de las células (Figura 6 a,b,d,e). Lo cual concuerda con Kong et al. (2018), que reportó que los polímeros de la pared celular probablemente constituyen un entorno restringido para la polimerización de FA, lo que provoca un acceso restringido para las resinas de FA, quedándose depositadas en la pared celular. A su vez también Thygesen et al. (2010), explica que las regiones ricas en lignina favorecen la polimerización de FA, lo que da como resultado un depósito preferido de las resinas de FA dentro de estas regiones. Y como se logró observar en *V. f* (Figura 6 a,b) y *E. c* (Figura d,e) el marco de la pared celular de la madera está constituido por fibras, cuyo componente principal es la lignina (Wang et al., 2019), por lo que la fluorescencia se emite con mayor brillo en estas regiones (L. G. Thygesen et al., 2010). A su vez es de esperar que en aquellas especies con menor absorción de las resinas la fluorescencia sea mínima o casi nula como lo ocurrido en *T. g* en los tres tratamientos (Figura 6g, h, i).

Finalmente, un aspecto relevante para promover el uso del proceso de furfurilación a escala industrial en maderas tropicales de rápido crecimiento, es el hecho de que la toxicidad del alcohol furfurílico podría constituir un inconveniente para este tratamiento, sin embargo, la toxicidad se reduce fuertemente después de la polimerización. Los resultados no mostraron una ecotoxicidad significativa, la combustión no liberó ningún compuesto orgánico volátil o hidrocarburos poliaromáticos por encima de los niveles normales para la combustión de madera (Lande et al. 2004b; Lande et al. 2004c; Pilgard et al. 2010a, b). De manera similar, Vetter et al. (2008) demostraron que la furfurilación protege la madera adecuadamente, sin representar una amenaza para el medio ambiente. Lo que ratifica que la furfurilación de la madera es un proceso seguro para el medio ambiente, que puede implementarse en maderas tropicales de rápido crecimiento para incrementar algunas de sus propiedades y dar mayor valor agregado a los productos que se fabrican a partir de ellas.

Conclusión

La furfurilación de maderas tropicales se logró con diferentes niveles de absorción de las soluciones de FA y FA- NPs Ag, fenómeno que está relacionado directamente con el tipo de especies. Esta tendencia claramente evidenció que las diferencias entre especies, observadas en este estudio, son atribuidas al flujo del líquido dentro de la madera o a la permeabilidad. La furfurilación mejoró la densidad de la madera, redujo la capacidad de absorber humedad,

aumentó la dureza, tuvo efecto en el color, en la estabilidad dimensional y en la anisotropía. Así mismo, disminuyó la pérdida de masa por efecto de hongos de pudrición blanca y café. Fue posible evaluar el desempeño del proceso mediante métodos indirectos tales como: espectroscopia de rayos-X FTIR, análisis termo gravimétrico TGA y microscopía de escaneo de láser confocal. Finalmente, quedó demostrado, a partir de los resultados obtenidos, que la aplicación de furfurilaciónen en madera de especies tropicales de rápido crecimiento es una alternativa viable para obtener productos de mejores características y consecuentemente con un mayor valor agregado.

Referencias

Acosta, Andrey Pereira, Schulz, Henrique Römer, Barbosa, Kelvin Techera, Zanol, Gustavo Spiering, Gallio, Ezequiel, Delucis, Rafael de Avila, & Gatto, Darci Alberto. (2020). Dimensional stability and colour responses of *Pinus elliottii* wood subjected to furfurylation treatments. *Maderas. Ciencia y tecnología*, Epub 05 de abril de 2020.https://dx.doi.org/10.4067/S0718-221X2020005000305

Ahmad, E. E. M., Luyt, A. S., & Djoković, V. (2013). Thermal and dynamic mechanical properties of bio-based poly(furfuryl alcohol)/sisal whiskers nanocomposites. *Polymer Bulletin*, *70*(4), 1265–1276. https://doi.org/10.1007/s00289-012-0847-2

ASTM. (1985). Standard test method for anti-swelling effectiveness of water-repellent formulations and differential swelling of untreated wood when exposed to liquid water environments. *Annual Book of ASTM Standards. Section 4, Construction. Volume 04.09, Wood*, 702–706. https://doi.org/10.1520/D4446-08R12.when

ASTM. (1999). Standard Guide for Moisture Conditioning of Wood and Wood-Based Materials 1. *Current*, *i*(Reapproved), 1–8. https://doi.org/10.1520/D4933-99R10.2

ASTM. (2005). Standard Practice for Calculation of Color Tolerances and Color Differences from Instrumentally Measured Color Coordinates 1. *Annual Book of ASTM Standards*, *i*, 1–10. https://doi.org/10.1520/D2244-16

ASTM. (2007). Standard test methods for direct moisture content measurement of wood and wood-base materials. *Annual Book of ASTM Standards*, *92*(December), 1–6. https://doi.org/10.1520/D4442-07.

Barsberg, S. & Thygesen, L. (2009). Poly(furfuryl alcohol) formation in neat furfuryl alcohol and in cymene studied by ATR-IR spectroscopy and density functional theory (B3LYP) prediction of vibrational bands. *Vibrational Spectroscopy*, 49(1), 52-63. 10.1016/j.vibspec.2008.04.013.

Bastani, A., Adamopoulos, S., & Militz, H. (2015a). Gross adhesive penetration in furfurylated,

N-methylol melamine-modified and heat-treated wood examined by fluorescence microscopy. *European Journal of Wood and Wood Products*, *73*(5), 635–642. https://doi.org/10.1007/s00107-015-0920-2

Bastani, A., Adamopoulos, S., & Militz, H. (2015b). Water uptake and wetting behaviour of furfurylated, N-methylol melamine modified and heat-treated wood. *European Journal of Wood and Wood Products*, *73*(5), 627–634. https://doi.org/10.1007/s00107-015-0919-8

Baysal, E., Ozaki, S. K., & Yalinkilic, M. K. (2004). Dimensional stabilization of wood treated with furfuryl alcohol catalysed by borates. *Wood Science and Technology*, *38*(6), 405–415. https://doi.org/10.1007/s00226-004-0248-2

Dong, Y., Ma, E., Li, J., Zhang, S., & Hughes, M. (2020). Thermal properties enhancement of poplar wood by substituting poly(furfuryl alcohol) for the matrix. *Polymer Composites*, *41*(3), 1066–1073. https://doi.org/10.1002/pc.25438

Dong, Y., Qin, Y., Wang, K., Yan, Y., Zhang, S., Li, J., & Zhang, S. (2016). Assessment of the Performance of Furfurylated Wood and Acetylated Wood: Comparison among Four Fast-Growing Wood Species. *BioResources*, *11*(2), 3679–3690. https://doi.org/10.15376/biores.11.2.3679-3690

Dong, Y., Yan, Y., Wang, K., Li, J., Zhang, S., Xia, C., Shi, S. Q., & Cai, L. (2016). Improvement of water resistance, dimensional stability, and mechanical properties of poplar wood by rosin impregnation. *European Journal of Wood and Wood Products*, *74*(2), 177–184. https://doi.org/10.1007/s00107-015-0998-6

Dong, Y., Yan, Y., Zhang, S., & Li, J. (2014). Wood/Polymer Nanocomposites Prepared by Impregnation with Furfuryl Alcohol and Nano-SiO2. *BioResources*, *9*(4), 6028–6040. https://doi.org/10.15376/biores.9.4.6028-6040

Dong, Y., Yan, Y., Zhang, S., Li, J., & Wang, J. (2015). Flammability and physical–mechanical properties assessment of wood treated with furfuryl alcohol and nano-SiO2. *European Journal of Wood and Wood Products*, *73*(4), 457–464. https://doi.org/10.1007/s00107-015-0896-y

Epmeier, H., Westin, M., & Rapp, A. (2004). Differently modified wood: Comparison of some selected properties. *Scandinavian Journal of Forest Research*, *19*, 31–37. https://doi.org/10.1080/02827580410017825

Esteves, B., Nunes, L., & Pereira, H. (2011). Properties of furfurylated wood (Pinus pinaster). *European Journal of Wood and Wood Products*, *69*(4), 521–525. https://doi.org/10.1007/s00107-010-0480-4

Gao, X., Dong, Y., Wang, K., Chen, Z., Yan, Y., Li, J., & Zhang, S. (2017). Improving Dimensional and Thermal Stability of Poplar Wood via Aluminum-based Sol-Gel and Furfurylation Combination Treatment. *BioResources*, *12*(2). https://doi.org/10.15376/biores.12.2.3277-3288

Gascon, P., Oliver-Villanueva, J.V., Ibiza-Palacios, M.S., Militz, H. , Mai, C. & Adamopoulos, S.

(2013). Resistance of wood modified with different technologies against Mediterranean termites (Reticulitermes spp.). *International Biodeterioration & Biodegradation*, *82*, 13-16. 10.1016/j.ibiod.2012.07.024.

Gérardin, P. (2016). New alternatives for wood preservation based on thermal and chemical modification of wood— a review. *Annals of Forest Science*, 73(3), 559–570. https://doi.org/10.1007/s13595-015-0531-4

Hadi, Y. S., Westin, M., & Rasyid, E. (2005). Resistance of furfurylated wood to termite attack. *Forest Products Journal*, *55*(11), 85-88.

Herold, N., Dietrich, T., Grigsby, W. J., Franich, R. A., Winkler, A., Buchelt, B., & Pfriem, A. (2013). Veneer treatments: DSC. In *BioResources* (Vol. 8, Issue 1). http://ojs.cnr.ncsu.edu/index.php/BioRes/article/view/3240

Keenan, F., & Tejada, M. (1987). *Maderas Tropicales como Material de Construcción en los países del Grupo Andino de América del Sur*. https://idl-bnc-idrc.dspacedirect.org/bitstream/handle/10625/8403/IDL-8403.pdf?sequence=1

Kong, L., Guan, H., & Wang, X. (2018). In Situ Polymerization of Furfuryl Alcohol with Ammonium Dihydrogen Phosphate in Poplar Wood for Improved Dimensional Stability and Flame Retardancy. *ACS Sustainable Chemistry & Engineering*, *6*(3), 3349–3357. https://doi.org/10.1021/acssuschemeng.7b03518

Kumari, D., Qian, X.-Y., Pan, X., Achal, V., Li, Q., & Gadd, G. M. (2016). Microbially-induced Carbonate Precipitation for Immobilization of Toxic Metals. In *Advances in Applied Microbiology* (Vol. 94, pp. 79–108). https://doi.org/10.1016/bs.aambs.2015.12.002

Lahtela, V., & Kärki, T. (2015). Determination and comparison of some selected properties of modified wood. *Wood Research*, *60*(5), 763–772. http://www.centrumdp.sk/wr/201505/08.pdf

Lande, S., Eikenes, M., & Westin, M. (2004). Chemistry and ecotoxicology of furfurylated wood. *Scandinavian Journal of Forest Research*, *19*, 14–21. https://doi.org/10.1080/02827580410017816

Lande, S., Eikenes, M., Westin, M., & Schneider, M. H. (2008). Furfurylation of wood: Chemistry, properties, and commercialization. *ACS Symposium Series*, *982*, 337–355. https://doi.org/10.1021/bk-2008-0982.ch020

Lande, S., Westin, M., & Schneider, M. (2004a). Properties of furfurylated wood. *Scandinavian Journal of Forest Research*, *19*, 22–30. https://doi.org/10.1080/0282758041001915

Lande, S., Westin, M., & Schneider, M. H. (2004b). Eco-efficient wood protection: Furfurylated wood as alternative to traditional wood preservation. *Management of Environmental Quality: An International Journal*, *15*(5), 529–540. https://doi.org/10.1108/14777830410553979

Larsson Brelid, P. (2013). *Benchmarking and State of the art for Modified wood*. http://www.diva-portal.org/smash/get/diva2:962771/FULLTEXT01.pdf

Li, W., Ren, D., Zhang, X., Wang, H., & Yu, Y. (2016). The Furfurylation of Wood: A Nanomechanical Study of Modified Wood Cells. *BioResources*, *11*(2), 3614–3625. https://doi.org/10.15376/biores.11.2.3614-3625

Li, W., Wang, H., Ren, D., Yu, Y., & Yu, Y. (2015). Wood modification with furfuryl alcohol catalysed by a new composite acidic catalyst. *Wood Science and Technology*, *49*(4), 845–856. https://doi.org/10.1007/s00226-015-0721-0

Lima, J., Gonçalez, J., Mori, F., Mori, C. & Trugilho, P. (2005). Caracterização da cor da madeira de clones de híbridos de eucalyptus spp. *CERNE. 11*, 137-146.

Mantanis, G. I. (2017). Chemical Modification of Wood by Acetylation or Furfurylation: A Review of the Present Scaled-up Technologies George. *BioResources*, *12*(2), 4478–4489. https://bioresources.cnr.ncsu.edu/wp-content/uploads/2017/05/BioRes_12_2_4478_Mantanis_Chemical_Modification_Wood_Review_Present_Technologies_11731.pdf

Mantanis, G., & Lykidis, C. (2015). Evaluation of Weathering of Furfurylated Wood Decks after a 3-year Outdoor Exposure in Greece. *Drvna Industrija*, *66*(2), 115–122. https://doi.org/10.5552/drind.2015.1425

Moya, R., Salas, C., Berrocal, A., & Valverde, J. C. (2015). Evaluation of chemical compositions, air-dry, preservation and workability of eight fastgrowing plantation species in costa rica. *Madera Bosques*, *21*, 31–47. http://www.redalyc.org/articulo.oa?id=61743003003

Nordstierna, L., Lande, S., Westin, M., Karlsson, O. & Furo, I. (2008). Towards novel wood-based materials: Chemical bonds between lignin-like model molecules and poly(furfuryl alcohol) studied by NMR. *Holzforschung*, *62* 709-713. https://www.degruyter.com/view/j/hfsg.2008.62.issue-6/hf.2008.110/hf.2008.110.xml.

Pilgård, A., Treu, A., Van Zeeland, A. N. T., Gosselink, R. J. A., & Westin, M. (2010). Toxic hazard and chemical analysis of leachates from furfurylated wood. *Environmental Toxicology and Chemistry*, *29*(9), 1918–1924. https://doi.org/10.1002/etc.244

Pranger, L., & Tannenbaum, R. (2008). Biobased Nanocomposites Prepared by In Situ Polymerization of Furfuryl Alcohol with Cellulose Whiskers or Montmorillonite Clay. *Macromolecules*, *41*(22), 8682–8687. https://doi.org/10.1021/ma8020213

Ringman, R., Pilgård, A., Brischke, C., & Richter, K. (2014). Mode of action of brown rot decay resistance in modified wood: a review. *Holzforschung*, *68*(2), 239–246. https://doi.org/10.1515/hf-2013-0057

Rowell, R. (2016). Dimensional stability and fungal durability of acetylated wood. *Drewno*, *59*(197), 139–150. https://doi.org/10.12841/wood.1644-3985.C14.04

Rowell, R. M. (2014). Acetylation of wood-A review. In *International Journal of Lignocellulosic Products* (Vol. 2014, Issue 1). http://ijlp.gau.ac.ir

Sarvaramini, A., & Larachi, F. (2017). Pyrolysis Kinetics of Pre-Torrefied Woody Biomass Based on Torrefaction Severity—Experiments and Model Verification. *Industrial & Engineering*

Chemistry Research, *56*(45), 12972–12983. https://doi.org/10.1021/acs.iecr.7b01123

Sejati, P. S., Imbert, A., Gérardin-Charbonnier, C., Dumarçay, S., Fredon, E., Masson, E., Nandika, D., Priadi, T., & Gérardin, P. (2017). Tartaric acid catalyzed furfurylation of beech wood. *Wood Science and Technology*, *51*(2), 379–394. https://doi.org/10.1007/s00226-016-0871-8

Shirmohammadli, Y., Moradpour, P., Abdulkhani, A., Efhamisisi, D., & Pizzi, A. (2019). Water resistance improvement by polyethyleneimine of tannin-furfuryl alcohol adhesives. *International Wood Products Journal*, *10*(1), 16–21. https://doi.org/10.1080/20426445.2019.1600814

Sodero Martins Pincelli, A. L. P., de Moura, L. F., & Brito, J. O. (2012). Effect of thermal rectification on colors of Eucalyptus Saligna and Pinus caribaea Woods. *Maderas. Ciencia y Tecnología*, *14*(2), 239–248. https://doi.org/10.4067/S0718-221X2012000200010

Sun, R. (2001). Fractional isolation, physico-chemical characterization and homogeneous esterification of hemicelluloses from fast-growing poplar wood. *Carbohydrate Polymers*, *44*(1), 29–39. https://doi.org/10.1016/S0144-8617(00)00196-X

Temiz, A., Terziev, N., Eikenes, M., & Hafren, J. (2007). Effect of accelerated weathering on surface chemistry of modified wood. *Applied Surface Science*, *253*(12), 5355–5362. https://doi.org/10.1016/j.apsusc.2006.12.005

Tenorio, C., Moya, R., Salas, C., & Berrocal, A. (2016). Evaluation of wood properties from six native species of forest plantations in Costa Rica. *Bosque*, *37*(1). https://doi.org/10.4067/S0717-92002016000100008

Thygesen, L. G., Barsberg, S., & Venås, T. M. (2010). The fluorescence characteristics of furfurylated wood studied by fluorescence spectroscopy and confocal laser scanning microscopy. *Wood Science and Technology*, *44*(1), 51–65. https://doi.org/10.1007/s00226-009-0255-4

Thygesen, L. G., Tang Engelund, E., & Hoffmeyer, P. (2010). Water sorption in wood and modified wood at high values of relative humidity. Part I: Results for untreated, acetylated, and furfurylated Norway spruce. *Holzforschung*, *64*(3), 315–323. https://doi.org/10.1515/hf.2010.044

van Gelder, H. A., Poorter, L., & Sterck, F. J. (2006). Wood mechanics, allometry, and life-history variation in a tropical rain forest tree community. *New Phytologist*, *171*(2), 367–378. https://doi.org/10.1111/j.1469-8137.2006.01757.x

Venås, T. M., Feldby, C., & Morsing, N. (2008). A study of mechanisms related to the fungal decay protection rendered by wood furfurylation. In *Faculty of Life Sciences*. https://www.forskningsdatabasen.dk/en/catalog/2398267464

Vetter, L., Depraetere, G., Janssen, C., Stevens, M., & Acker, J. (2008). Methodology to assess both the efficacy and ecotoxicology of preservative-treated and modified wood. *Annals of Forest Science*, *65*(5), 504–504. https://doi.org/10.1051/forest:2008030

Wang, Y., Deng, L., Xiao, Z., Li, X., Fan, Y., & Li, C. (2019). Preparation and properties of bamboo/polymer composites enhanced by in situ polymerization of furfuryl alcohol. *Materials Express*, *9*(7), 712–722. https://doi.org/10.1166/mex.2019.1550

Westin, M., Rapp, A., & Nilsson, T. (2006). Field test of resistance of modified wood to marine borers. *Wood Material Science and Engineering*, *1*(1), 34–38. https://doi.org/10.1080/17480270600686978

Worasuwannarak, N., Sonobe, T., & Tanthapanichakoon, W. (2007). Pyrolysis behaviors of rice straw, rice husk, and corncob by TG-MS technique. *Journal of Analytical and Applied Pyrolysis*, *78*(2), 265–271. https://doi.org/10.1016/j.jaap.2006.08.002

Xie, Y., Fu, Q., Wang, Q., Xiao, Z. & Militz, H. (2013). Effects of chemical modification on the mechanical properties of wood. *European Journal of Wood and Wood Products*, *71*(4), 401–416. https://doi.org/10.1007/s00107-013-0693-4

Yang, T., Cao, J., & Ma, E. (2019). How does delignification influence the furfurylation of wood? *Industrial Crops and Products*, *135*, 91–98. https://doi.org/10.1016/j.indcrop.2019.04.019

Anexo 1